The Coverage, Capacity and Coexistence of Mixed High Altitude Platform and Terrestrial Segments

Muhammad Danial Bin Zakaria

Doctor of Philosophy

University of York

Electronic Engineering

July 2019

Abstract

This thesis explores the coverage, capacity and coexistence of High Altitude Platform (HAP) and terrestrial segments in the same service area. Given the limited spectrum available, mechanisms to manage the co-channel interference to enable effective coexistence between the two infrastructures are examined. Interference arising from the HAP, caused by the relatively high transmit power and the antenna beam profile, has the potential to significantly affect the existing terrestrial system on the ground if the HAP beams are deployed without a proper strategy. Beam-pointing strategies exploiting phased array antennas on the HAPs are shown to be an effective way to place the beams, with each of them forming service cells onto the ground in the service area, especially dense user areas. Using a newly developed RF clustering technique to better point the cells over an area of a dense group of users, it is shown that near maximum coverage of 96% of the population over the service area can be provided while maintaining the coexistence with the existing terrestrial system.

To improve the user experience at the cell edge, while at the same time improving the overall capacity of the system, Joint Transmission – Coordinated Multipoint (JT-CoMP) is adapted for a HAP architecture. It is shown how the HAP can potentially enable the tight scheduling needed to perform JT-CoMP due to the centralisation of all virtual E-UTRAN Node Bs (eNodeBs) on the HAP. A trade-off between CINR gain and loss of capacity when adapting JT-CoMP into the HAP system is identified, and strategies to minimise the trade-off are considered. It is shown that 57% of the users benefit from the JT-CoMP.

In order to enable coordination between the HAP and terrestrial segments, a joint architecture based on a Cloud – Radio Access Network (C-RAN) system is introduced. Apart from adapting a C-RAN based system to centrally connect the two segments together, the network functional split which varies the degree of the centralised processing is also considered to deal with the limitations of HAP fronthaul link requirements. Based on the fronthaul link requirements acquired from the different splitting options, the ground relay station diversity to connect the HAP to centralised and distributed units (CUs and DUs) is also considered.

Table of Contents

List of Figures

Acknowledgement

Being always in the state of remembrance towards The Almighty, while ever longing for His blessings and forgiveness, it is only natural that my utmost thanks is reserved only for Him, the Most Gracious, the Most Merciful. Peace and blessings be upon His servant and messenger, Muhammad s.a.w.

I am indebted eternally grateful to my supervisors Professor David Grace and Dr Paul Mitchell for their patience, ever-presence, dedication and invaluable guidance throughout the period of this research, without which this work would not have come this far. My sincere appreciation also goes out to many other individuals who either directly or indirectly contributed to the completion of this thesis.

Success is always enhanced by the emotional support of the family and loved ones. Thank you to my parents Zakaria Ibrahim and Rosidah Mohd Amin, my wife Amelia Akashah Amiruddin, our children, Muhammad Affan and Aafiyah, my siblings, Muhammad Mustaqim, Sarah Nasuha, and Hajar Kamilah, and other family members whose constant support made this achievement possible.

With great fondness, my special thanks to the members of the Communication Technologies Research Group and Department of Electronic Engineering for creating a friendly, supportive, enjoyable and comfortable environment at the workplace.

Lastly, I would like to thank my sponsor, Universiti Sultan Zainal Abidin, Malaysia for giving me the opportunity to work and study for my Ph.D in Electronic Engineering.

To all those mentioned, either by name or otherwise, please let it be known that "thank you" is just a small and modest phrase used to express my gratitude to all of you; if there is ever a bigger and ostentatious alternative, I would have used it. Thank you.

Declaration

All the work presented in this thesis, to the best knowledge of the author are original in contribution. References and acknowledgements to other researchers have been appropriately given.

Part of the research materials have been used to form an initial patent filing [1], and several papers that were published in conferences and a journal [2-4].

List of Publications

Patent

M. D. Zakaria, D. Grace, and P. D. Mitchell, "Service Cell Selection," Patent Pending 1901060.2, 2019

Journal Articles

M. D. Zakaria, D. Grace, P. D. Mitchell, T. M. Shami, and N. Morozs, "Exploiting User-Centric Joint Transmission – Coordinated Multipoint With a High Altitude Platform System Architecture," Published in *IEEE Access*, 2019.

Conference Papers

M. D. Zakaria, D. Grace, and P. D. Mitchell, "Antenna array beamforming strategies for high altitude platform and terrestrial coexistence using K-means clustering," Published in *2017 IEEE 13th Malaysia International Conference on Communications (MICC)*, 2017.

M. D. Zakaria, D. Grace, P. D. Mitchell, and T. M. Shami, "User-centric JT-CoMP for High Altitude Platforms," Published in *2018 26th International Conference on Software, Telecommunications and Computer Networks (SoftCOM)*, 2018.

Glossary

1G 1st Generation

5G 5th Generation

BBU Baseband Unit

C-RAN Centralised – Radio Access Network

CAPEX Capital Expenditure

CB Coordinated Beamforming

CDF Cumulative Distribution Function

CINR Carrier to Interference plus Noise Ratio

CNR Carrier to Noise Ratio

CoMP Coordinated Multipoint

CS Coordinated Scheduling

CSI Channel State Information

CU Centralised Unit

DU Distributed Unit

DoA Direction of Arrival

eNodeB E-UTRAN Node B

FBW Full Bandwidth

FSO Free Space Optics

FSPL Free Space Path Loss

Gbps Giga Bit per Second

GRS Ground Relay Station

HAP High Altitude Platform

HBW Half Bandwidth

ICIC Inter-cell Interference Coordination

INR Interference to Noise Ratio

IoT Internet of Things

IP Internet Protocol

ITU-R International Telecommunication Union – Radio Communication

JT-CoMP Joint Transmission – Coordinated Multipoint

LC Listening Cell

LoS Line of Sight

LTE Long Term Evolution

Mbps Mega Bit per Second

MIMO Multiple Input Multiple Output

NFV Network Function Virtualisation

OBF Opportunistic Beamforming

OPEX Operational Expenditure

PSO Particle Swarm Optimisation

QoS Quality of Service

RF Radio Frequency

RRU Remote Radio Unit

RSSI Received Signal Strength Indicator

SDN Software Defined Network

TVWS Television White Space

UE User Equipment

Symbology

Σ Summation

{ } Set

| Such that

∪ Union

∩ Intersection

∈ Elements of

⊖ Symmetric difference

| | Number of elements in a set

⌈ ⌉ Rounding up

CHAPTER 1

1. Introduction

Contents

1.1 Overview

The evolution of wireless communication networks from the 1st generation (1G) until the 5th generation (5G) is largely driven by the demands of coverage and capacity. There are many reasons for the observed rise in network traffic, including the significant increase in the number of connected devices such as smartphones and tablets with the addition of heavy data usage applications like video streaming and video calls [5]. All these convenient services have changed user behaviour and internet usage. Previously, internet activity was limited to within the home or office, but now people can stay connected even when they are outside. The amount of Internet Protocol (IP) data handled by wireless networks has increased by over 100 fold; with approximately 3 exabytes in 2010, rising to a predicted value greater than 500 exabytes by 2020, and potentially 5 zettabytes in 2030 [6, 7]. The challenge for researchers and engineers is keeping pace with the enormous data traffic increase in the delivery of reliable and sustainable wireless networks.

Several solutions regarding the improvement of network capacity have been studied, but more cost-effective solutions are to be considered because massive networks are needed to

accommodate the data growth. Therefore, the idea of deploying cells from the above ground has surfaced. High Altitude Platforms (HAPs) are widely regarded as a flexible, mobile, cost-effective and alternative way to provide wireless communication services (e.g. broadband and cellular services) [8, 9]. HAPs are airships or aircraft, operating in the stratosphere approximately 17-22 km above ground [10, 11]. This height range is well above commercial airplanes and suffers from less atmospheric turbulence than lower altitudes. HAPs that are not currently in service can be repositioned to replace failed communication infrastructure and provide extra coverage and capacity when needed, e.g. for a temporary large crowd events [12]. In terms of permanent service, HAPs are suited to filling coverage holes in areas lacking in terrestrial infrastructure. HAPs have the potential to provide a useful alternative to the traditional terrestrial provision because their higher altitude operation provides a better chance of achieving Line of Sight (LoS) connectivity which means there is a lower chance of shadowing compared to terrestrial systems. HAPs are capable of deploying many transmission/reception beams which can be directed anywhere inside a service area for the purpose of forming cells to provide wireless communication services. With a multi-beam deployment capability, a HAP will need less infrastructure to serve more users over a larger service area compared to a corresponding terrestrial system.

The International Telecommunications Union – Radiocommunication Sector (ITU-R) has issued recommendations for HAPS, and allocated spectrum at 47/48 GHz for worldwide use and a 28/31 GHz band for Asian countries with an available bandwidth of 300 MHz for both uplink and downlink [13]. HAPs have also been authorised to provide IMT - 2000 (3G band) service worldwide [14] and potentially the television (TV) white space band which is the ultra high frequency (UHF) band could be exploited due to the gap left in TV networks for buffering purposes [15] and as a result of switchover to digital TV, more gap in spectrum is left unused. However, given the prominence of terrestrial infrastructure, there will be many situations where HAPs are deployed in the same service area as existing terrestrial networks (e.g. where additional capacity density is required). Given the limited spectrum available, mechanisms to enable effective coexistence between the two infrastructures are needed. Use of the same bands will

generate interference from a HAP to an existing terrestrial system, and the amount of interference the systems can tolerate will depend on the application(s). In the case of the TV white space bands, coexistence is very strict, but in the case of cellular systems, more interference can be tolerated, especially if a sharing agreement is in place between the two systems.

1.2 The Coexistence of High Altitude Platform (HAP) and Terrestrial Network Challenges.

HAPs are suitable for providing coverage in rural areas where the locations are geographically hard to reach or considered not cost-effective to build terrestrial infrastructure. To provide total coverage, one way is by deploying the beams based on a regular hexagonal grid, but it is only applicable when no other network operates in the area concerned using the same spectrum. There will be a situation where the service area already has terrestrial provision and the deployment of highly concentrated signal power on a specific area without proper management over the interference will cause the degradation in performance of the existing terrestrial system that shares the common frequency band. Naturally, an appropriate strategy is needed to deploy the HAP beams to provide total coverage without causing high interference to the existing terrestrial network.

Coexistence between HAP and terrestrial networks can be achieved by keeping a certain separation distance between active cells (HAP and terrestrial cell). However, in order to ensure the interference remains below a minimum level, a gap between the cells may be needed which could mean that the users in the region will be unserved, so to enable contiguous coverage, the separation distance should be shortened which will result in an increase in interference levels especially for users at the edge of a cell. To counter this problem, interference mitigation techniques such as inter-cell interference coordination (ICIC) can be adapted which exchanges information between base stations or cells about resource reservations through an X2 interface so that the user in one cell can use the reserved resource blocks without interference from the other cell that was informed to reserve the resource blocks [16]. Alternatively, using a similar approach,

coordinated multipoint (CoMP) reserves specific resources for users that are profoundly affected by interference from two or more cells and turns the strongest interfering transmission into useful signal by requiring the formerly interfering cell to send the same packet simultaneously on the same resources [17]. Both techniques will benefit the users at the edge of a cell and/or even improve the overall system capacity.

However, the interference mitigation techniques will not be available between HAP and terrestrial cells with no centralisation and coordination between the two systems. A conventional HAP system is assumed to have one or more base stations on the platform, so it is safe to assume there will be an insufficient degree of inter-segment control to enable ICIC and CoMP between the terrestrial and HAP systems. Thus, techniques like ICIC and CoMP might only be feasible between the HAP cells. With this system, maintaining a separation distance with an interference to noise ratio (INR) threshold of X dB at key sites will be the best option to enable effective coexistence which is a common spectrum management method. Alternatively, a more centralised approach could be introduced on a HAP such as making it part of a Cloud – Radio Access Network (C-RAN) so that techniques like CoMP and ICIC can be implemented across the HAP and terrestrial system. Introducing a new approach for HAP system deployment is required to support coordination of the two different systems and enable HAP technologies fill a gap in delivery of 5G services.

The system layout to evaluate the performance of the schemes, architectures, and systems in this work, as well as the coexistence environment with the terrestrial system, is shown in Figure 1-1. It consists of a HAP and a macro base station (T-BS). HAP users (H-UE) and Terrestrial users (T-UE) are randomly distributed across the 30 km radius service area and two additional groups of users are generated randomly in smaller areas as hotspot coverage areas. The HAP is located at an altitude of 20 km above ground, while the macro base station is deployed at the centre of the service area which is at the sub-platform point of the HAP. We consider the HAP to be equipped with a 25 x 25 element phased array antenna to perform beamforming and deploying HAP beams where in previous work for example, the CAPANINA project [18], considered a 121

beam structure over a 30 km radius service area and a three sector antenna for the macro base station cell deployment. Details about the phased array antenna profile will be briefly discussed in Chapter 3.

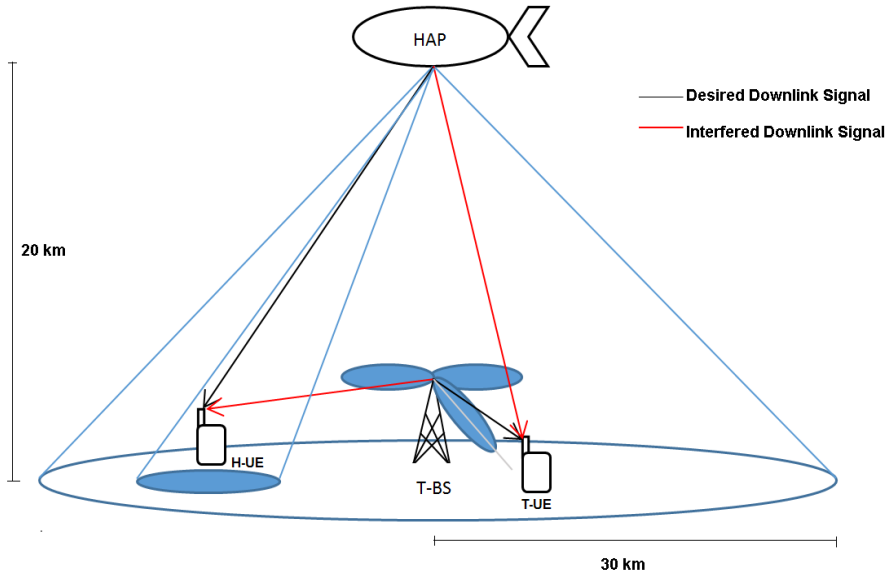

Figure 1-1 The coexistence scenario of HAP and terrestrial networks with downlink transmission.

1.3 Hypothesis and Objectives

The hypothesis on which this research is based is:

"*A HAP can coexist with a terrestrial network sharing a common frequency band while restricting degradation in terrestrial network performance, so as to maintain a minimum quality of service (QoS).*"

In order to realise the hypothesis, the following objectives were defined:

I. To develop a suitable strategy for a HAP beam-pointing technique so that total coverage and coexistence can be achieved with a terrestrial network.

II. To mitigate the interference between cells especially at the cell edges, while improving overall system performance.

III. To enable coordination between HAP and terrestrial networks, and therefore to achieve a new degree of coexistence capability between the two systems.

1.4 Thesis Outline

The rest of the thesis is organised as follows:

- **Chapter 2** provides background information of essential elements related to the author's research work including a brief description of related projects and other research in the field. It is divided into an overview of High Altitude Platform (HAPs), the coexistence of HAPs and terrestrial networks, a summary of Cloud - Radio Access Network (C-RAN), and an overview of interference management techniques.
- **Chapter 3** explains the methodology for experimental evaluation used in this thesis. It describes the phased array antenna profile, proposed HAP architecture, performance metrics (e.g. CINR), propagation model for both HAP and terrestrial macro base station, phased array antenna profile for HAP, three-sector antenna profile for a macro base station, the channel capacity model, and lastly the traffic model.
- **Chapter 4** proposes novel beam-pointing techniques to control the coverage and capacity of a HAP system while providing adequate protection for terrestrial users coexisting in the cellular spectrum. An intelligent beamforming strategy based on RF clustering is used to assist the HAP in determining the locations to avoid the terrestrial system, while providing coverage for user groups that are demanding service from the HAP.
- **Chapter 5** investigates how joint transmission coordinated multipoint (JT-CoMP) can be extended to a new High Altitude Platform (HAP) system architecture by exploiting a phased array antenna, which generates multiple beams that form cells, each of which can map on to pooled virtual base station equipment, thereby replacing various terrestrial cell sites. This chapter focuses on enhancement of user’s experience at the edge of the HAP cells, although the terrestrial macro base station is still present.
- **Chapter 6** presents jointly controlled HAP and terrestrial segments by introducing a new joint HAP and terrestrial architecture, via a new 5G C-RAN based system variant. A network functional split for a C-RAN based system is shown to be important to provide tight

coordination between High Altitude Platform (HAP) and terrestrial segments that form joint networks.

- **Chapter 7** concludes all the work done in this thesis, revisits the objectives, and shows how the work done has complimented the objectives and contributes to novel findings of each of the works. Later, some suggestions are made regarding the future work, and how to take the research forward beyond what was covered in this thesis.

CHAPTER 2

2. Literature Review

Contents

2.1 Introduction

This chapter presents background information about important elements related to the author's research work including a brief description of related projects and other research work. It is divided into an overview of High Altitude Platforms (HAPs), the coexistence of HAPs and terrestrial networks, an overview of Cloud – Radio Access Network (C-RAN), and a summary of interference management techniques.

2.2 High Altitude Platforms

The development of HAPs started as early as 1969 and since then, a lot of research and development has been undertaken by both industry and academia. However, commercial exploitation of HAPs has been limited to date, because of aeronautics technological challenges mainly related to the need for lightweight structures (material), energy harvesting and storage [19], but HAPs are now starting to become available. We are starting to see the first long endurance HAPs produced for commercial sale. For airships and balloons, the envelope material needs to be able to withstand damage, low temperatures, and have low permeability to the lifting gas [20]. As for aircraft, reducing weight is the critical factor because of the limitations on payload weight, volume and power. Typically, the wing structure consists of a tubular spar and ribs made of carbon fibre [21]. The weight of various components (e.g. batteries on the Zephyr) is distributed along the wingspan to minimise the structural stress on the wing [22].

The potential cost to build, operate, and maintain a HAP varies depending on the HAP category, whether it is an airship or aircraft. According to [23], an airship can cost up to €36 million, and an aircraft approximately €5 million for both capital and al expenditure (CAPEX and OPEX) per annum [24]. It is only natural that operators want to select the most economical option, but they have to deal with the trade-off of more limited payload weight, volume and available power compared with airships. This calls for innovative ways to provide communication services.

Unmanned airships or aircraft means that the vehicle is fully automated by some flight control or even artificial intelligence (AI). When the technology is ready, there will be many HAPs in the sky which opens up possibilities of collisions between HAPs. It is therefore essential that there will be some effective communication between HAPs to avoid collisions, with the control systems designed to be failsafe [23].

To be able to maintain a long duration flight (e.g. three months proposed for Facebook's Aquila), the plane for project Aquila needs to be able to regenerate and store energy so that it can

enable a longer duration flight in the stratosphere. 5kW of power is required to supply their propellers [23], payloads (e.g. telecommunication, Earth monitoring) and avionics. At 18 – 27 km, the dominant energy source is solar, and solar power can be efficiently harvested using solar panels and stored in batteries or fuel cells. To make up for the non-harvesting time (during the night), the solar panels need to harvest at least 10kW during the day [23]. There are ways to maximise the energy accumulated from solar power; one factor is to optimize the area of the solar panel array. The larger the usable surface area of the HAP, the greater the size of solar panel array can be installed; hence more energy can be harvested. Secondly, advanced technology such as the triple-junction solar cells by SolAero Technologies Corp can be used to make the photons absorb 3 times more than the average solar cells, due to relatively high-efficiency levels approximately around 32% [23]. Unfortunately for the upper latitudes in the northern hemisphere, they will have a problem to rely solely on solar power, due to shorter days, and the energy harvested from solar power is unlikely to be sufficient. To counter this problem, an alternative source can be used which is the regenerative fuel cell. It works by fusing hydrogen gas (which will come in a tank on a HAP) and oxygen resulting in electricity and water (H_2O).

2.2.1 Wireless Communication Services via HAPs

HAPs are seen as an essential way to deliver wireless communication services such as cellular and broadband, which is often referred to as "connectivity from the sky" [25]. HAPs are referred to as the "middle ground" in between terrestrial and satellite provision. For instance, HAPs are capable of serving a larger area than terrestrial, while at the same time having a better link budget than satellites due to their shorter distance to the ground. More comparisons between terrestrial, HAP (airships and aircraft), and satellite are presented in Table 2-1.

A considerable amount of research has been carried out regarding wireless communication service provision from HAPs for both broadband and cellular communications. A typical HAP communication architecture consists of the access network (user's link), backhaul/fronthaul (depending on the type of the platform), inter-platform link, and alternative backhaul through

satellite [9]. The authors in [11] discussed the potential role of HAP in beyond 3G networks, where a HAP is part of a hybrid terrestrial-HAP-satellite system. The service (which in this case is a 4G service) can be mapped to either to terrestrial or HAP and satellite to provide an alternative backhaul link depending on the bit rates. High bit rate classes are mapped onto the terrestrial component, while medium and it rate classes are mapped onto the HAP component of the system. For a broadband service, [26] evaluates the performance of worldwide interoperability for microwave access (WiMAX) from HAPs with multiple antenna payloads, at the same time examining the coexistence behaviour with several terrestrial WiMAX base stations for both downlink and uplink performance sharing the same 30 km radius coverage area. With better Line of Sight (LoS) connectivity from HAP, millimetre-wave (mm-wave) technology is seen as a promising medium to deliver broadband service from a HAP [26]. In [27], four transmissions options from four different modulation schemes were proposed, corresponding to the quality of the mm-wave link. The better the link budget, the higher modulation scheme is available which can enable maximum bit rate per cell up to 120 Mbps hence more application like internet access, video-on-demand- video conference, and telephony will be available with such data rates.

According to [28], even with sufficient link budgets, coverage by mm-wave will still be limited due to physical random access channel (PRACH). To overcome this, they propose a re-transmission mechanism for PRACH sequences. The proposed algorithm can potentially double the coverage area [28]. Authors in [29] were looking at the deployment of HAP on frequency above 10 GHz in desert and semi-desert area. In these type of area, the sand storm which contribute to the attenuation by the dust in the air. They proposed some modification to an existing dust attenuation model to comply with real dust scenario. It was shown that the dust attenuation degraded the CINR by around 20 dB [29].

Apart from being used as infrastructure on a permanent basis in a specific service area, HAPs can also be a used for temporary events where sudden large crowds form such as at a football match or concert in a stadium, and more importantly for emergency use following a disaster. According to the Freepress report [30], when Hurricane Sandy hit New York back in 2012,

thousands of people were left without access to communication networks when they needed them most. Later in 2014, there was a severe flood that occurred in the Kelantan State of Malaysia, and the report says that one of the reasons that complicated the rescue mission was communication infrastructure failure [31]. A case in 2015 was the flooding in York, where all the cellular communication and even fibre connections were not available for a whole day. Aerial platforms in disaster relief situations have been studied thoroughly in [32-34]. In [32] the aerial platform and a hybrid satellite-aerial-terrestrial (HSAT) networks was studied for emergency situations. They found that the HSAT networks can compensate for the failure of terrestrial networks due to emergency occurrences with the high availability and easy set up characteristics of aerial platforms. Authors in [33] show that a damaged network can be compensated and recovered up to 70% compare to pre-disaster by using a HAP to form cells and provide coverage temporarily.

Table 2-1 Wireless Communication Provision Comparison [23]

	Terrestrial	Airship	Aircraft	Satellite
Height	5 – 250 m	3 – 22 km	16 – 19 km	500 – 30000 km
Life time	up to 15 years	up to 5 years	-	up to 15 years
Capacity	high	medium	medium	low
Cell coverage	only land	everywhere	everywhere	everywhere
	0.1 – 1 km	1 – 10 km	1 – 10 km	50 – 400 km
Maintenance	easy to schedule	more difficult to schedule	more difficult to schedule	too expensive to relaunch
Remarks	proven and well known technologies many infrastructures required	power constraint too costly	more power contain than airship	proven and well known technologies

IoT has become a hot topic in recent years in term of technical, social and economic significance [35]. When hundreds of thousands IoT devices are expected to demand connection, there are concern of whether supporting these IoT devices would significantly burden the current network infrastructures. The authors in [35] have proposed a reliable IoT network based on HAPas an alternative standalone network that is well positioned to provide a seamless connectivity. However, HAPs are susceptible to various factors in the sky that may resulting degradation of service [36]. To ensure GoS, author proposed a DOA method based on the lates long short-term memory (LSTM) through multiple beamforming for 5G HAPS IoT networks [36]. In [37], the author also suggest that HAPs unstable movement may effect on the handover performance. They discussed vertical and swing movement which are affecting the path loss. They found that swing movement has greater influence on the handover probability than the vertical movement [37].

2.2.2 HAPs Related Projects by both Industry and Academia

The potential advantages of HAPs have encouraged their development over the last 40 years. Many organisations, companies and even countries have funded various projects to develop HAPs for many applications; such as broadband communication.

Even though airship based HAPs cost significantly more than aircraft, many projects have been undertaken to develop them, due to their potential to have significantly higher payload capabilities. The Airship High Platform II built by the Raven Company with the support from the US Navy was one of the earliest experiments carried out in HAP research. This project started in 1969 in order to analyse the feasibility of such platforms. The platform was solar powered, was 25 m in length, weighed 62 kg, and had electric propulsion with the propeller as shown in Figure 2-1. The flight succeeded for more than an hour, reaching an altitude of 21km in 1970 [38].

Figure 2-1 High Platform II Airship, Raven [38].

The HiSentinel project aimed for a low-cost unmanned airship system with a payload capability of 9 – 90 kg at stratosphere level, with an expected flight duration of at least 30 days. It was developed by the Southwest Research Institute (SwRI) and was sub-contracted to the American company Aerostar International of the Raven Group for envelope manufacturing and flight test purposes. The HiSentinel family consists of three different vehicles: HiSentinel20,

HiSentinel50, and HiSentinel80 with 9, 23, and 36 kg payload capabilities respectively [39]. Only one flight test was conducted which lasted 8 hours at an altitude of 20 km. It failed to meet the early expectation of 24 hour flight due to propulsion system failure and the project lasted from 2007 – 2012 [40].

In the Far East, Japan also started their HAP program called the Japanese Stratospheric Platform (SPF) in 1998 with the objective to develop a system based on a large unmanned airship that can maintain position at 20 km altitude above ground with future telecommunication and earth observation as the applications with an 8 year development plan [41]. The full-scale SPF airship would have been 245 m in length with a 1 ton payload. The airship was intended to be solar powered during the day, with regenerative fuel cells (RFC) used at night. The SPF project was funded by the Millennium Project, promoted by the Japan's Prime Minister Office [41]. Two prototypes SPF-1 and SPF-2 were developed for demonstration and flight test. SPF-1 successfully reached 16 km altitude in August 2003 [42], while SPF-2 was demonstrated at lower altitude focusing on some of SPF key technologies like flight control, earth observation, and telecommunications. In 2004, SPF-2 was tested for flight eight times at lower altitude [43]. The SPF programme was terminated in 2005 after spending approximately $200 million and was not further supported for full scale development. However, the research for key technologies such as RFC and lightweight materials was continued by the Japan Aerospace Exploration Agency (JAXA) [44].

The Korean Stratospheric Airship Program started in 2000 for a 10 year development program, and was aiming to develop a 200 m long airship (VIA 200), capable of carrying around 1000 kg of payload [45-47]. The project was supported by the Korean Ministry of Commerce, Industry and Energy (MOCIE). The first phase of the project was completed in 2004 with a 50 m long airship (VIA 50). The airship successfully achieved a 5 km altitude carrying a 100 kg payload with a new hangar built in southern region of Korea. Phase two which was aimed at developing VIA 200 was halted in 2005 and there is no further information about the current development of

the project [45]. However, there is an active aircraft project (EAV-3), where a flight test at 14 km altitude was conducted in August 2015 [48].

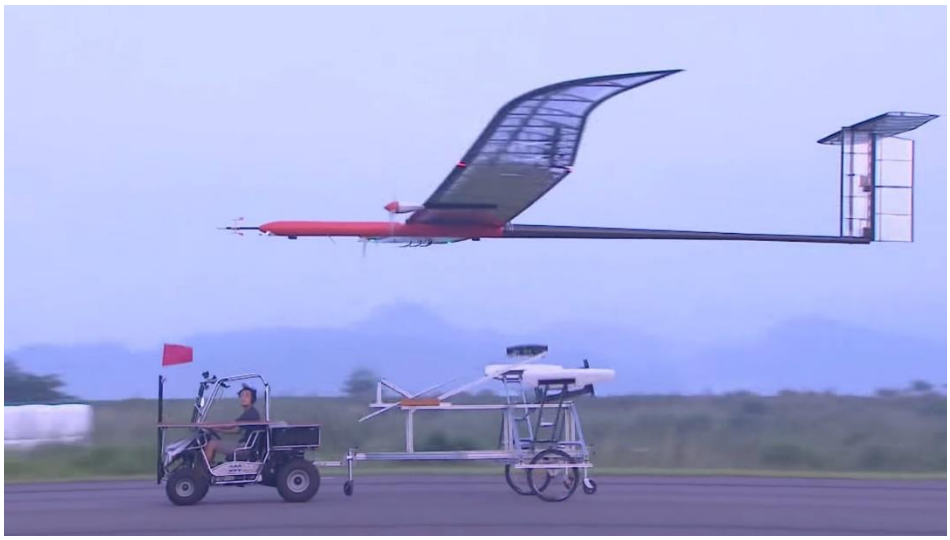

Figure 2-2 EAV-3 takes off with assisted from its trailer at Korean Airport (Directly reproduced from [45]).

In 2010, Thales Alenia Space started the Stratobus project. The Stratobus is an unmanned airship 100 m long, 33 m diameter, and can carry a 250 kg payload [49]. The Stratobus features some innovative designs which include the use of transparent upper body to allow the reflected sunlight to be directed to solar panels inside the Stratobus.[50], and during the night, energy is provided by the RLC. This platform will have 5 years lifetime but will have to land one week every year for maintenance purposes. It was reported that the product may be commercialised after 2023.

CAPANINA was a project funded by EU Framework 6 from November 2003 to January 2007. It involved 14 global partners, including the University of York which coordinated the project [51]. Their aim was to deliver a low cost broadband service with data rate up to 120 Mbps which is about 200 times faster than the fixed line broadband at that time. The use of millimetre wave (mm-wave) as the medium to deliver broadband service was the highlight of the

CAPANINA project. The platform was assumed to serve at least a 60 km diameter coverage area. With the HAP's unique wide area and high capacity coverage capability, the aim was for it to be beneficial for rural and "hard to reach" areas [8]. The most future oriented part of CAPANINA work was the delivery of high speed broadband (backhaul) to high-speed trains travelling up to 300 km/h via a steerable antenna on the roof. The backhaul link enabled integration with on-board WLAN access points. It was found out at that at the time, none of current broadband standards were universally suitable for this kind of service, however IEEE 802.16SC (single carrier) is the closest match, so it was selected for further study and adaptation [18].

As for aircraft, several projects have been undertaken considering the lower cost compared to airships. Known as the first European Union (EU) HAP project, the HeliNet project started on January 2000 to May 2003 and was funded by the EU Framework 5 Programme. The University of York was one of the ten European partners [27]. A study was carried out in order to develop a parts of a scaled size prototype HAP named the HeliPlat, from which broadband communication and other services could be delivered [10]. In [10], it is concluded that the main constraints are the limited payload and power. However, the methods and techniques may be applied in the future when the aeronautical technology is ready.

The Environment Research Aircraft and Sensor Technology (ERAST) Program was conducted by National Aeronautics and Space Administration (NASA) which was started in 1994. In conjunction with industry, the ERAST program's aim was to develop and demonstrate aircraft for the stratosphere for long-duration missions for environment monitoring [52]. The unmanned solar energy aircraft developed by AeroVironment for the program reached an altitude of 21.48 km with the Pathfinder, and 29.52 km for Helios. Helios had a wingspan of 75 m and weighed up to 1052 kg, and was tested with two different configurations (10 and 14 electric motors) [21]. AeroVironment stated that for Helios to be commercialised, $300 million of investment was needed plus $50 million for the prototype. The ERAST program was finally closed in 2014 and one of the reasons is the Helios prototype crashed after being caught up in turbulence near the island of Kauai, Hawaii in June 2003 [21, 53].

The development series of drone projects called the Zephyr began in 2001 [22]. The Zephyr 7, developed by the British company QinetiQ, managed to establish the current flight record of approximately 14 days at 18 km altitude in July 2010. In 2013, Airbus Defence and Space purchased the Zephyr project from QinetiQ. Developing the latest version of Zephyr, the twin tail Zephyr T will have a payload carrying capability of 20 kg which is an upgrade from the previous version due to an increase in the wingspan [54]. In February 2016, the UK Ministry of Defence requested two units of the Zephyr S worth £13 million. Airbus continuously flew its Zephyr S for over 23 days recently, significantly exceeding previous flight endurance records for aircraft [55].

Facebook is also participating in developing HAPs and their motivation is to connect more people across the globe. In March 2014, Facebook purchased the British drone making company, Ascenta along with its staff who were involved in the development of the Zephyr. The project named Aquila was a flying wing with a 42 m wingspan and about 400 kg weight. Equipped with four propellers, it was driven by electric motors and solar powered. The aim was that it will fly at altitude 18 – 27 km for a 3 month flight duration. It was expected to use a laser connection for a high speed communication network and switch to a lower frequency when there is non-line of sight (nLoS) conditions. In February 2016, an attempt to deploy Aquila was denied by the Indian authorities. According to Facebook, the service would have connected millions of Indian citizens who currently have no access to the Internet [19]. Facebook has since formed a partnership with Airbus to perform wireless communication service tests towards the end of 2018, using its Zephyr S aircraft [56].

Also, with the motivation to connect more people to the internet, Google bought the American company Titan Aerospace. The project called Solara 50 was announced back in 2013 [57]. The aircraft has a wingspan of 50 m and is capable of carrying 32 kg payload. Solara 50 was expected to fly at 20 km altitude, maintaining the flight up to 5 years [58]. In May 2015, Solara 50 failed its first flight test after it crashed immediately after take-off in a test area in New Mexico. It was due to a wing structural failure due to air currents at low altitude. Despite of high risk of failure like Titan and Helios, AeroVironment Inc., a global leader in unmanned aircraft systems

(UAS) recently announced a joint venture with the Japanese SoftBank to fund development and production of solar-powered high-altitude unmanned aircraft systems with a contract value of $65 million [59]. Their 5G vision is to have a ‘Super Cell Tower’ in the stratosphere [60].

Softbank and AeroVironment Inc. developed HAWK30, and automated pilot aircraft for telecommunication platform that aims to be operated at 20 km altitude. Several communication services are expected to be available with HAWK30 such as drone utilisation, IoT, as well as 5G [61]. HAWK30 is approximately 78 meters long, with 10 propellers along its wing and can fly at approximately 110 km/h in average. HAWK30 is expected to have mass production and service launch by 2023 [61].

Avealto, a manufacturer of HAPs based in the United Kingdom said that HAP service will be available in Indonesia in the next few years according to an Indonesia portal [62].Avealto’s HAP trial is to be held in mid 2020. As soon the trial is completed, and HAP legal issues is solved, HAPs are certainly available in Indonesia soon [62]. Article from [63] discussed on what regulation is HAPs should fall into, looking specifically on the Thales Alenia, the Stratobus. It was concluded that HAPs will be considered as aircraft and will fell under aircraft legal status.

2.2.3 The Coexistence of HAP and Terrestrial Networks

A coexistence scenario is where multiple systems or cells share the same frequency band in the same service area. It is known that co-channel interference from the HAP antenna serving the cells sharing the same band is the main source of interference in this coexistence scenario [64]. To minimize the co-channel interference, there are a few techniques that can be applied to the system, for example power control, beamforming, and radio resource management. In the past, significant research has been carried out to counteract this problem.

In [65], the downlink performance of WiMAX from HAP and terrestrial base stations sharing the same 3.5 GHz band was tested through simulation. Both the HAP and user devices were equipped with directional antennas, and the terrestrial base station was assumed to have an

omni-directional antenna with different separation distances and an overlapping cell scenario was investigated. They presented a power control strategy based on the interference-to-noise-ratio (INR) level of users at the edge of both cells, to improve the coexistence capabilities of terrestrial and HAP systems. It was concluded that such a strategy could be applied for both systems, and that they could coexist with a minimum CINR of 7 dB and 17 dB for the HAP and terrestrial system respectively. Then in [66], the same scenario was used once again to study the downlink performance by varying the HAP spacing radius; a user was placed at the cell edge as the performance indicator and a terrestrial WiMAX cell placed adjacent to the HAP cell. It showed that the HAP antenna gain gradually falls when the HAP moves away from the centre of the cell towards the opposite direction from the user location, while the gain fall more rapidly when HAP moves towards the user and terrestrial WiMAX location because of the interference from the terrestrial network. Varying the HAP spacing radius across the cell was just showing the effect of the HAP moving away from its antenna boresight and nearer to the interference source. By varying the beamwidth of the HAP antenna and user antenna as examined in [67], optimised coexistence performance could be achieved. HAP antennas of 43-degree and 72-degree beamwidth were compared and it was shown that for this scenario, the wider 72-degree beamwidth gave better performance as 50% of area inside the coverage region received a higher CINR of 25 dB and a higher CINR at the cell edge. By varying the user antenna beamwidth, it was concluded that a narrower beamwidth will require greater antenna pointing accuracy if movement of the HAP is considered.

For a HAP to serve several cells in a service area, multiple beams must be deployed from the HAP which will also cause interference between the beams, assuming that they share the same frequency band. A HAP delivering multiple beam coexistence with terrestrial networks sharing the same frequency band was examined in [64]. The terrestrial and user set up is the same as in [65]. They evaluated the downlink performance of this coexistence scenario with a configuration of different possible frequency reuse patterns for the HAP. For the uplink, the performance of the same scenario as in [64] varying the frequency reuse pattern was evaluated. It was to focus on

mitigating the co-channel interference from the terrestrial network to the HAP. The co-channel interference in the downlink and uplink were both being reduced subject to the reuse distance; hence the HAP system can effectively share the same band as the terrestrial network. The coexistence scenario is also feasible if a low rate modulation scheme such as BPSK modulation is used. The percentage coverage area served and percentage coverage area not served was defined by set theory [68].

The coexistence performance of HAP and terrestrial systems using Gigabit (Gb) communication links to serve specialist users was studied in [69]. The users are normally served by satellite links, but due to the demanding requirements of delivering HDTV signals, which requires a data rate up to 3 Gigabit per second (Gbps) for an uncompressed video stream, HAPs would be the possible solution to overcome capacity limitations. The carrier frequency selected was 28 GHz. Since it will share the same band as the terrestrial system, the coexistence scenario between the HAP and terrestrial system was examined. The solution to make the coexistence feasible was to use a highly directive antenna for each HAP antenna, terrestrial base station antenna, and also the specialist user. The beamwidth of the HAP antenna and terrestrial base station was set to 5-degrees and for the user antenna was 1-degrees. The pointing accuracy to deliver the optimum CINR level at the user positions was the main concern in this paper. For that, they implemented three schemes to adjust the pointing direction of the HAP spot beam which are the small step size scheme, half distance scheme, and switched beam scheme. A technique to enhance the performance by switching off the antenna beams below the CINR threshold value is also suggested in order to improve the CINR level of other specialist users.

Dealing with users equipped with directional antennas will be beneficial to control interference, as the directional antenna at both ends will provide more gain for a better link budget. On contrary, considering users with omni-directional antennas such as mobile phones and tablets in a coexistence scenario will be more challenging, as the link budget for the desired signal is poorer compared with users with directional antennas, thus experiencing a higher interference level. However, research has been carried out where they considered omni-directional user

antennas such as in [70]. Disaster scenarios were considered like earthquakes, flooding, and tornados where the terrestrial system can be disabled. The performance of 19 HAP cells deployed overlaying 37 terrestrial cells in suburban macrocell, urban macrocell, and urban microcell environments were shown, with the terrestrial base station shut off gradually. It was shown that 3G HAP networks offer a higher capacity than terrestrial networks, especially in suburban macrocell and urban microcell environments, due to their propagation characteristics [70]. The coexistence of HAP and terrestrial systems gave an impact on the terrestrial signal in suburban and urban macrocell environments but is not so crucial on the urban microcell environment. It was concluded that in disaster scenarios, the terrestrial systems can be shut off and the overlay HAP cell can provide more than enough coverage and capacity. The antenna radiation pattern in this work is modelled based on ITU-R M. 1456. However, the use of elliptical beam derived from the cosine function with variable values of the n roll-off factor to get the optimum antenna power roll-off is also shown to reduce the cell overlapping hence, reduce the interference to other cells [71, 72].

While in [73], the scenario of coexistence of HAP and terrestrial for mobile WiMAX downlink systems was evaluated. The performance of the overall system was evaluated to find the best frequency reuse pattern for this scenario. A frequency reuse pattern of 1 does not meet an acceptable GoS as required for mobile WiMAX services, and a reuse pattern of 3 and above can be used, but there is always a trade-off between minimising the interference and system capacity. Recently, a paper has examined the deployment of LTE from a lower altitude platform, an unmanned aerial vehicle (UAV) coexisting with terrestrial eNodeB [74]. The work was evaluated by both real experiments and simulations with the UAV transmitting 10 dBm power following the LTE standard requirements for small cells. The UAV was tested at altitudes of 150 m and 300 m to see which altitude gave the optimum performance. It was concluded that even a low-power UAV introduced a per square kilometre decrease in the overall CINR, and therefore it was suggested that only with better dynamic interference management, will the coexistence scenario be feasible.

Two spectrum etiquettes were developed to aid the coexistence of HAP and terrestrial networks on the downlink in [75]. The spectrum etiquettes vary the transmit power of a newly activated system when serving a specific user, called the INR-based and CINR-based schemes. The INR-based scheme controls the transmit power of the newly activated system based on the INR level at the receiver of a user as a reference. On the other hand, the CINR-based scheme controls the transmit power of the newly activated system based on the CINR level at the receiver of a user as a reference. Focusing on minimizing the impact to the terrestrial network, these schemes were implemented on the HAP system with various user antenna beamwidths and different types of modulation scheme as performance indicators. At the end of the experiment, it was shown that the CINR-based schemes offer better performance because they use the margin of CINR levels to set the modulation scheme thresholds which gives more flexibility with respect to whether to upgrade the performance or to use it for the upcoming new system activation.

Apart from beamforming and power control techniques, channel assignment strategies are another way of dealing with the co-channel interference for the coexistence scenario. In [76], a fixed channel assignment strategy was applied to the HAP spot beams. With appropriate spatial separation, effective channel reuse can be obtained and the frequency allocations were uniformly split to provide cluster sizes of 3, 4, and 7. At the user terminal, the sub-channels were allocated dynamically based on the Personal Access Communications – Unlicensed B (PACS-UB) protocol. The effect of overlapping HAP spot beams and hexagonal cells were evaluated based on the blocking probability for the PACS-UB system with different cluster sizes. It was shown that the performance with the overlapping cells is better in terms of blocking probability, because for fixed channel assignment, call blocking occurs due to a lack of resources rather than interference. From the results, it was shown that the overlapping cells between HAP and terrestrial network can be exploited to improve system performance with this channel assignment strategy. While in [77], the author performed an investigation to enhance the capacity from various fixed channel assignment techniques and to exploit the overlapping cells from a HAP. A technique derived from the Erlang B distribution was described to impose certain restrictions to limit the

proportion of the channels allocated to the overlap areas and retain some for use in non-overlap areas. This technique controls the number of channels being allocated without partitioning the coverage area into smaller regions, thereby increasing the capacity. In [78], a new channel assignment strategy which is Uniform Fixed Channel Allocation II (UFCA II) for a broadband multi-beam HAP architecture was developed to exploit the cell overlapping scenario. In previous work [77], the UFCA scheme was used successfully to achieve uniform blocking levels between the regions, but in different regions, users will experience a different data rates. To ensure fairness in terms of uniform data rates and uniform blocking, every user will have to pass a bits per second (bps) threshold check for all available channels. All the channels will be released and the user will be blocked if the data rate threshold is not met. A new user that will potentially affect the active user will be dropped. It was shown that the blocking probability was reduced from 4% to 2.6% by exploiting this technique. Although the technique discussed in [77, 78] was designed for an overlapping HAP cell, it is possible to implement this technique for coexistence of HAP and terrestrial networks.

In [79], spectrum sharing for HAP networks with the ground network was examined by applying stochastic geometry. An optimal altitude for HAP was obtained where the HAP network capacity is optimised [79]. In [80], the problem of deploying HAP to provide wireless communication service to the terrestrial users by modelling the problem as a potential game. A restricted spatial adaptive play (RSAP) learning algorithm was introduced for the game. With the RSAP algorithm, HAPs network can be deployed to serve the users in self-organised manner and achieved the required GoS [80]. On the other hand, authors in [81] looked at coordinating multiple HAPs for a service area. They compared the application of reinforcement learning (RL) and swarm intelligence (SI) based methods to solve the problem to coordinate multiple HAPs [81].

2.2.4 HAP Beam-pointing Techniques

The deployment of beams from a HAP onto the ground such that each of the beams then forms a cell in the intended service area which is typically up to 30 km radius will directly

determine the overall performance of the HAP system. It is because the interference power between the cells are determined by their geographic location, assuming that the frequency reuse of the system is 1. The same concept is applied to the existing infrastructure on the ground, so when the importance of the cell placement is considered, there is significant research that studied how the cell placement or beam-pointing should be executed. In [82], cell layouts of 121 and 313 cells for an elliptic beam lens antenna are compared. Two methods were used to derive the co-channel interference for both cell layouts when the cluster size was 3, and regular hexagonal grid layout. While in [83], the analysis on HAP movement models is done to predict the coverage in the case of shifting and the mechanism of steerable antennas movement is studied. The 127 cell layout with cell cluster of 4 scenario is applied. Moving on from a regular cell structure, the authors in [84] presented a smart cell design technique for irregular shaped cells for the HAP system. It is said that the smart cell design can reduce the co-channel interference because the irregular shape can reduce the overlapping cell, hence reduce the co-channel interference. The technique works by dividing the coverage area into a grid of small pixel spots and the smart cell is formed by clustering some pixel spots regardless of the shape of the smart cell.

One of the critical factors is to localise the users to efficiently deliver wireless communication services. A challenge was highlighted in [85] that to localise users from HAPs using two-dimensional direction of arrival (2D-DOA) will have high computational complexity over the large service area. However, the author proposed an efficient reduced processing time 2D-DOA by using two successive stages; starting with a low resolution 2D-DOA estimation Barlett algorithm and normalised the Barlett 2D-DOA spectrum with suitable threshold as a window for subsequent stage higher resolution 2D-DOA such as MUSIC algorithm. In [86], the authors proposed user clustered opportunistic beamforming schemes with a K-Means clustering algorithm for stratospheric communication. To avoid overwhelming the capacity gain because of the feedback from the large number of users that require Channel State Information (CSI), they adopted Opportunistic Beamforming (OBF) on HAPs which only requires CINR information for the purpose of clustering [87, 88].

2.3 Cloud – Radio Access Network (C-RAN)

C-RAN is a promising radio access architecture that aims to improve radio resource sharing and to reduce CAPEX/OPEX. It is also said to be one of the key features for upcoming 5G networks [89-91].The C-RAN system was first introduced back in 2009 by China Mobile which was intended to help solve the problem of the 100 fold increase in data requirements by 2020 [92]. To accommodate the increase in data, operators have to upgrade their infrastructure. In 5G, the number of devices per service subscriber is expected to increase, especially with the introduction of Internet of Things (IoT), so revenues are expected to be smaller [92]. A C-RAN based system will allow more flexibility in a network deployment (e.g. allowing for the turn on and off of the RRU) and also more dynamic deployments with network virtualization which allows multiple operators to run their network on virtual machines on single physical resources (in this case the CU and DU) as graphically illustrated in Figure 2-3, thus being more cost efficient. A C-RAN system consists of RRHs which are distributed, connected to CUs and DUs (in cloud) based on a common CU and DU pool (centralized) via fronthaul (FH) links. RRU, CU and DU are the new 5G terminologies [93, 94]. Looking back at 4G Long Term Evolution (LTE), the RRU is equivalent to the remote radio head (RRH), and CU and DU are equivalent to the baseband unit (BBU).

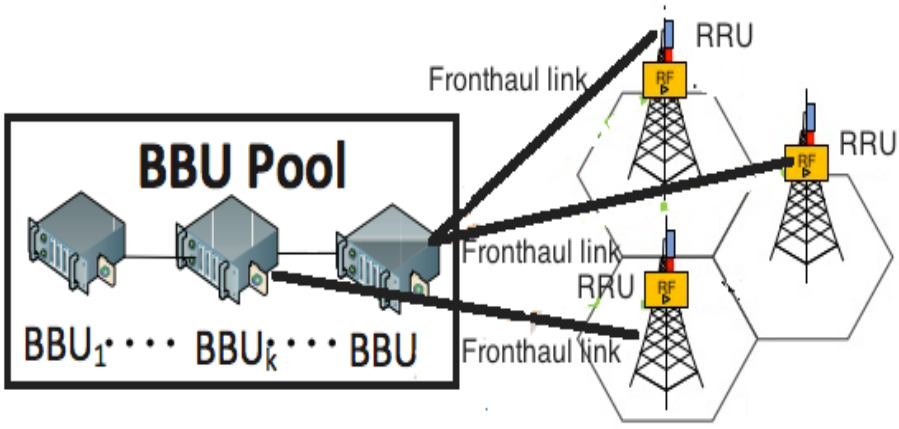

Figure 2-3 C-RAN architecture components (directly reproduced from [92]).

There have been a considerable number of research efforts related to a C-RAN based system with the aim of adapting to the requirements of 5G networks, such as the work in [95] which considered a 5G platform based on the C-RAN architecture, with a full virtualised RAN and a wireless or optical fronthaul link connection. The link domain is controlled by the Software Defined Networking (SDN) controllers. The author proposed to use a modular E-UTRAN Node B (eNodeB) where the virtualised BBU and RRH are implemented together with Commercial Off-The-Shelf (COTS) for their testbed. The rational dynamic adjustment to the connection between RRHs and BBUs is not to be neglected. According to [90], if this feature is neglected, there is a possibility that the blocked calls and poor connections will be faced by the users of the system. Therefore, the authors suggested to use particle swarm optimisation (PSO) to minimise the blocked calls and balance the processing load between the BBUs. Another application that is possible with a C-RAN based system is the network slicing that is considered as a key technology for the upcoming 5G networks [96]. The authors in [96] demo a prototype for managing the network slices in a C-RAN based system. Based on the resource requirements of each slice, the prototype will deal with how to efficiently share the bandwidth among the slices.

2.3.1 Network Functional Split in a C-RAN Based System

Recently, more ways have been developed to implement a C-RAN system that is able to dynamically balance how many CU and DU functions should be centralised, thereby reducing the fronthaul load. This can be achieved by adapting the C-RAN with a network functional split. Functionality is divided into several split options of the RRU and, CU and DU. There are eight main split options with option 8 being the conventional C-RAN system which has only the RF function on the RRU and the rest are centrally located in the CU and DU. Other split options down to option 1 see more functionality being added to the RRU side making them less centralised. Every option has its own requirement and behaviour, with the differing levels of functional split allowing systems to be tailored according to need.

Significant network functional split related research has been undertaken in the past few years. In [97, 98], evaluation of mobile fronthaul optical bandwidth and CoMP transmission and reception performance was carried out experimentally. Split-physical (PHY) processing (SPP) is proposed to locate some of the BBU functions at the RF side which can reduce the data to be transported by over 90% data through the mobile FH link. SPP employs its own CoMP scheme so that the CoMP performance is comparable to the conventional C-RAN. The authors in [99] suggested that reducing the fronthaul load by using a split might result in increased delay. They study the impact of different levels of splitting and different packetisation methods on the packet-based fronthaul network. Some insights are provided into the number of remote radio heads (RRHs) that can be supported over a single Ethernet-based fronthaul link. Also mitigating the fronthaul requirements, the authors in [94] consider the challenging task of selecting an appropriate split. A virtual network embedding (VNE) algorithm is proposed to flexibly select the most appropriate split for each small cell in the system.

2.4 Interference Mitigation Techniques

To accommodate the demand for scarce bandwidth, a potentially efficient choice is to reuse the frequency with a frequency reuse of one. This will result in co-channel interference, which is also known as inter-cell interference, to be high, which may reduce the Quality of Service (QoS). Therefore, a technique to mitigate the inter-cell interference is needed in order to improve the user experience, especially those who are heavily affected by the interference.

2.4.1 Inter-cell Interference Coordination (ICIC)

ICIC is a technology to reduce the inter-cell interference and improve the performance of the users at the cell-edge by informing the neighbouring eNodeBs to reserve bandwidth that is currently in use so that the user that occupies the bandwidth will not receive interference from the neighbouring eNodeBs [16, 100]. The ICIC consists of centralised, distributed, and hybrid ICIC. Centralised ICIC will have all the information control sent to a central entity which then makes decisions like resource allocation. This solution can achieve optimal resource allocation with the price of high overhead signalling, while the distributed ICIC is the other way around, which means that each eNodeB will have to make decision regarding resource allocation independently [101].

2.4.2 Coordinated Multipoint (CoMP)

The advantage of CoMP is not only to reduce the number of interfering signals, but also in some cases to convert them into useful signals. There are three types of CoMP: Coordinated Scheduling (CS), Coordinated Beamforming (CB), and Joint Transmission (JT). CoMP was first introduced by the third generation partnership project (3GPP) release 11 [102], in order to mitigate inter-cell interference particularly at the cell-edge, thereby improving the capacity of the cell-edge users. JT-CoMP can enable two or more simultaneous data transmissions to an intended user for both downlink and uplink cases. Tight synchronization between the cooperative cells will be required to perform JT-CoMP. Tight synchronization can normally be achieved with the

centralization of all eNodeBs, so JT-CoMP would be an appropriate choice compared to CS and CB CoMP.

Significant research has been carried out on JT-CoMP for terrestrial networks. It has been shown in [103-105] that JT-CoMP can provide significant SINR gain; however, JT-CoMP consumes additional bandwidth, as a user that is served by JT-CoMP requires all of its cooperative BSs to reserve an identical physical resource block (PRB) to transmit the same data. This means that if a PRB is reserved by one of a users' serving BS, none of the other cooperating BSs of this user can reuse it. As a result, resource allocation should be taken into account when the performance of JT-CoMP is investigated. User-centric JT-CoMP clustering is considered in this work as it has proven its superiority in improving cell-center and cell-edge throughput compared with static clustering [104, 106].

There have been a considerable number of research efforts on JT-CoMP, with the aim of finding an optimal user-centric cluster size and allocating radio resources in an efficient way. Nevertheless, most research on JT-CoMP deals with developing an optimal user-centric cluster size and allocating the corresponding resources separately. In [106], optimal and suboptimal user-centric clustering algorithms are proposed to enhance the performance of users located at the edge. The work in [107] has applied user-centric JT-CoMP clustering to tackle inter-cell interference in multi-tier networks. In the proposed approach, users can operate under two different modes: a non-CoMP mode and a CoMP mode. A user operates in CoMP mode only if its second strongest received power is comparable with its strongest received power. The authors in [108] proposed a user-centric algorithm with the aim of maximising energy efficiency in multi-tier networks. A user in the user-centric approach chooses the BSs that provide strong received signal strength as its cooperative BSs. Recently, the authors in [109] applied JT-CoMP in a decoupled control/data architecture with the objective of balancing the load and maximising spectral efficiency. A user selects the n strongest BSs provided that n does not exceed a maximum user-centric clustering size.

Some research has addressed user-centric JT-CoMP clustering and resource allocation jointly. The authors in [110] proposed a two-step joint user-centric clustering and resource scheduling in ultra-dense multi-tier networks. As a first step, game theory is utilised to design a load aware clustering algorithm. Based on the clustering results obtained in the first step, graph colouring is employed to allocate resources.

2.5 Summary

This chapter has briefly discussed the background information that is useful for the work in this thesis. Some important history of research and development in producing HAPs has been presented to show how this technology has grown and that there is now a serious interest in seeing HAPs actually being deployed for many purposes including communication services. For the coexistence part, management of interference in order for two system to coexist has clearly been a main concern, given the breadth and depth of work in the literature. In the author's opinion, a good and efficient beam-pointing technique from HAPs is needed. It is mentioned in the literature that HAPs are limited in power, so a pointing technique that requires high processing complexity and power should be avoided

To provide total coverage, the separation distance between the cells should be minimised so that a contiguous cell layout could be achieved. In order to mitigate the rising inter-cell interference due to close proximity, or even overlap between the cells, the interference mitigation techniques such as CoMP could be considered. Based on the literature, despite providing an increase in CINR levels, resources will be more limited due to the bandwidth reservation for the overlapping regions. A proper resource allocation strategy or how to provide balance between improving CINR and a loss of resources should be studied.

In the background study above, no research has been done that considers exploiting the architecture that is regarded as one of the key features for 5G technology, which is the C-RAN based system for HAPs. One of C-RAN features is the dynamic configuration of RRU and CU/DU

which can potentially solve the lack of energy on the aerial platform. All of these will be covered in Chapter 6 of this thesis.

CHAPTER 3

3. System Modelling and Performance Evaluation

Contents

3.1 Introduction

In this chapter, the specifications that were used to model all parts of the system such as the traffic, antenna, propagation, and channel capacity model are explained in detail. All the parameters used to present the results of the simulation are also explained. This is to make sure that the system is modelled to a standard where the results can be verified and recognized by fellow researchers and industry. Firstly, the simulation tools used for this work are discussed, followed by the parameters used, and lastly the methodology for modelling the simulation is introduced.

3.2 Simulation Software

As simulation plays a significant role in creating solutions in various disciplines, many simulation tools such as C/C++, OPNET, and MATLAB are capable of modelling wireless communication. Each of them has their own advantages and disadvantages. The simulation environment used to build up the network model in this thesis is MATLAB. It is suitable for modelling wireless communication systems because it offers robust numerical computing, powerful tools for graphics in two and three dimensions, advanced matrix manipulation capability, and is widely used. There are hundreds of predefined commands and functions and can be further enlarged by user-defined functions and also powerful commands for solving linear systems with one single command, and for performing advanced matrix manipulations [39].

3.3 HAP System Architecture

In this work, we consider a planar phased array antenna as part of the remote radio unit (RRU) on the HAPs, which is capable of deploying multiple beams at a time, while also pointing and steering beams anywhere in the service area. The approach taken for the antenna array is to have each beam form a cell to provide a wireless communication service to a group of users. Overall, from the access protocol perspective, the architecture behaves almost identically to a traditional terrestrial network. The configuration of this new architecture mirrors the traditional configuration, hence many aspects such as mobility will be handled in the same way as in a terrestrial system. To realise such an approach, the HAP architecture is proposed as in Figure 3-1. The limitation of power on HAPs is one of the reasons why we choose not to put the whole physical eNodeBs on the platform which will be discussed in more details in Chapter 4 and 5. Later in Chapter 6 the limitation of power on HAP will be dealt differently from Chapter 4 and 5 by adapting the C-RAN based system. One of the key functions in the phased array controller is the function that maps each of the beams to the virtual eNodeBs so that each beam can be treated as a cell.

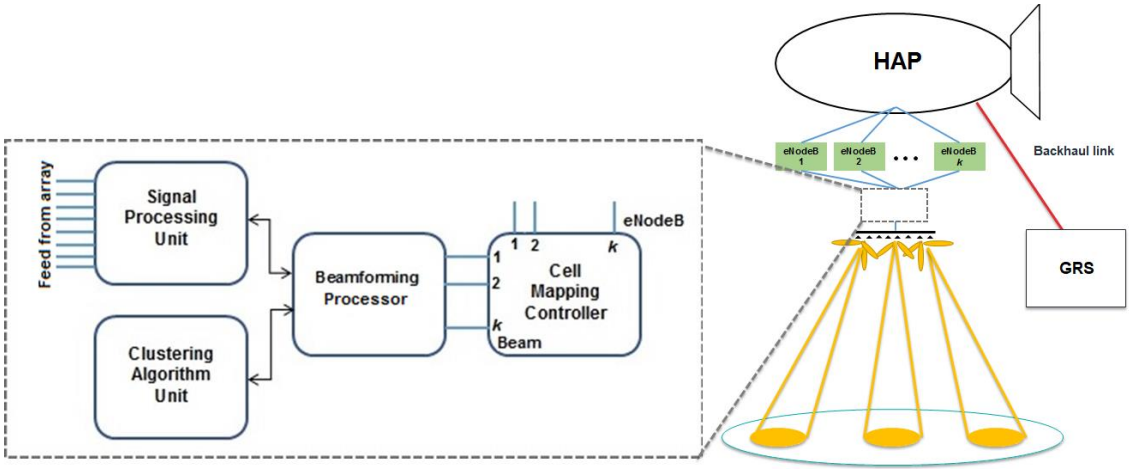

Figure 3-1 HAP system architecture with phased array antenna and phased array controller.

The phased array controller acts as the entity to control and connect the antenna array beams with the virtual E-UTRAN Node Bs (eNodeBs). The controller consists of a signal processing unit which connects directly to the antenna array. This unit is responsible for setting the weights of the individual antenna elements in order to perform beamforming. The second unit is the Beamforming Processor. This processor acts as the central unit where information about the HAP beams and associated user information (e.g. CINR levels) are collected, processed and forwarded to all connected units. The third unit is the Clustering Unit, which in this work adopts the K-means clustering algorithm. It clusters the users in order to optimise the beam pointing location. This information is passed to the Beamforming Processor. The generated beams will be mapped onto the virtual eNodeBs using the Cell Mapping Controller, which manages the feed from the beamforming processor. Using virtual eNodeBs to manage the individual beams as cells provides equivalence to the traditional terrestrial system cell approach, enabling easy integration with existing (including hybrid) systems. Co-location of (virtual) eNodeBs and operation with the same HAP antenna array provides for tight clock synchronization and phase alignment which greatly assists with applications like CoMP and also facilitates handover. Alternatively, a HAP system could have completely centralized processing, where all beams are managed by a single eNodeB, as seen in massive MIMO applications. However, given number of potential beams (delivering fully functional cells) that can be provided by a HAP system and the resulting

capacity, this multiple eNodeB approach with separation of beamforming from higher level functions is much more scalable.

3.4 Performance Metrics

The following sections describe the key parameters used in evaluating the system performance in this work. Some of the parameters are widely used as indicators for performance evaluation in this field of research work.

3.4.1 Link Quality Measurement

To identify the link quality, we measure the signal and interference experienced by the users in the system for downlink transmission by using parameters that are established and widely used. Based on the scenario in Figure 1-1 in Chapter 1, we use Carrier to Noise Ratio (CNR), Carrier to Interference plus Noise Ratio (CINR) and Interference to Noise Ratio (INR). To measure CNR, CINR and INR, we must first measure the received power level of a user. The received power level, P_R at the user device can be measured as follows:

$$P_R = \frac{(P_T.G_T.G_R)}{P_L} \tag{3.1}$$

$$CNR = \frac{P_R}{P_N} \tag{3.2}$$

$$CINR = \frac{P_R}{P_N + \sum P_I} \tag{3.3}$$

$$INR = \frac{\sum P_I}{P_N} \tag{3.4}$$

where P_T is the transmit power emitted by the transmitter located at the HAP, G_T is the antenna of the transmitter antenna of the HAP, G_R is the receiver antenna gain, and P_L is the path loss which will be explained later in (3.9, 3.10).While P_N is the noise power and $\sum P_I$ is the summation of the interference power from the neighbouring cells. CNR is measured by taking the ratio of the

signal of the associated cell received by a user, and the noise power. Most of the time, CNR is used as a threshold in forming a cell for both HAP and terrestrial system with the value of at least 9 dB according to the requirements of the GSM standard [111]. While CINR is measured based on the ratio of the signal of the associate cell received by a user, and the total interference by the neighbouring cells plus the noise power. Lastly, INR is measure of the ratio of the sum of the total interference to the noise power. As for the measurement for uplink transmission, the same equation 3.2, 3.3, and 3.4 will be used except for it will be measure at the array antenna on HAP (for scenario as Figure 1.1).

3.4.2 Channel Capacity Measurement

In a wireless communication network, the channel link quality can be determined by the level of CNR or CINR. In practice, each link has a maximum CINR or CNR that actually can be used for a device or user equipment which gives rise to a high rate modulation scheme such as 64 QAM and 256 QAM. To determine the data rate of the channel, given that CNR/CINR is calculated, a Truncated Shannon Bound [112] is used in this work. The data rate of a link can be compute using the equation from the model as follows:

$$C = \begin{cases} 0\ , & CINR_{dB} < CINR_{\ min} \\ \alpha\ B_c\ log_2(1 + CINR), & CINR_{\ min} \leq\ CINR_{dB} \leq CINR_{\ max} \\ \alpha\ B_c\ log_2(1 + CINR_{\ max}), & CINR_{dB} > CINR_{\ max} \end{cases} \quad (3.5)$$

where α is the attenuation that was set to 0.65, B_c is the bandwidth per channel. $CINR_{\ min}$ is set to 1.8 dB which is the minimum CINR threshold for the system, and $CINR_{\ max}$ is set as 22 dB, which is the maximum CINR set by the Truncated Shannon Bound.

3.5 System Specification Models

In this section, the main system models used are briefly described which meet the requirements of the system design.

3.5.1 Antenna Models

Two different antenna models considered, as two types of base station are considered: the high altitude platform (HAP) and the macro base stations. For a macro base station, the 3GPP has suggested an antenna profile for each sector of the macro base station, while HAPs require a phased array antenna to cope with the dynamic configuration of the HAP beams.

A. Phased Array Antenna Model

A phased array antenna is a flexible solution for a beam deployment capability allowing the HAP to electronically steer its beam anywhere within a service area. It consists of multiple antenna elements forming a composite antenna which can form a very narrow beam.

A phased array antenna (also known as a smart antenna) needs to configure the element weights to perform beamforming in a specific direction. It is achieved by emitting a copy of the same signal from closely spaced antenna elements, but with slightly different delays and phases. By doing so, such signals from every element are added up in phase and amplified in the desirable direction, while cancelling each other out in every other direction when combined together. In this work, a 25 × 25 element phased array antenna is used, with elements spaced λ/2 apart where λ is the wavelength of the carrier frequency.

The array factor, $G_{AF}(\alpha_{XZ}, \alpha_{YZ})$ for a uniform rectangular phased array with λ/2 spacing can be calculated by treating the 2D phased array problem as two separate linear phased arrays along the X and Y axis and multiply them together to get the G_{AF}. The formulation is as follows:

$$G_{AF}(\alpha_{XZ}, \alpha_{YZ}) = \frac{1}{N}\left|\left(\sum_{n} w_{XZ}[n] \times e^{j(n-1)\pi \sin \alpha_{XZ}}\right) \times \left(\sum_{m} w_{YZ}[m] \times e^{j(m-1)\pi \sin \alpha_{YZ}}\right)\right|^2$$ [4] (3.7)

where $\boldsymbol{w_{XZ}}$ and $\boldsymbol{w_{YZ}}$ are the beamforming coefficients for the linear phased arrays derived in XZ and YZ planes. $\pi \sin \alpha_{XZ/YZ}$ is the fixed phase lag increments due to the element spacing.

This antenna element spacing is commonly used in phased array antenna design to achieve a smooth antenna pattern without grating lobes. The size of the cell formed by the beam and also the inter-cell interference, directly correspond to the width of the main lobe and the attenuation of the sidelobes respectively. These features can be manipulated by using a windowing function which in this work is the Blackman-Harris window, which dramatically compresses the sidelobe levels to approximately -90 dB of peak gain but at the same time causes the main lobe to increase in width. The Blackman-Harris windowing function can be described as follows:

$$w(n) = 0.36 - 0.48Cos\frac{2\pi n}{N} + 0.14Cos\frac{4\pi n}{N} - 0.01Cos\frac{6\pi n}{N}, 0 \leq n \leq N-1 \text{[4]} \quad (3.8)$$

where *N* are uniformly spaced samples and are assumed to be even numbers.

A two-dimensional phased array is required in order to create and steer narrow beams in the users' direction on the ground as seen in Figure 3-2. The direction of the beamforming can be determined based on the angles in XZ and YZ planes; vertical orthogonal planes aligned with the length and width of the array antenna mounted on the HAP

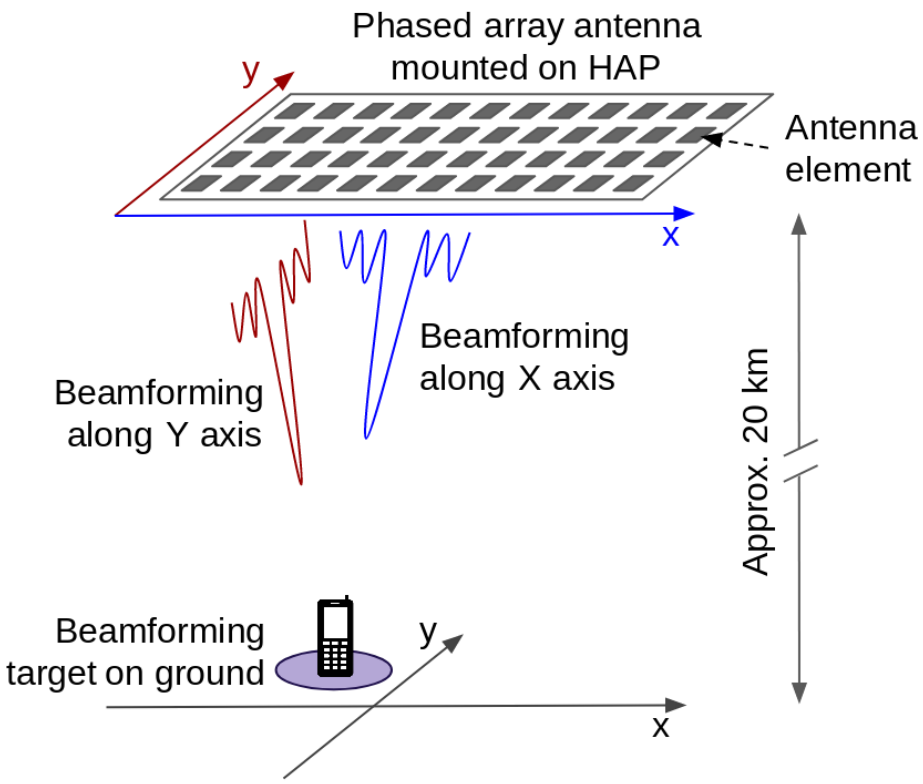

Figure 3-2 Horizontally orientated rectangular phased array antenna mounted on a HAP forming a beam to a target location [4].

Figure 3-3 shows a beamforming example that was designed to point a beam in the direction of the target location at (3, 5) km, aligned with the X and Y axis of the phased array antenna. It is performed on a 20 km altitude HAP equipped with a 25 × 25 element array, using the Blackman-Harris window function.

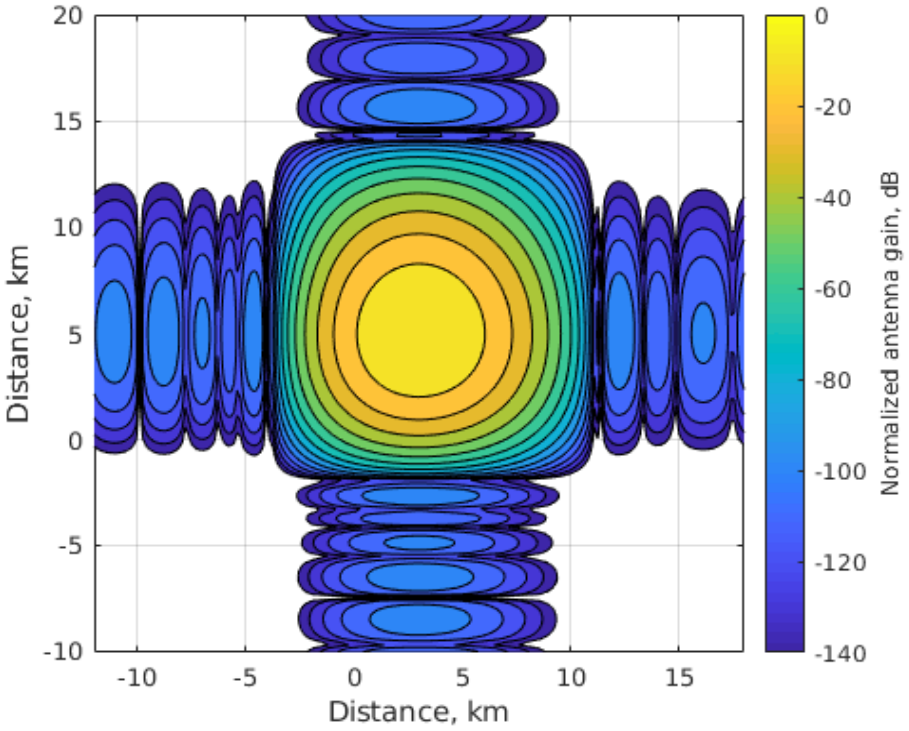

Figure 3-3 Ground projection of the antenna gain pattern at the target location of (3,5) with a 25 × 25 elements antenna array with Blackman-Harris windowing and λ/2 element spacing [4, 113].

B. Three-sector Antenna Model

The macro base station requires a three-sector antenna profile because of the division of the macro cell into three sectors in order to increase the capacity of the cell. Each sector will have full access to the resource block groups which means a frequency reuse of 1 is available, with resources assignment taking interference from neighbouring cells and sectors into account. However, a fractional frequency reuse could be an answer to the co-channel interference which involve in reserving a specific frequency at the cell-edge. It can be done with inter-cell interference coordination (ICIC) or coordinated multipoint (CoMP), and more details will be discussed in Chapter 5. A directional antenna is needed to properly divide the sector to minimize the co-channel interference. Therefore, there is a standard from technical report [114] for a three sector antenna as seen as follows:

$$A(\theta) = -\min\left[12\left(\frac{\theta}{\theta_{3dB}}\right)^2, A_m\right] \quad (3.8)$$

θ is the elevation angle between the user position and the macro base station, θ_{3dB} is the 3dB beamwidth in degrees, and Am is the maximum attenuation which in this case also described as the sidelobe floor. For a 3dB beamwidth of 70 degrees, the gain at boresight is 14 dBi. The three sector antenna is plotted in Figure 3-4.

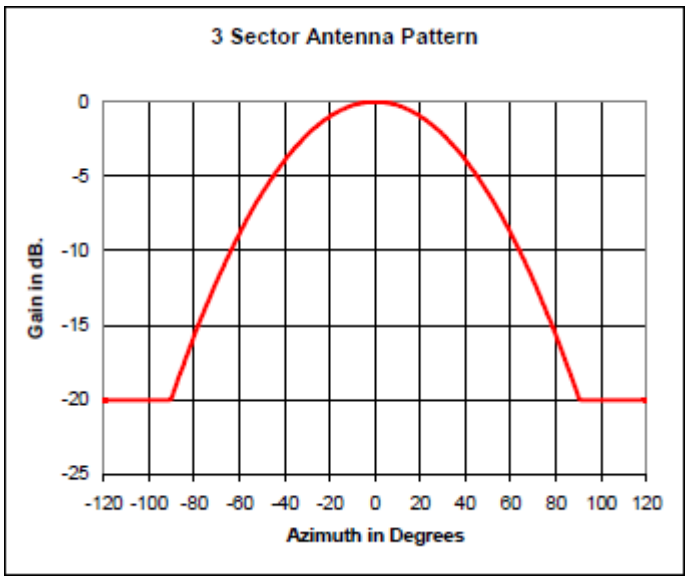

Figure 3-4 Normalised antenna pattern for three sector cell (directly taken from [114]).

3.5.2 Propagation Models

Signals transmitted over a wireless network link will be attenuated due to a number of factors such as natural phenomenon and man-made constructions. The factors can be categorized as path loss which attenuates the signal over the distance, shadowing loss which is due to phenomena like reflections and diffraction that result mostly from man-made constructions, and multipath fading. In this work, only the path loss and shadowing loss are considered, while the multipath fading is neglected in the propagation model for a long term performance such as clustering and we are not looking at specifically exploiting multipath fading in optimisation for different multiple input multiple output (MIMO) techniques.

A HAP is considered to have a higher chance in achieving line of sight connectivity due to its high elevation angle, thus the free space path loss (FSPL) is used to define the signal attenuation for HAP in this work. There are no models tested in a real life HAP scenarios yet so no propagation models for HAP can be claimed as perfectly accurate. The FSPL can be defined as follows:

$$FSPL_{dB} = 20\log_{10}(d) + 20\log_{10}(f) + 92.45 \quad (3.9)$$

where carrier frequency, f and the separation distance between transmitter and receiver, d is measured in GHz and km respectively.

While for the terrestrial part of the system, the propagation model considered has been selected from the 3GPP standard. This model is exclusively for the macro cell and applicable for a test scenario in urban and suburban areas [115]. The model can be expressed mathematically as follows (in dB):

$$Pl_{dB} = 40(1 - 4 \times 10^{-3}h)\log_{10}(d) - 18\log_{10}(h) + 21\log_{10}(f) + 80\ dB + LogF \quad (3.10)$$

where *h* is the height of the base station antenna above the average rooftop level and it is assumed to be 15 m, *d* is the separation distance between transmitter and receiver in km, and *f* is the carrier frequency in GHz. The *LogF* is log-normal distributed shadowing loss with standard deviation (δ) added together in the path loss calculation. The model is valid for a non-line of sight case and describes a worse case propagation model because it quantifies a large signal attenuation. This path loss model is valid for antenna height, *h* in range between 0 – 50 m and designed mainly for separation distance, *d* from few hundred meters to kilometres and not very accurate for short distances. This model is chosen due to suitability with this work that considers a kilometre unit scale for the all distances.

In comparing the HAP and terrestrial (macro base station) propagation models, they are expected to have different ranges of received power. This is a common problem arising in heterogeneous networks where it could result in load imbalance between the cells. Cells are referred to the

network distributed on the ground bounded by either distance or signal strength (e.g. CNR). The non-compatibility of the received power range is partly caused by the assumptions made by a specific propagation model, and a power control scheme is needed to normalise the relative power difference between the HAP and macro base station. In this work, setting up the cell boundary by using a CNR threshold of 9 dB helps at least to normalise the received power at the cell edge because we only consider the adjacent cells situation. In real life situations, the relative power difference might not exist at all because of the possibility of lack of preciseness on modelling the signal attenuation.

3.5.3 Traffic Model

The communication link is usually occupied by a user device when they need a service such as a file transmission or voice call. It could be dynamically shared with another user from another communication node, and it will remain idle when user is inactive. There are two types of traffic model that are commonly used. 3GPP File Transfer Traffic Model 1 (FTP 1) considers a user pool in which the users have their own unique arrival and departure times generated based on the Poisson distribution. The system will experience different levels of data traffic over time so it is good to see how the system performance with variation of traffic levels is. Alternatively, to model only the worst case scenario of spectrum sharing in the downlink transmission (high traffic), all users that share the same spectrum from other nodes or cells are assumed to be active (unlimited receiving/downloading data) at all times and results are presented as snapshots. Having all the users active means a subject user will receive interference from all the presence cells around the user associated cell. Network is modelled to reach its maximum capacity usage to users to characterise a scenario during network congestion, so with worst case interference scenario it would be easier to study and solve this co-channel interference issues. This adopted model is known as the Full Buffer Traffic Model.

3.6 Summary

In this chapter, the framework to model the system in this thesis has been described in detail. The proposed HAP system architecture was introduced. MATLAB was chosen as the platform to carry out the simulation of this work. The modelling of the system consists of specific models for each part of the simulation such as the propagation and antenna models for both HAP and macro base stations, the traffic model, and channel capacity model. All the performance parameters used to present the results of this work are generally well established and widely used.

CHAPTER 4

4. Antenna Array Beam-pointing Techniques for High Altitude Platforms

Contents

4.1 Overview

The purpose of this chapter is to show how intelligent beamforming strategies can be used to control the coverage and capacity of a HAP system, while providing adequate protection for terrestrial users coexisting in cellular spectrum. HAPs can deploy many beams which can be directed anywhere inside a service area for the purpose of forming cells to provide wireless communication services. Unfortunately, HAP beam deployments can do more harm than good for both HAP users and terrestrial users if the decision of where to deploy the beams does not account for the presence of the terrestrial system. As a solution to this problem, we present an

intelligent beamforming strategy based on RF clustering, which is used to assist the HAP in determining the locations to avoid the terrestrial system, while providing coverage for user groups that are demanding service from the HAP. It is considered as intelligent because it has a decision making, information gathering, and communicating capabilities. The contributions of this work are the development of novel intelligence-based beamforming approaches based on an RF clustering algorithm to achieve effective and dynamic coexistence with the terrestrial system.

In [116, 117], two clustering schemes were invented for the purpose of selecting the cluster heads to form clusters. One of the schemes selects the cluster heads based on the highest accumulation of received signal strength indicator (RSSI), received from neighbouring nodes. The nodes will compete with each other to be the first to achieve a threshold of the accumulated RSSI value, hence becoming the cluster heads. The RSSI sensing allows the nodes to learn about its positioning significance. The accumulation of RSSI method is the inspiration of the RF clustering scheme that is proposed in this chapter.

K-means clustering is an established data mining method to cluster sets of data, based on the mean value of the data sets that are associated with the formed cluster. In the ABSOLUTE project [118], a K-means clustering algorithm was used to determine the information that was exchanged between eNodeBs and also to discover the groups of users that frequently use the Virtual Resource Blocks (VRBs) of the system. The system was employed on an aerial eNodeB.

4.2 Coexistence Controlling Parameter

There are two types of coexistence to be considered during the beam-pointing process in this chapter: the coexistence between HAP cells and the coexistence between a terrestrial macro cell and HAP cells. CINR and INR levels of the UEs are used as the parameters to control both coexistence scenarios respectively. Both INR and CINR thresholds are implemented so that the two systems (HAP and terrestrial) and intra HAP cells can coexist without heavily degrading the performance of the users in each of the cells because of interference. Effective coexistence is achievable through controlling the separation distance or the level of overlapping between the cells by measuring the signal quality (INR or CINR) of the affected users of a particular cell. Both thresholds are considered as **TWO** constraints in the beam-pointing techniques which are essential in this work. Note that all the pointing techniques in this work will need to satisfy these **TWO** constraints. The controlling parameters can be illustrated as follows:

4.2.1 CINR Threshold

CINR is used to control the separation distance as well as the level of overlap between HAP cells. CINR levels are used as the threshold because it is the right medium to make sure the users in surrounding cells would not be affected by the newly deployed cell. The cell-edge users who are most affected by the inter-cell interference (as they receive the weakest signal from their associated cell and at the same time receive the strongest interference signal from a neighbouring cell) can also be guaranteed a certain quality link by using CINR as a coexistence threshold. A cell-edge user who is closest to the newly deployed cell is used as benchmark, where its CINR level is compared to the CINR threshold as seen in Figure 4-1. A CINR threshold equal to 0 dB occurs where the cells meet at a tangent point. Further decreasing the threshold will result in overlap between the cells.

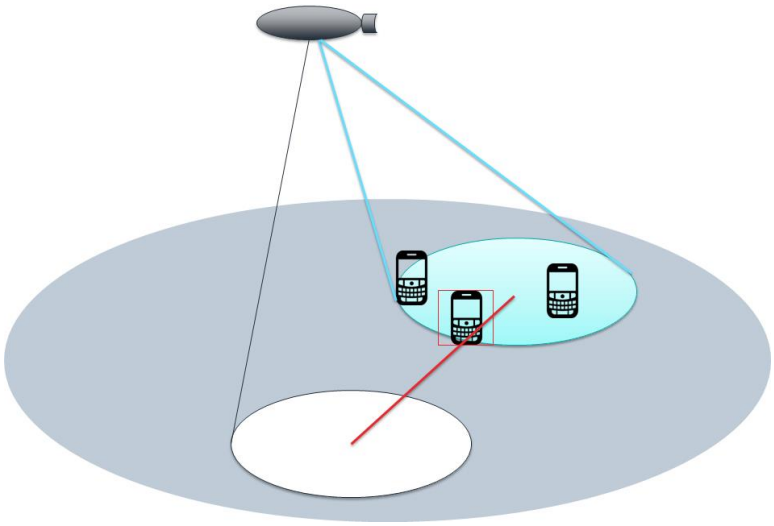

Figure 4-1 Identifying the closest HAP UE which is on the red line of an established HAP cell (blue oval) to the newly deployed cell (white oval) for the use of CINR threshold.

4.2.2 INR Threshold

Minimising the impact of interference for the terrestrial users will be the second part of the coexistence. Effective coexistence of HAP and terrestrial users can also be achieved by keeping an appropriate separation distance between the HAP cells and terrestrial macro cell. INR levels of a terrestrial user will be measured to keep the interference at an appropriate level. The INR level is a good parameter to be considered as in some cases regulations are applied to protect the primary system, similar to this scenario where the terrestrial system is considered as being the primary. The regulations normally set a strict maximum power boundary by the secondary systems (interference) sharing the same spectrum, so INR levels are the most appropriate parameter to monitor and control interference power. For example, in ITU-R Recommendation F.758-6 [119], the criteria for sharing between fixed wireless systems was issued where it is stated for a system sharing with more than one primary service with a frequency range between 30 MHz to 3 GHz the INR threshold should be set at -6 dB. The INR level of a terrestrial user which is closest to the newly deployed HAP cell will be selected as the benchmark as it is geographically most affected by the interference signal as illustrated in Figure 4-2.

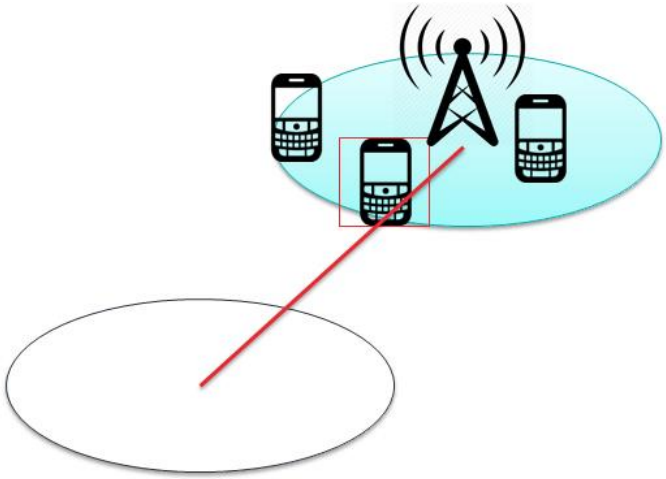

Figure 4-2 How the closest terrestrial UE which is on the red line to the newly deployed cell (white oval) is identified for the use of INR threshold.

4.3 RF Clustering Algorithm

This novel clustering technique adapts the traditional user equipment (UE) and cell association procedure while at the same time it exploits this procedure to perform efficient user clustering to enable more efficient cell formation. The aim of this process is to make more efficient use of the scarce resources on the HAP system, such as the available power and possible capacity available. This will help high altitude platform (HAP) systems to better provide coverage and capacity to those areas most densely occupied by UEs, by providing the best coordinates to point the beams that will form the cells on the ground. Figure 4-3 shows the flow process of how the clustering works. When a HAP is activated or reconfigured in a particular service area, it deploys listening cells (LCs) in a regular hexagonal grid to initiate the clustering process. Each LC will compute how many UEs are associated with it, e.g. based on (aggregate) received carrier to noise ratio (CNR) or through use of association control messages described in detail below. The service cells (red hexagonal cells) are activated if there is a sufficient number of UEs in the LC while the others are turned off.

In Figure 4-4, the flow chart of the RF clustering approach is presented. First, the phased array antenna will deploy the listening cells (LCs) over the service area based on a regular hexagonal grid. This is to make sure the LCs will cover the entire service area. Then the UEs will

associate with the closest/strongest signal LC around them (refer to Figure 4-5 for more details of this process). Each LC calculates how many UEs are associated with each of them and clusters the UEs together. The UE association is counted based on a counter function using the CNR of individual association messages as follows:

ALGORITHM I: UE ASSOCIATION COUNTER

```
I.    Counter(1:k) = 0;
II.   i = 1;
III.  While ( i < k )
IV.   {
V.    For j = 1:1:( no. of UE )
VI.   {
            If ( index of max CNR(j,:) is i & CNR(j,i) ≥ 9 dB
            )
                  Counter (i) ++;
            End
VII.  }
VIII. End
IX.   i++
X.    }
XI.   End
```

where k is the number of LCs, and Counter is a vector of the number of UEs associated with each LC.

At this stage all the LCs have the information on how many UEs are clustered in their coverage area. They then check to see if they meet the requirement to activate a service cell (e.g. no. of UEs in cell ≥ minimum no. of UEs required per cell) – the center of the LCs then become the new beam-pointing coordinates. The requirement to activate service cells can be different depending on the specific requirement from the telecommunication operators. For example, a minimum user per cell requirement or priority based requirement (cell with highest number of users will activate first). This process will therefore help maximise the number of users served within the service area, when power constrained.

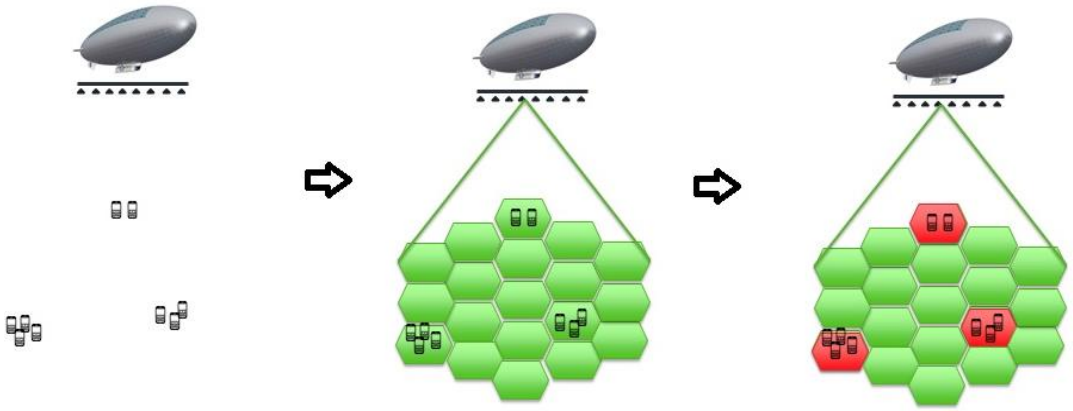

Figure 4-3 Graphical illustration of the RF clustering flow process.

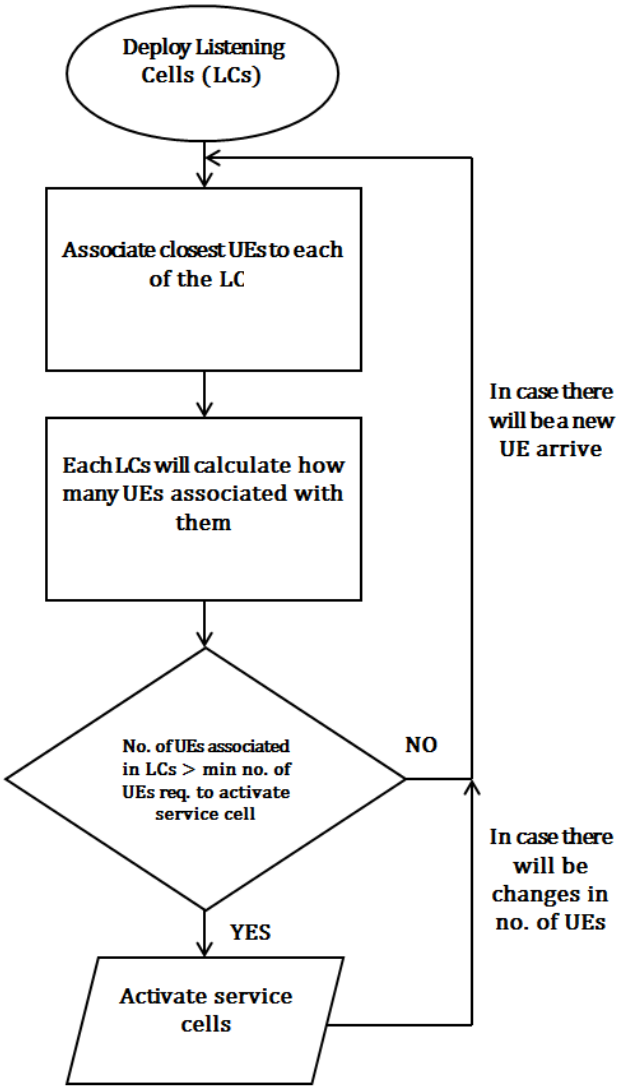

Figure 4-4 Flow chart of the RF clustering.

Figure 4-5 shows the interaction and control message exchanges between a UE and a LC during the association process. LCs will broadcast a beacon signal so that the UEs can associate with a LC. A UE will first identify which LC is the closest to it by determining which LC provides the highest received power level (Pr). Then the UE will send a request for connection to the LC with the strongest Pr. The LC will check the CNR level of the requesting UE to see if its CNR is at least 9 dB. This threshold will form the cluster and later help form the cell boundary. If the CNR is sufficient, then it will accept the request to associate and send a successful acknowledgement message. The UEs in a LC are then clustered together by connecting to the same LC, with each LC knowing precisely the number of UEs in its cluster.

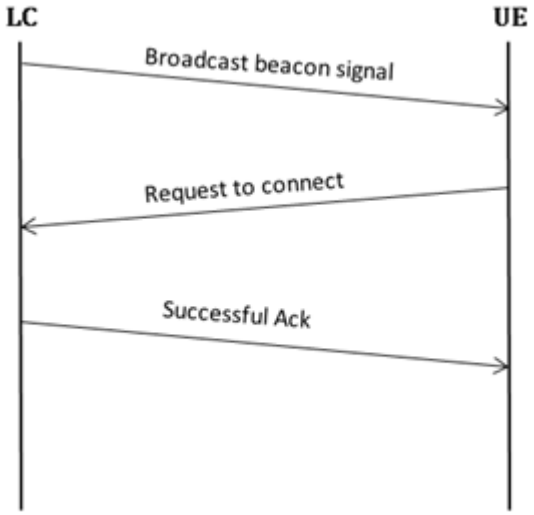

Figure 4-5 Process of UE association to the nearest/strongest signal LC. Note that this process happens to all LCs with all users in the service area.

The Phased Array Controller is part of the remote radio head (RRH) which will handle all the processing of the data coming in and out from the array antenna. Specifically, the Clustering Unit consists of two different sub-units which are the RF Clustering Unit and K-means Algorithm Unit as illustrated as sub-system block diagram in Figure 4-6. The RF Clustering Unit will receive information such as the UEs' CNR levels, and it will also process connection requests. The RF Clustering Unit will pass on the information about the LC that are activated as service cells and

also the UEs that are clustered in the LC. Alternatively, if the successful LC is to have its location further optimised, the RF Clustering Unit will pass the coordinates to K-means Algorithm Unit. The K-means Algorithm Unit will optimise the beam pointing coordinates as described in detail in the next section.

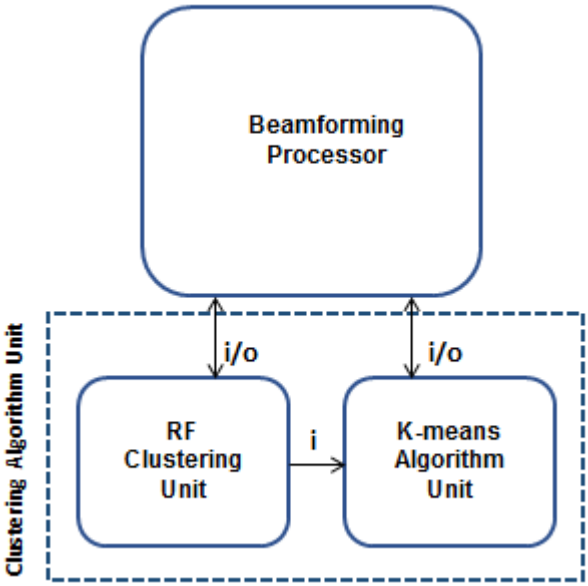

Figure 4-6 Apparatus to implement RF and RF + K-means clustering algorithm.

4.4 K-Means Clustering Algorithm

K-means clustering is an optimisation algorithm that is used to move the initial centroid based on the mean value of the associated user position. Here users are associated with formed clusters based on their CNR levels instead of distance. The CNR levels of users based on all the centroids available will be calculated and the centroid that gives the highest CNR value and a value higher than the CNR threshold will have that user associated with its cluster. If none of the CNR values pass the CNR threshold, it will not be part of any cluster. The steps for this algorithm are as follows:

ALGORITHM II: K-MEANS CLUSTERING

I. Decide how many clusters (k) the system will operate with, which correspond to the number of HAP beams.
II. Generate k centroids randomly within the X km radius service area.
III. Check that the generated centroid points meet the TWO constraints. If not, repeat step ii.
IV. Assign users to the cluster delivering the highest CNR level passing the CNR threshold requirement.
V. Recalculate the position of the centroids based on the mean values of the associated users' position that is known at the HAP following information exchange as shown in Figure 4-8.
VI. Repeat steps 4 and 5 until the centroid position is exactly the same as in the previous cycle.

In Figure 4-7 below, the flowchart of K-means clustering is illustrated to help in understanding the flow of the algorithm.

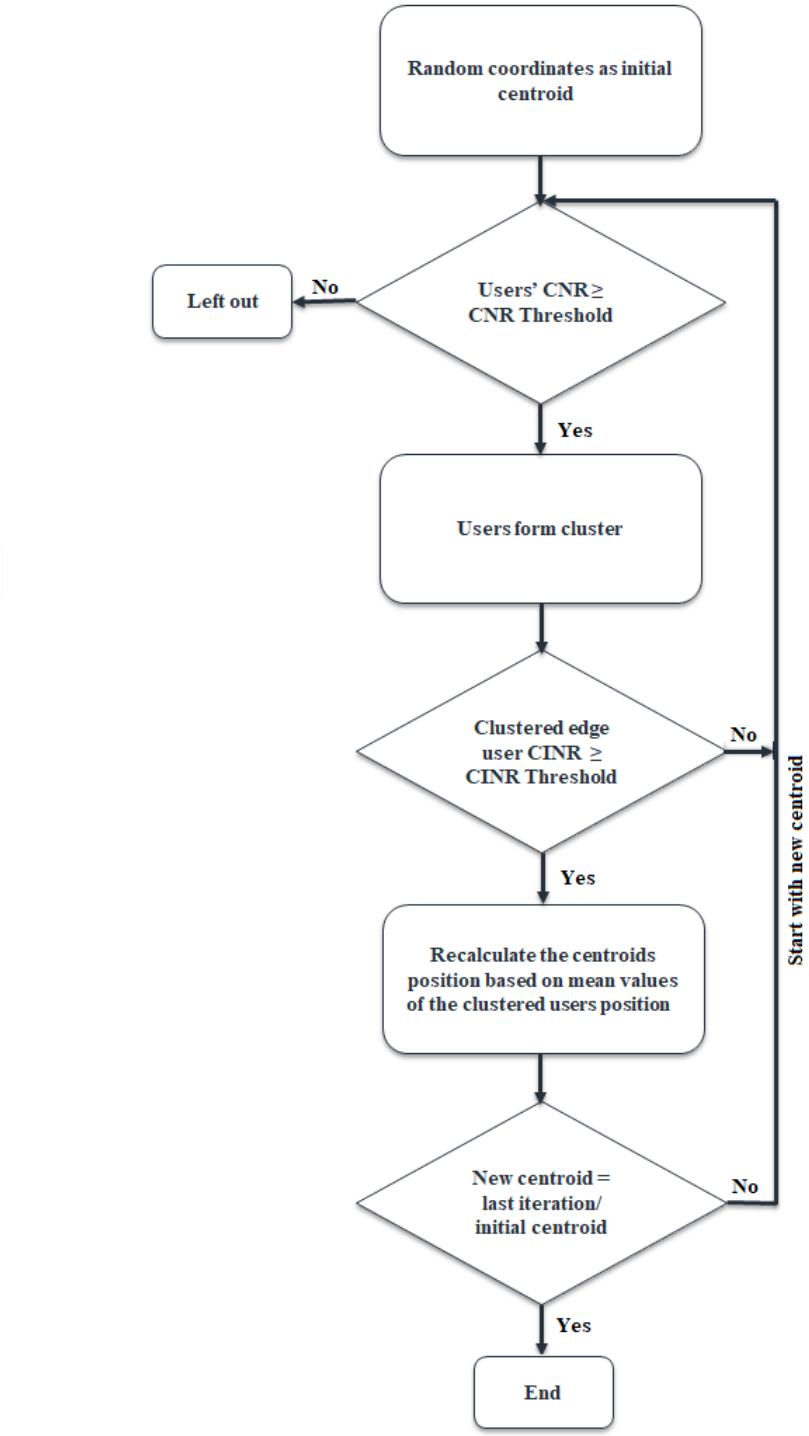

Figure 4-7 Steps of how K-means algorithm is performed in every iteration until it obtains the optimised centroid.

4.4.1 K-Means Algorithm as Further Optimisation for RF Clustering

In this work, two different implementations of a K-Means clustering algorithm are considered. The first implementation uses random points as the initial centroids. The second implementation uses the LC coordinates as initial centroids and to further optimise the coordinates obtained by the RF clustering scheme. After a LC passes the requirement to activate as a service cell, the LC will be activated to begin wireless communication service. Alternatively, the location of the center of the successful LC can be optimised before deploying a service cell. The same steps are still applicable as in Figure 4-5, apart from the fact that its initial centroids are obtained from the successful LC coordinates.

To reach the optimum coordinate for the beam-pointing location, the centroid will use the successful LC coordinate and form a temporary cell and it will go through the same interactions and signals exchange with UE as shown for RF clustering. For the K-means algorithm to work, the specific location is needed at the Clustering Unit, and the exchange process shown in Figure 4-8 below is used to obtain this.

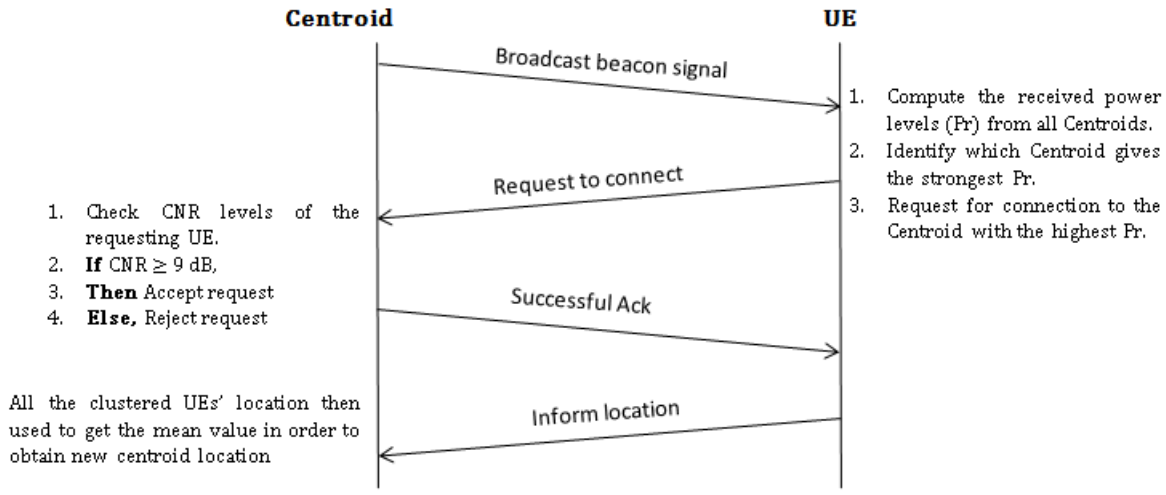

Figure 4-8 The information exchange between the temporary cell and a UE during the optimisation process.

In every iteration, checking the CINR levels of the user at the cluster edge closest to the interfering cells (neighbour cells) is essential to control the level of overlap between the HAP cells. Practically with this optimisation, the service cells are shifted from the original hexagonal grid. The graphical illustration of this process can be seen in Figure 4-9. This is an example of two iterations of the K-means clustering algorithm. The (K-means) clustering is used to better locate the cells onto the dense areas occupied by UEs (red dots).

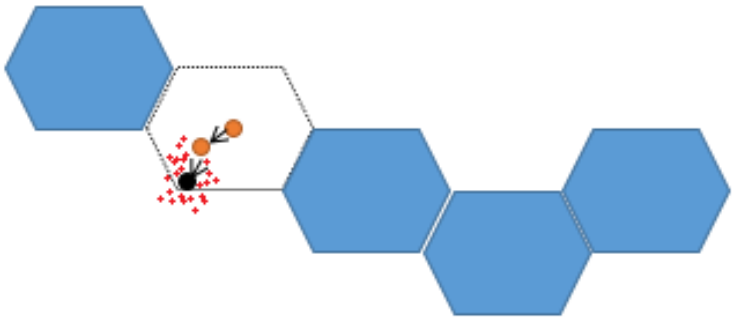

Figure 4-9 Illustration of shifting centroid as two iterations of the K-means algorithm on the center of LC.

4.5 Conventional Pointing Technique

For the purpose of comparing the performance of the newly proposed schemes, two conventional pointing techniques are adopted in this work. These two techniques are random and regular pointing.

4.5.1 Random Pointing

Random pointing is considered as the most basic pointing method, which is directing the HAP beams onto the points that are randomly generated inside the service area as long as they obey the **TWO** constraints. This technique may only be suitable for experimental purposes because pointing the beams randomly without identifying where the user groups are could be a waste of energy.

4.5.2 Regular Pointing

Regular pointing is a beam pointing technique that arranges the HAP beams within 30 km inside the service area. As the number of beams increase, the arrangement forms a ring. When the beams are packed at the edge of the service area, the beams will be arranged closer to the centre of the service area which forms the outer and inner rings of HAP beams. If one of the **TWO** constraints are not met, the beam will be reallocated based on the next order of the arrangement.

4.6 Results and Discussion

All schemes are simulated using the same system layout as discussed in chapter 1 earlier and the parameters are presented in Table 4-1. The number of HAP beams is varied from 2 to 42 to determine the difference in performance of each scheme and the impact the HAP has on the terrestrial users in terms of interference. The purpose in each case is to achieve maximum coverage while focusing on the user's priority in providing service, at the same time providing effective coexistence with the terrestrial system.

Table 4-1 Simulation Parameters

Parameter	**Value**
Macro BS Transmit Power	40 dBm
HAP Transmit Power	40 dBm
Receiver Antenna Gain	0 dBi
HAP Antenna Gain (Boresight)	32 dBi
Three-sector Antenna Gain (Boresight)	14 dBi
Bandwidth per Resource Block Group (RBG)	727 kHz
Carrier Frequency	2.6 GHz
Noise Power	-100 dBm
CNR Threshold	9 dB
CINR Threshold	0.5 dB
INR Threshold	-10 dB
Number of Users	2900

Figure 4-10 shows the median CINR levels of all users across the 30 km radius service area for the downlink. Users will connect to either the HAP or the macro cell base station, based on whichever they receive a stronger signal from (higher CNR levels). From Figure 4-10, it can be seen that the median CINR performance has the same general behaviour for all schemes, as the number of beams is varied from 2 to 42, which decreases the CINR values due to the increasing number of interfering sources. Even though they have the same general behaviour, the more complex schemes are still needed to efficiently deploy the beams. RF based schemes (RF and RF + Kmeans clustering) start well, but as soon as the number of HAP beams increase, the CINR values reduce to the lowest level compared to all other schemes and eventually perform the best at 42 beams. RF clustering is developed to spot high density user groups which should have service priority. This explains the sudden decreases of median CINR when the number of beam increases from 2 to 4 beams. RF clustering still focuses on the high density user groups and directs more beams towards these user groups causing high interference in that region. On the other hand, schemes like K-means clustering will require several scanning iterations depending on the initial placement of centroids to precisely detect the dense user group. Most of the time, with fewer beams, K-means clustering, Random and Regular pointing will have the beams placed at a distance from each other causing lower interference.

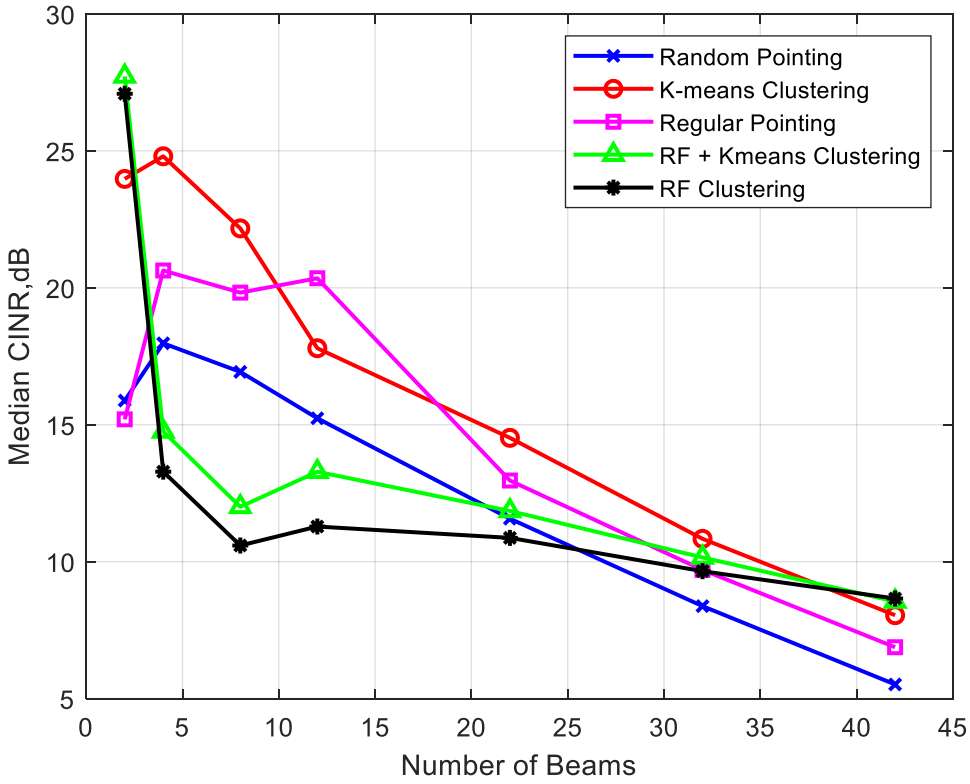

Figure 4-10 Median CINR performance for all schemes.

Figure 4-11 shows the percentage of users covered by the HAP beams for all schemes meaning that those users are served including the terrestrial users. It shows how well the pointing schemes can provide coverage to the service area. Overall, the K-Means clustering scheme covers more with 8 to 32 HAP beams. However, as discussed earlier the RF based schemes focuses more beams on the hotspot region (high density user groups). It is shown more clearly by looking at a lower number of beams, that both the RF based schemes start by covering approximately 42% of the users, but barely cover an additional 5% more users with 4 more HAP beams, while other schemes improve their coverage by at least 10% with additional 4 HAP beams. This happens because even with up to 8 beams, the RF based scheme still cover the denser user group while other schemes already start covering users at different locations. With 42 beams, the RF + Kmeans and K-means clustering managed to cover up to 96% of the users in the service area, meeting the requirements of network operators which often are obliged to cover at least 95% of the population of a specific place or country.

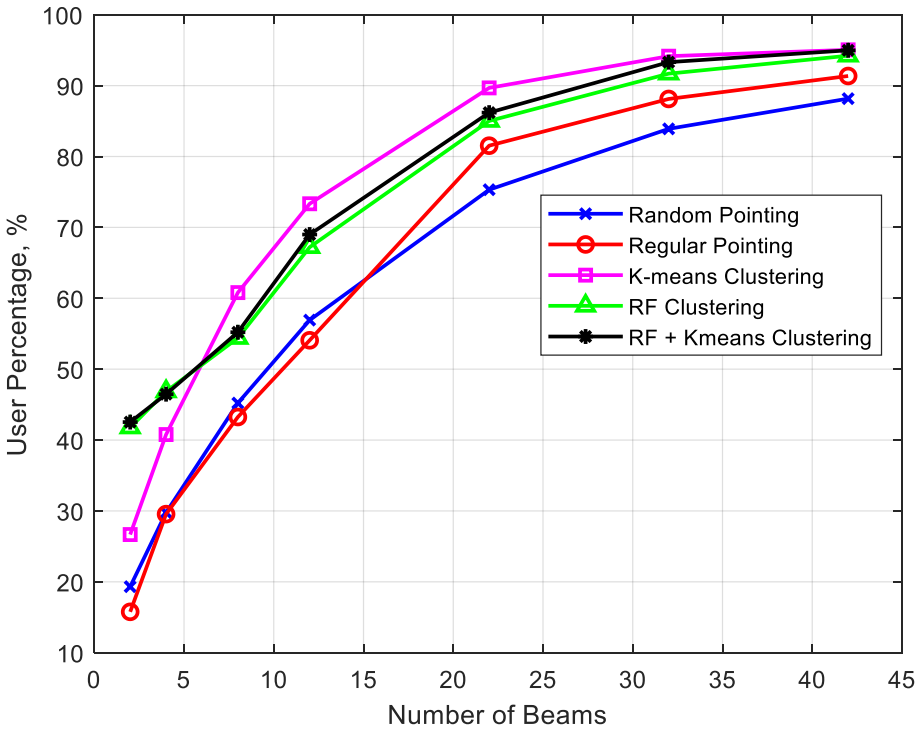

Figure 4-11 User percentage covered for all schemes which indicate the coverage percentage using 25 × 25 elements for the service area.

The percentage of users covered for all the schemes when using a 40 × 40 elements phased array antenna has also being looked at to see if the behaviour of the beam-pointing schemes will still behave the same as 25 × 25 elements phased array scenario especially the K-means and RF clustering scheme. Figure 4-12 shows that the RF based schemes perform better in terms of the user percentage covered than the K-Means clustering scheme for all scenarios with different number of beams. The K-Means clustering scheme performs better with a lower number of elements when a 25 × 25 phased array antenna is used which deploys smaller beam footprint on the ground. With bigger beams, a bigger cluster of users can be achieved, hence it provides an advantage for an algorithm like K-Means to better locate an optimum centroid among the clustered users. As for the RF based schemes, whatever the size of the beams, they are able to precisely locate the dense user group even with lower number of beams.

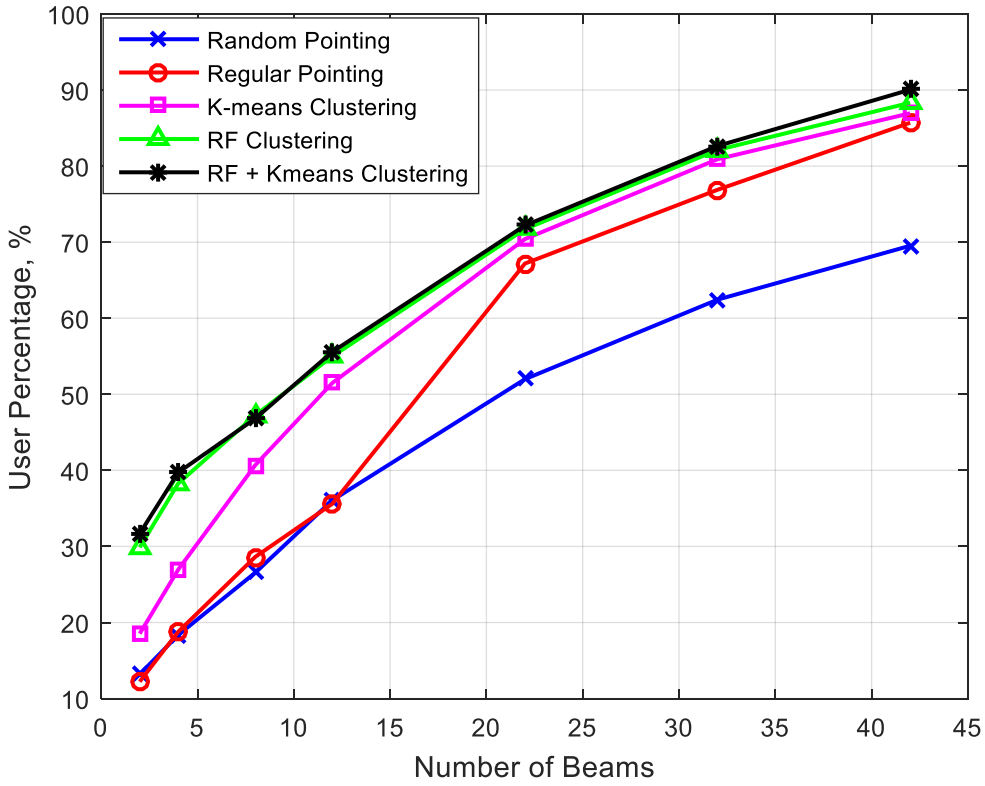

Figure 4-12 User percentage covered for all schemes which indicate the coverage percentage for the service area using 40 × 40 elements phased array antenna.

To further support the statement regarding the user percentage above, the average number of users per beam is presented in Figure 4-13. The overall trend shows that the average number of users per beam decreases as the number of beams increases, but the numerical figures show that the overall number of users supported is significantly increased, with an associated increase in the overall system capacity. With a low number of HAP beams, both RF and RF + K-means clustering serve more users per beam because these schemes are able to find regions of higher user density, so they have a higher probability of covering more users with fewer HAP beams. For Regular Pointing, the average number of users per beam increases up until it reaches 4 HAP beams. This is because of the specific regular pointing strategy used, where the HAP beams initially form an outer ring arrangement, then the inner ring arrangement is used until it reaches the center of the service area. This strategy does not consider the need to locate high density user groups which is similar to the Random Pointing scheme except that the HAP beams are pointed randomly in this latter case.

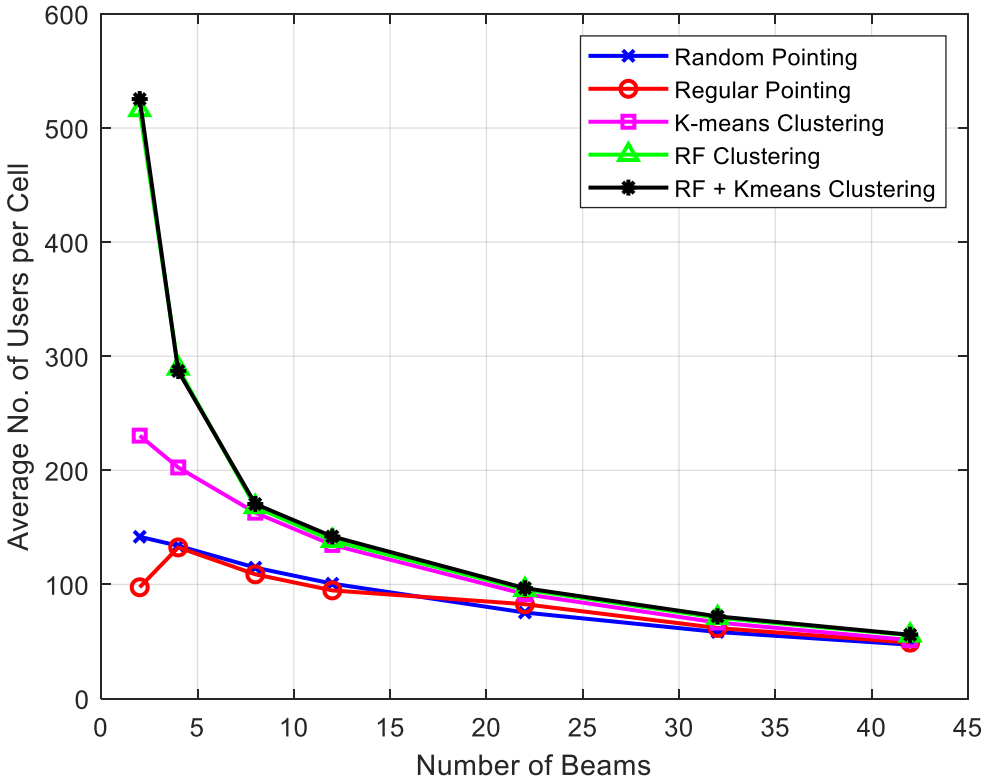

Figure 4-13 Average number of users per beam for all schemes.

For the terrestrial part of the system, the protection of terrestrial users is successful as seen in Figure 4-14. The interference contributed by the HAP system increases as the number of beams is increased. Even with 42 beams deployed, 95 % of the terrestrial users do not experience interference from HAP beams exceeding the given threshold (red line; 10 dB threshold). The implementation of the INR threshold in order to protect the terrestrial users is seen to gain control of the interference level caused by the HAP. This shows that a HAP is able to coexist effectively with the terrestrial system.

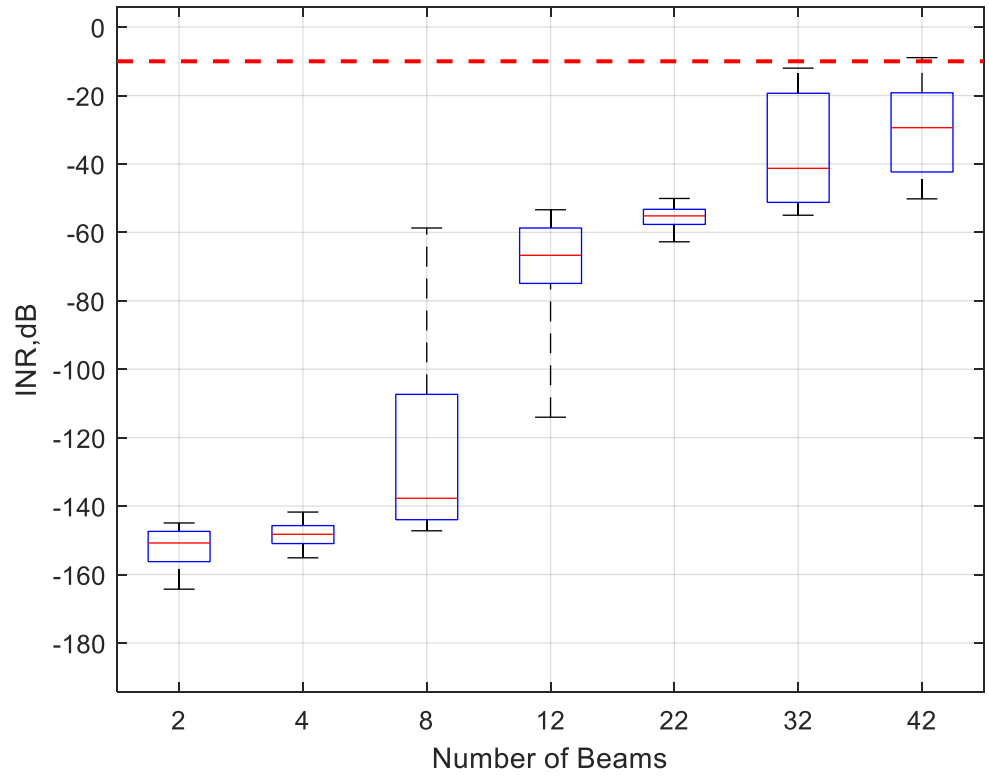

Figure 4-14 Terrestrial INR box plot performance for RF + Kmeans clustering contributed by the HAP with the upper whisker indicates the 5th percentile, red line indicates the median, and lower whisker indicates 95th percentile.

Figure 4-15 (a), (b), (c), (d), (e), and (f) show contour plots of the Random, Regular, RF Clustering, RF + Kmeans Clustering, K-Means (25 × 25), and K-Means (40 × 40) pointing schemes respectively with a 12 HAP beam deployment. The reason why snapshots of a 12 beam deployment are chosen is because with lower the number of beams, it is easier it is to differentiate the behaviour of each scheme, thereby providing further justification to support the earlier discussions. For Random pointing as seen in Figure 4-15 (a), the HAP beams are more distributed. This kind of strategy to point beams is likely to waste resources because no optimisation is made, and the users will be served solely based on luck. In Figure 4-15 (b), we can see that the pattern of a ring is formed from the Regular pointing scheme. As with Random pointing, users will be served based on luck, the only difference is Regular pointing is formed sequentially, rather than being random. Both had no intention to detect high density user groups. Initially based on random points, but with optimisation, this will highlight the chance of detecting high density user groups.

With the K-Means algorithm, the point will move to the centre of a user group with several iterations, which is eventually able to pick up the high density user group if the initial centroid is anywhere near it. In Figure 4-15 (e), it is shown that K-Means algorithm is able to detect the high density user group, but not as well as the RF and RF + Kmeans clustering in Figure 4-15 (c) and (d). For RF clustering, 8 from the total of 12 beams are focused on the high density user group intending to provide higher capacity density for that area. It illustrates the preciseness by which this scheme can spot the high density user group. To further optimise the RF clustering, K-Means algorithm is added to the process by using the output from the RF clustering as the initial centroids. It can be seen in Figure 4-15 (d) that some of the centroids are moved from their original positions (refer Figure 4-15 (c)) in order to provide more coverage. Also, the comparison between different number of elements of 25 × 25 and 40 × 40 can be seen in Figure 4-15 (e) and (f) respectively which both are using K-Means clustering pointing scheme. As discussed earlier, it can be seen from the contour plot of (f) that the beams are much smaller than in (e) and because of that, the precision of detecting high density user group is lower.

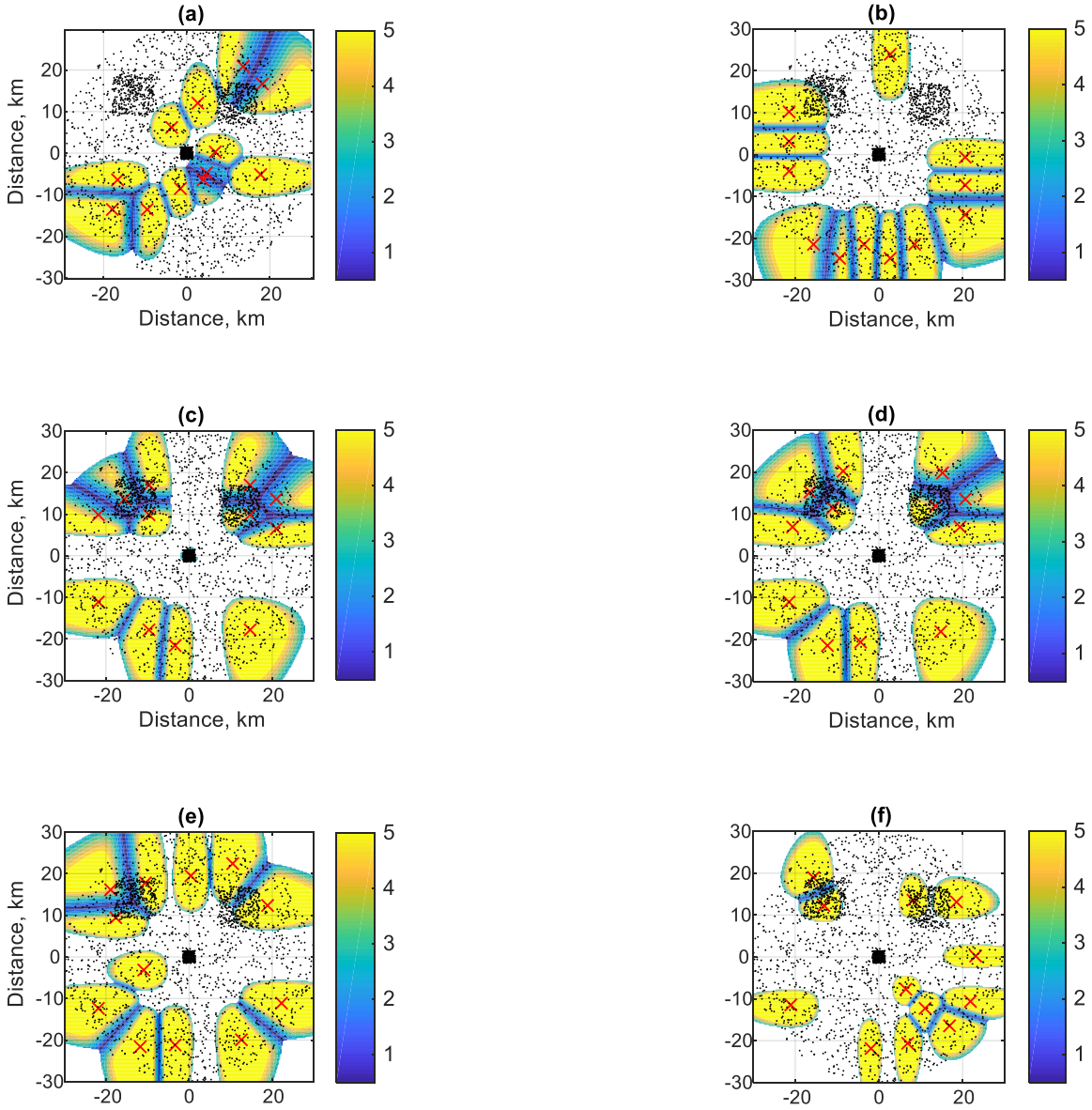

Figure 4-15 Contour plot of (a) Random pointing (b) Regular pointing (c) RF Clustering (d) RF + Kmeans clustering (e) K-Means Clustering 25 × 25 elements and (f) K-Means Clustering 40 × 40 elements schemes with the red 'X' indicate the boresight of the beams, black dot indicate the user distribution, and the colour bar represents the capacity per user in Mbps.

4.7 Summary

This chapter has investigated the coexistence of terrestrial and HAP systems with multiple beams to provide effective coverage of the users in the service area. A new scheme based on the RF clustering and K-means algorithms has been considered and compared with alternative approaches. We have shown that coverage is controlled by varying the number of HAP beams, in which a near maximum coverage of 96% can be achieved. It is achievable with the K-means, and RF + Kmeans clustering schemes with 42 beams while still enabling coexistence with the terrestrial system. It is also shown that the RF based schemes are very effective in locating beams in highly populated areas. The impact of the HAP system on the existing terrestrial system is shown to be minimal, through evaluation of the INR levels experienced by the terrestrial users. The focus here has been to maximise the coverage, without taking the capacity density into consideration. Although the CINR levels are shown to decrease with an increasing number of beams and hence more interference, especially with the RF based schemes, there are interference mitigation techniques can be considered such as coordinated multipoint (CoMP) and inter-cell interference coordination (ICIC) to help mitigate this issue.

CHAPTER 5

5. Exploiting User-Centric Joint Transmission – Coordinated Multipoint with a High Altitude Platform System Architecture

Contents

5.1 Overview

The purpose of this chapter is to show how joint transmission – coordinated multipoint (JT-CoMP) can be integrated into a HAP system, and how JT-CoMP can increase the capacity of HAP cell-edge users by adapting HAP phased array antenna systems to better integrate with existing approaches to delivering cellular infrastructure. Implementing CoMP is possible because of the newly proposed HAP architecture that was introduced in Chapter 3 which enables the system to treat individual HAP beams as a serving cell which can be managed by virtual eNodeBs.

This provides equivalence to the traditional cell approach adapted by the terrestrial systems, thus providing the capability to perform such functions in a flexible way.

The novelty and contributions of this work are:

- Demonstration of the use of a new HAP system architecture which integrates techniques like JT-CoMP.
- A method to better balance the CINR gain and capacity loss trade-off via a new bandwidth allocation technique.
- A new flexible CINR threshold that better selects users who will benefit from CoMP.

HAPs can deploy multiple beams simultaneously, with each beam reusing the same spectrum, which causes interference between the cells. Typically, the users at the edge of the cell will experience most interference from the neighboring cells due to closer proximity. This factor makes the user CINR levels vulnerable. Due to the interconnected layout of HAP cells, there is a trade-off where users will receive less bandwidth compared to when a system does not use CoMP. To solve this issue, we present four different schemes in order to find the appropriate group of users to be included in the CoMP region.

Notation in the chapter	
$\mathcal{H}$	Set of HAP cells
$\mathcal{U}e_i^{\mathcal{H}}$	Set of active UEs associated with HAP cell
$\mathcal{C}c$	Set of cooperative cells to form JT-CoMP
$\mathcal{N}$	The non-CoMP set
$\mathcal{C}_{2w}$	2 ways CoMP set
$\mathcal{C}_{3w}$	3 ways CoMP set
$\mathcal{U}e_n^{\mathcal{H}}$	Set of non-CoMP UEs associated with BS_m
$\mathcal{U}e_c^{xy}$	Set of 2 ways CoMP UEs associated with $H_x$as the primary and $H_y$as secondary cells
$\mathcal{U}e_c^{xyz}$	Set of 3 ways CoMP UEs associated with $H_x$as the primary, $H_y$as secondary and $H_z$as the third cells
$\mathcal{B}$	Total bandwidth available in the system

5.2 Set Theoretic User Definition

To implement CoMP it is helpful to correctly define the users within the systems especially when the condition of a user or how a user will operate depends on its specific location. A Venn diagram in Figure 5-1 represents the system in general (set S), and the users will be defined using the set theory. Sets A, B, and C represent the HAP cells. The sets are described as follows:

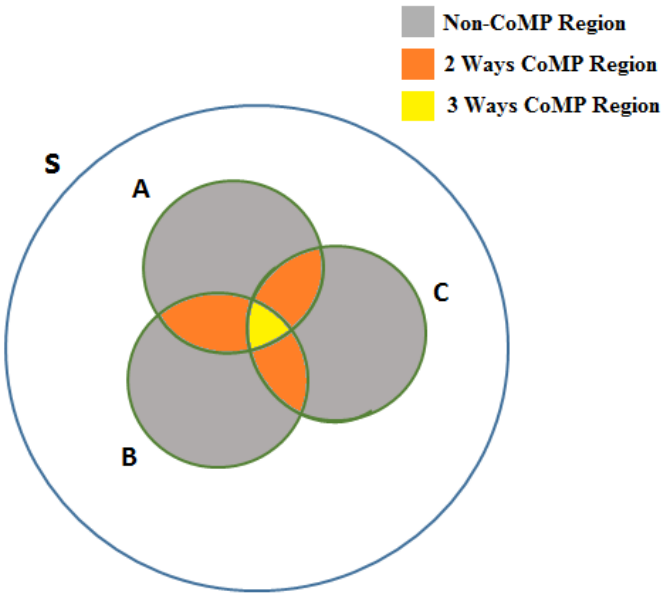

Figure 5-1 Venn diagram representing the service area and overlapping HAP cells.

$$S = \{\mathcal{U}e : \mathcal{U}e \; is \; user \; demanding \; service \;\} \tag{5.1}$$

$$A \cup B \cup C = \{\mathcal{U}e_i | \mathcal{U}e_i \in S, \mathcal{U}e(CNR) \geq 9 \; dB\} \tag{5.2}$$

$\mathcal{U}e$ is a user equipment distributed randomly across the service area and demanding wireless communication service. A $\mathcal{U}e$ demanding service will have to associate with a cell to be served, subject to a certain CNR threshold being met. In the context of set theory, a $\mathcal{U}e$ needs to be included in either set A, B or C meeting the requirement of having at least CNR of 9 dB. A $\mathcal{U}e$ that belongs to either set A, B or C will be included in the system is known as $\mathcal{U}e_i$ as described in (5.2). In the intersection of sets as seen in Figure 5-1 a user suffers from a great deal of interference, which is why CoMP is needed to reduce the interference. When CoMP is applied, the sets are as follows:

$$A \cap B | C \cap A | B \cap C \geq \mathcal{C}_{2w} \tag{5.3}$$

$$\mathcal{C}_{2w} = \{\mathcal{U}e_c | \mathcal{U}e_c \in A \cup B \cup C, \mathcal{U}e_i(CINR) < \gamma\} \tag{5.4}$$

$$A \cap B \cap C \geq \mathcal{C}_{3w} \tag{5.5}$$

$$\mathcal{C}_{3w} = \{\mathcal{U}e_c | \mathcal{U}e_c \in A \cup B \cup C, \mathcal{U}e_c(CINR_c) < \gamma\} \tag{5.6}$$

$$A \ominus B \ominus C < \mathcal{N} \tag{5.7}$$

$$\mathcal{N} = \{\mathcal{U}e_n | \mathcal{U}e_n \in A \cup B \cup C, \mathcal{U}e_i(CINR) \geq \gamma\} \tag{5.8}$$

The intersections of set A and B, or C and A, or B and C as seen in the Venn diagram in Figure 5-1 represent the overlapping regions of the cells and known as the CoMP regions ($\mathcal{C}_{2w}$ and $\mathcal{C}_{3w}$). For the CoMP set, user $\mathcal{U}e_i$ with CINR lower than the CINR threshold γ will be included in the $\mathcal{C}_{2w}$. These users are then defined as $\mathcal{U}e_c$. $\mathcal{U}e_c$, with new $CINR_c$ checked again to see whether it meets the CINR threshold requirement γ. If the $CINR_c$ is still lower than γ, then the user will then be included in the $\mathcal{C}_{3w}$. Meanwhile, the users that belong to set A, B, or C but not their intersections are in $\mathcal{N}$ as shown in Figure 5-1, where $\ominus$ is the symmetric difference or

disjunctive union in (5.7). These users typically have CINR of at least equal to γ and are known as $\mathcal{U}e_n$.

5.3 CoMP User CINR Threshold (γ)

5.3.1 Centralised Threshold

To determine appropriate CoMP users ($\mathcal{U}e_c$) and Non-CoMP users ($\mathcal{U}e_n$), we set a range of CoMP user CINR threshold levels (γ) centrally for all cells involved so that we can differentiate the performance of various sizes of CoMP and non-CoMP sets as illustrated in Figure 5-2. This enables an optimal value of γ to be determined. The set of cooperative cells ($\mathcal{C}c$) that serves the $\mathcal{U}e_c$ in this work is defined as follows:

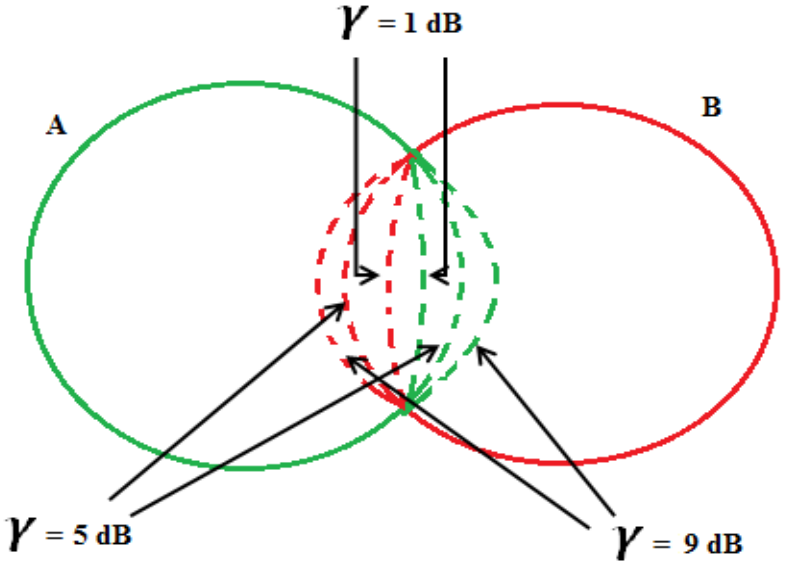

Figure 5-2 .Illustration of the impact of different CINR thresholds in determining the overlapping region.

$$Cc = \begin{cases} \{x_1\} & if\ CINR \geq \gamma \quad (\mathcal{N}) \\ \{x_1, x_2\} & if\ \ CINR < \gamma \quad (\mathcal{C}_{2w}) \\ \{x_1, x_2, x_3\} & if\ CINR_c < \gamma \quad (\mathcal{C}_{3w}) \end{cases} \tag{5.9}$$

where x_1, x_2, x_3 are the cells that provide the strongest, second strongest, and third strongest received power level P_R to a particular user respectively, and γ is the CoMP user CINR threshold.

The initial CINR is measured based on (3.3), to determine whether a user is heavily affected by the interference. $CINR_c$, is a re-measurement of CINR after taking into account nullifying the strongest interference from x_2 and possibly x_3 is then turned into a useful signal. The $CINR_c$ can be defined as follows:

$$CINR_c = \frac{\sum_{j \in \mathcal{C}c} P_{R_j}}{P_N + \sum_{k=|\mathcal{H}|;\, k \notin \mathcal{C}c} P_{I_k}} \quad (5.10)$$

where P_R in this case is the summation of the useful signals based on (3.1). Two signals from x_1 and x_2 will be added for a two way CoMP, and the third signal of x_3 will be added if the user is activated in a three way CoMP. Whilst the rest of the signals not included in $\sum P_R$, are $\sum P_I$, which are the remaining interference powers.

The steps to define a user are as follows:

ALGORITHM I Centralised Threshold

For $Ue_i \in S$,

i. Calculate CINR based on (9).
ii. If CINR > γ, then
iii. $\mathcal{U}e_i = \mathcal{U}e_n$
iv. Else,
v. included in $\mathcal{C}_{2w}$ CoMP region; $\mathcal{U}e_i = \mathcal{U}e_c$
vi. End
vii. Calculate $CINR_c$ based on (21).
viii. If $CINR_c > \gamma$, then
ix. Stays in $\mathcal{C}_{2w}$CoMP region.
x. Else, included in $\mathcal{C}_{3w}$ region; recalculate $CINR_c$.
xi. End

Based on (5.9), a user with CINR less than γ will operate in $\mathcal{C}_{2w}$ mode as $\mathcal{U}e_c$, and will receive signals from both cell x_1 and x_2; otherwise the user will operate in a non-CoMP mode as

$\mathcal{U}e_n$. It is because a user with CINR less than γ is regarded as highly affected by interference and located at the cell edge nearest to the strongest interference source. The $\mathcal{U}e_c$ will have their CINR re-calculated using (5.10) and again checked if the $CINR_c$ is less than γ. Not passing the threshold again will result in an activation of $\mathcal{C}_{3w}$ because of the possible location of the user closer to x_2 and at the same time closer to x_3 which means the interference is still high even after removing the interference and turning it into useful signal of the x_2. The use of CINR of the users to determine whether the particular user is a $\mathcal{U}e_c$ or $\mathcal{U}e_n$ has never been used previously. This method is more straightforward as CINR is more widely used as the threshold to determine whether a user has a minimum quality of link needed to operate in allocated bandwidths.

5.3.2 Flexible Threshold

Implementing a centralised threshold will affect some users in the system as a trade-off to maximise the capacity of the cell-edge users due to the inclusion of the non-beneficiary users in the CoMP set. A non-benefitting user means a user that does not benefit from the implementation of CoMP because their CINR improvement cannot compensate for the reduction in bandwidth needed to deliver CoMP and on the contrary, benefitting users are those that benefit from CoMP. The boundary between benefitting and non-benefitting users varies for each of the cells as it depends on geographical factors of the users associated with each cell, thus the centralised approach cannot be used in solving this matter. So a flexible CoMP user CINR Threshold (γ) is proposed to deal with this unevenness. This flexible threshold means that each of the cells will have their own γ which results from the derived equation below:

$$Capacity, C \leq Capacity_{CoMP}, C_c \quad (5.11)$$

$$B_c \log_2(1 + CINR) \leq kB_c \log_2(1 + CINR_c) \quad (5.12)$$

∴

$$\log_2(1 + CINR) \leq k\log_2(1 + CINR_c) \quad (5.13)$$

where *k* represents the fractional value of the initial bandwidth. The initial bandwidth is assumed to be 1. The variable *k* depends on the bandwidth allocation scheme that will be applied together with this flexible threshold. It will be explained more in detail in the later section. Using the equation in (5.13), we can acquire the suitable CINR levels that can be used as the threshold, γ for each cell. Redefining γ using (5.13) will help to reduce the number of non-benefitting users included in the CoMP set.

The steps to get the γ for each cell are as follows:

ALGORITHM II Flexible Threshold

1. Determine all $\mathcal{U}e_i$ of the cell whether they meet the requirement of equation (5.13).
2. If (TRUE), then
3. $\mathcal{U}e_i = \mathcal{U}e_{pass}$
4. $\gamma = \min(\, CINR\ of\ all\ \mathcal{U}e_{pass}\,)$
5. Else $\mathcal{U}e_i = \mathcal{U}e_n$
6. End

5.4 Bandwidth Allocation Approaches

Two types of overlapping region are considered in this work. According to the illustration in Figure 5-3, it can be seen that cells X, Y, and Z overlap with each other forming two different types of overlapping regions. An overlapping occurrence between two cells that forms the $\mathcal{C}_{2w}$ region creates two different sub-regions, for example the overlapping region of cells X and Y; sub-region xy where the users are associated to cell X as the primary and Y as the secondary cell,

and sub-region yx where the users are associated to cell Y and X as the secondary cell. These sub-regions will have to be defined specifically even though they form one overlapping region because these sub-regions are likely to have a different number of users, which will have an impact on the bandwidth allocation. There are regions where the three cells overlap, and when a user is inside this area the user will experience increased interference, without CoMP. This is because the user is further away from the associated cell's centre of coverage, while at the same time it is affected by two strong interfering sources. In this case, only removing one interference source and turning it into a useful signal will be insufficient to improve the CINR, hence the need to turn the second interference source into a useful signal, thereby creating $\mathcal{C}_{3w}$. Based on Figure 5-3, sub-regions xyz, yzx, and zxy will form the three way CoMP region. The two types of overlapping region are defined as follows:

1. ***$\mathcal{C}_{2w}$ CoMP region*** *– An overlapping region involving two cells for example in Figure* 5-3*, it is formed by the xy and yx sub-region.*
2. ***$\mathcal{C}_{3w}$ CoMP region*** *– An overlapping region involving three cells for example in Figure* 5-3*, it is formed by the xyz, yzx, and zxy sub-region.*

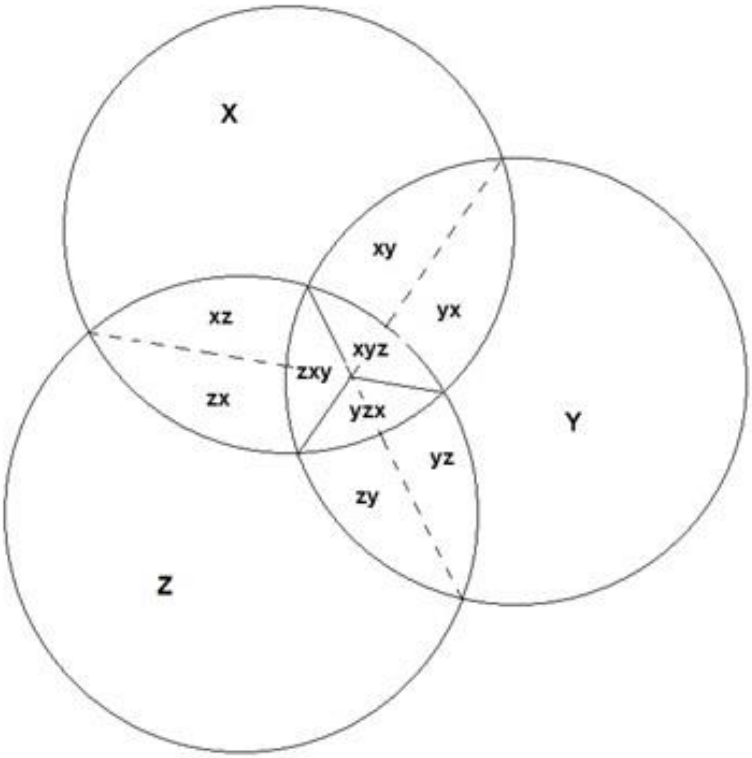

Figure 5-3 Overlapping cells.

Bandwidth allocation is non-trivial, especially when implementing CoMP in HAP systems due to the potential high degree of tessellation and overlap. It is also an important element in providing balance between improving CINR and losing the capacity. The cooperating cells will have to agree to allocate the same exact bandwidth to the overlapping CoMP region, and the allocated bandwidth cannot be reused by the cooperating cells. One way to allocate the bandwidths to the CoMP and non-CoMP regions is to allocate X% of the available bandwidths to CoMP region while the remaining is allocated to the non-CoMP region. This method may be relatively simple, but will result in an inefficient use of bandwidth because of the unevenness of the number of the users in the sub-regions. When encountering such a problem, we propose a strategy of using the number of users in both the CoMP and non-CoMP regions to decide what the ratio of bandwidths should be allocated between these regions. For the case of a $\mathcal{C}_{3w}$ region, the number of users in cooperating two-way CoMP regions and the number of users in the $\mathcal{C}_{3w}$ region will be considered.

From this strategy of allocating bandwidths and based on diagram in Figure 5-3, we propose two different schemes for allocating the bandwidths as follows:

5.4.1 Full Bandwidth (FBW) Scheme

The FBW scheme allocates the same amount of bandwidth per user as what they would receive if there is no CoMP applied in the system. The FWB scheme can be computed as below:

For $\mathcal{C}_{2w}$;

$$BW_X = \frac{\mathcal{B}}{|\mathcal{U}e_i^X|}|\mathcal{U}e_c^{xy}| \tag{5.14}$$

$$BW_Y = \frac{\mathcal{B}}{|\mathcal{U}e_i^Y|}|\mathcal{U}e_c^{yx}| \tag{5.15}$$

$$BW_{CoMP_{XY}} = Min(BW_X, BW_Y) \tag{5.16}$$

$$FBW_2 = \frac{BW_{CoMP_{XY}}}{|\mathcal{U}e_c^{xy}| + |\mathcal{U}e_c^{yx}|} \tag{5.17}$$

This is an example of bandwidth allocation computation between cell X and Y. The proposed bandwidth allocation for the CoMP region, BW_X for region X or BW_Y for region Y B are calculated based on the total number of users and number of Ue_c (e.g. number of users in xy ($\mathcal{U}e_c^{xy}$) and yx ($\mathcal{U}e_c^{yx}$) region respectively) in both cell X and Y. Both bandwidths are then compared between each other in (5.16) and the cell with lower bandwidth will be chosen. The other party will have to agree with the chosen bandwidth and allocate the same bandwidth to the CoMP region. The reason for this step is because with FBW the cell already offers the maximum bandwidth for the CoMP region, and going beyond that means that bandwidth for the Non-CoMP region will be sacrificed. Selecting the cell with the lower bandwidth offering will prevent the sacrificing of the Non-CoMP bandwidth. We then acquire the CoMP bandwidth per user for the $\mathcal{C}_{2w}$ region (FBW_2) by dividing the total bandwidth allocated to the CoMP region ($BW_{CoMP_{XY}}$) with the total number of users in the CoMP region in this case xy and yx sub-regions.

For $\mathcal{C}_{3w}$;

$$BW_{XY} = \frac{BW_{CoMP_{XY}}}{|\mathcal{U}e_c^{xy}| + |\mathcal{U}e_c^{yx}|} |\mathcal{U}e_c^{xyz}| \quad (5.18)$$

$$BW_{YZ} = \frac{BW_{CoMP_{YZ}}}{|\mathcal{U}e_c^{yz}| + |\mathcal{U}e_c^{zy}|} |\mathcal{U}e_c^{yzx}| \quad (5.19)$$

$$BW_{ZX} = \frac{BW_{CoMP_{ZX}}}{|\mathcal{U}e_c^{zx}| + |\mathcal{U}e_c^{xz}|} |\mathcal{U}e_c^{zxy}| \quad (5.20)$$

$$BW_{CoMP_{XYZ}} = Min(BW_{XY}, BW_{YZ}, BW_{ZX}) \quad (5.21)$$

$$FBW_3 = \frac{BW_{CoMP_{XYZ}}}{|\mathcal{U}e_c^{xyz}| + |\mathcal{U}e_c^{yzx}| + |\mathcal{U}e_c^{zxy}|} \quad (5.22)$$

In the case where a user activates the $\mathcal{C}_{3w}$, based on the illustration in Figure 5-3, it will involve three 2 way CoMP sub-regions and the bandwidth will be allocated from $BW_{CoMP_{XY}}$, $BW_{CoMP_{YZ}}$, and $BW_{CoMP_{ZX}}$. The bandwidth for the $\mathcal{C}_{3w}$ (e.g. BW_{XY}) will be decided based on the total number of Ue_c (e.g. users in xy ($\mathcal{U}e_c^{xy}$) and yx ($\mathcal{U}e_c^{yx}$) sub-region) and the number of $\mathcal{C}_{3w}$ users (e.g. users in xyz ($\mathcal{U}e_c^{xyz}$) region). Just as in the $\mathcal{C}_{2w}$ CoMP case, the lowest bandwidth among the three regions will be selected based on (5.21) for the same reason. If one of the sub-region results in zero bandwidth assignment, which means that there are zero $\mathcal{C}_{3w}$ users in that region, the $\mathcal{C}_{3w}$ region of cell X, Y, and Z will be shut down and all the other $\mathcal{C}_{3w}$ users from other sub-regions will be revert back to being $\mathcal{C}_{2w}$ users. This is to make sure that the sub-sections that have zero $\mathcal{C}_{3w}$ users do not need to reserve any bandwidth for the $\mathcal{C}_{3w}$ region which will results in degradation in the $\mathcal{C}_{2w}$ users' performance. Finally, the CoMP bandwidth per user for the $\mathcal{C}_{3w}$region (FBW_3) can be calculated by dividing the total bandwidth allocated ($BW_{CoMP_{XYZ}}$) with the total number of $\mathcal{C}_{3w}$ users ($\mathcal{U}e_c^{xyz}$, $\mathcal{U}e_c^{yzx}$, and $\mathcal{U}e_c^{zxy}$).

5.4.2 Half Bandwidth (HBW) Scheme

The HBW scheme allocates half of amount of bandwidth per user compared with what they receive if no CoMP is applied in the system. The HBW scheme can be computed as follows:

For $\mathcal{C}_{2w}$;

$$BW_X = \frac{\mathcal{B}}{|\mathcal{U}e_i^X| - |\mathcal{U}e_c^{xy}|/2} |\mathcal{U}e_n^X| \tag{5.23}$$

$$BW_Y = \frac{\mathcal{B}}{|\mathcal{U}e_i^Y| - |\mathcal{U}e_c^{yx}|/2} |\mathcal{U}e_n^Y| \tag{5.24}$$

$$BW_{CoMP_{XY}} = Max(\mathcal{B} - BW_X, \mathcal{B} - BW_Y) \tag{5.25}$$

$$HBW_2 = \frac{BW_{CoMP_{XY}}}{|\mathcal{U}e_c^{xy}| + |\mathcal{U}e_c^{yx}|} \tag{5.26}$$

To calculate the $\mathcal{C}_{2w}$ HBW, we first find out the bandwidth for the non-CoMP region for both cells X and Y (BW_X and BW_Y) by dividing the total bandwidth of the system with total number of users in the cell minus half of the total $\mathcal{U}e_c$ of that cell and multiply it with the number of $\mathcal{U}e_n$. To decide on the CoMP allocation, the CoMP bandwidth from both cells is the total bandwidth minus the bandwidth for non-CoMP region. The bandwidth in each cell is compared and the highest bandwidth that both cells can offer is assigned to the CoMP region, as in (5.25). This approach is different from the FBW scheme because for HBW only half of the bandwidth is considered, so if we choose the lowest bandwidth available the other cell that can offer more will have a much reduced bandwidth allocation. Hence, this will result in a much lower bandwidth allocation for $\mathcal{U}e_c$, and fails to deliver the capacity improvements in many cases arising from the improved CINR. With the $BW_{CoMP_{XY}}$ decided, the CoMP bandwidth per user (HBW_2) can be calculated by dividing $BW_{CoMP_{XY}}$ with the total number of $\mathcal{U}e_c^{xy}$ and $\mathcal{U}e_c^{yx}$.

For $\mathcal{C}_{3w}$;

$$BW_{XY} = \frac{BW_{CoMP_{XY}}}{|\mathcal{U}e_c^{xy}|+|\mathcal{U}e_c^{yx}|-|\mathcal{U}e_c^{xyz}|/2}\left(\left|\mathcal{U}e_c^{xy}\right| + \left|\mathcal{U}e_c^{yx}\right| - \left|\mathcal{U}e_c^{xyz}\right|\right) \quad (5.27)$$

$$BW_{YZ} = \frac{BW_{CoMP_{YZ}}}{|\mathcal{U}e_c^{yz}|+|\mathcal{U}e_c^{zy}|-|\mathcal{U}e_c^{yzx}|/2}\left(\left|\mathcal{U}e_c^{yz}\right| + \left|\mathcal{U}e_c^{zy}\right| - \left|\mathcal{U}e_c^{yzx}\right|\right) \quad (5.28)$$

$$BW_{ZX} = \frac{BW_{CoMP_{ZX}}}{|\mathcal{U}e_c^{zx}|+|\mathcal{U}e_c^{xz}|-|\mathcal{U}e_c^{zxy}|/2}\left(\left|\mathcal{U}e_c^{zx}\right| + \left|\mathcal{U}e_c^{xz}\right| - \left|\mathcal{U}e_c^{zxy}\right|\right) \quad (5.29)$$

$$BW_{CoMP_{XYZ}} = Max(BW_{CoMP_{XY}} - BW_{XY}, BW_{CoMP_{YZ}} - BW_{YZ}, BW_{CoMP_{ZX}} - BW_{ZX}) \quad (5.30)$$

$$HBW_3 = \frac{BW_{CoMP_{XYZ}}}{|\mathcal{U}e_c^{xyz}|+|\mathcal{U}e_c^{yzx}|+|\mathcal{U}e_c^{zxy}|} \quad (5.31)$$

To calculate the $\mathcal{C}_{3w}$ for the HBW case, all the cooperative sub-regions will calculate the bandwidth they can offer for the $\mathcal{C}_{3w}$ region by first determining the bandwidth for their 2 way sub-region (BW_{XY}, BW_{YZ}, and BW_{ZX}) by considering the number of $\mathcal{C}_{2w}$ users and $\mathcal{C}_{3w}$ users. Each of the bandwidth assignments can be offered to the $\mathcal{C}_{3w}$ region which is the total bandwidth allocated to the CoMP region (e.g. $BW_{CoMP_{XY}}$) minus bandwidth for the $\mathcal{C}_{2w}$ region (e.g. BW_{XY}) are compared and the highest among the three offers are selected as the $\mathcal{C}_{3w}$ bandwidth ($BW_{CoMP_{XYZ}}$). Lastly, the $\mathcal{C}_{3w}$ region bandwidth per user (HBW_3) is calculated by dividing $BW_{CoMP_{XYZ}}$ with the total number of $\mathcal{C}_{3w}$ users ($\mathcal{U}e_c^{xyz}$, $\mathcal{U}e_c^{yzx}$, and $\mathcal{U}e_c^{zxy}$).

5.5 Simulation Results and Discussion

Figure 5-4 illustrates the system, where the HAP is located at the centre of a 30 km radius service area at an altitude of 20 km above ground. The HAP cells are then deployed in the service area with overlapping areas between the cells. Three are shown, but in practice there can be many more. Two types of user are considered in the system which are the non-CoMP user equipment ($\mathcal{U}e_n$) and CoMP user equipment ($\mathcal{U}e_c$). Users are randomly distributed across the service area according to a uniform distribution. The HAP is considered to be equipped with a 25 x 25 element planar phased array antenna that uses beamforming, which forms the multiple cells used to deliver a wireless communication service. The locations of the cells are determined based on the clustering of users using the K-Means clustering algorithm as discussed in Chapter 4. The algorithm determines the optimum centroid positions using the mean of clustered user's positions. The process of determining centroid positions will be achieved by iterating until the optimum point is reached. With this clustering algorithm, specific high density user groups can also be identified inside the service area according to the work in [5].

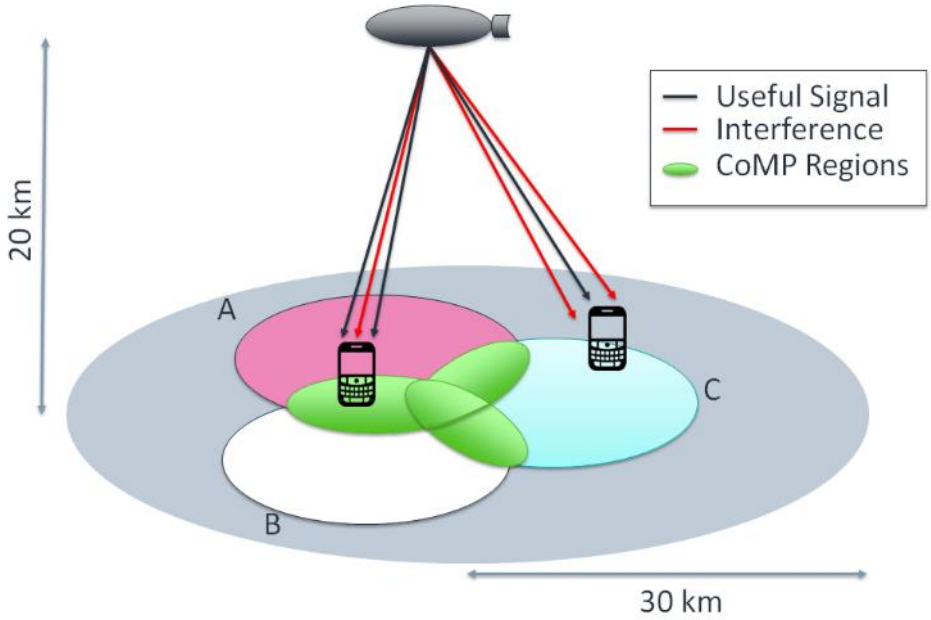

Figure 5-4 HAP cell footprints and the overlapping region as CoMP region.

In order to evaluate all the proposed methods and schemes, simulations using MATLAB were carried out based on the system layout in Figure 5-4. Traffic is modelled based on the full-buffer traffic model. The parameters are presented in Table 5-1 below:

Parameter	Value
HAP Transmit Power	40 dBm
Receiver Antenna Gain	0 dBi
HAP Antenna Gain (Boresight)	27.9 dBi
Carrier Frequency	2.6 GHz
Noise Power	-100 dBm
CNR Threshold	9 dB
CINR Threshold	0 dB
Number of Users	2900

Table 5-1 SIMULATION PARAMETERS

Figure 5-5 shows the percentage of Ue_ns and Ue_cs for several γ values from 0 to 19 dB used throughout the simulation. At γ of 0 dB, 0% users operate in the CoMP region while 100% users operate in the non-CoMP region, i.e. it can be assumed that the system operates with no CoMP. As γ increases, the percentage of Ue_c increases, and contrarily, the percentage of Ue_ndecreases. This is because the higher the γ, the more users that are included into the CoMP region, hence the increase of Ue_c and the decrease of Ue_n as a percentage.

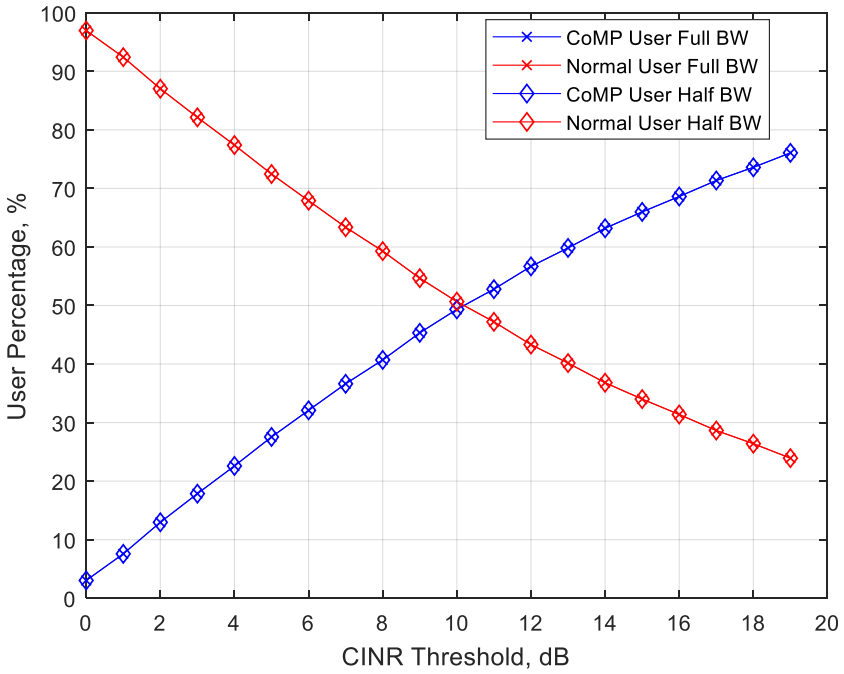

Figure 5-5 Percentage of CoMP and non-CoMP users with variation of the CINR threshold.

Implementing CoMP means that users can improve their CINR levels. In Figure 5-6, the CDF plot of CINR levels of no CoMP, $\mathcal{C}_{3w}$ (1, 5, 9 dB), $\mathcal{C}_{2w}$ (9 dB), and inter-cell interference coordination (ICIC) are presented. It is also observed that with higher γ, more users are included in CoMP region and hence have a better CINR performance. Besides that, it can be clearly seen that $\mathcal{C}_{3w}$ CINR is better than $\mathcal{C}_{2w}$ CINR, also ICIC obviously performs poorly compared to CoMP in terms of CINR performance. $\mathcal{C}_{3w}$ CINR should be higher than $\mathcal{C}_{2w}$ CINR because $\mathcal{C}_{3w}$ users will have one extra signal source (the addition of 3 signal sources) and one fewer interference source compared to $\mathcal{C}_{2w}$. For ICIC, one interference source will be removed because

the bandwidth used for ICIC will not be reused by the neighboring cell [120], but it will not benefit from the simultaneous data transmissions like CoMP. If we consider an outage at CINR of 10 dB, it can be seen that with no CoMP, there is 55% of users will be left out of the system. After CoMP is implemented with 1 dB threshold, it begin to show an improvement in CINR levels with the outage users dropped to 45%, followed by 30%, 13%, and 9% for CoMP with 5 dB, 9dB (two ways), and 9 dB (three ways) respectively. This clearly indicate that the higher CINR threshold for CoMP, the higher CINR improvement which is beneficial for the system. However, Figure 5-7 might suggest otherwise.

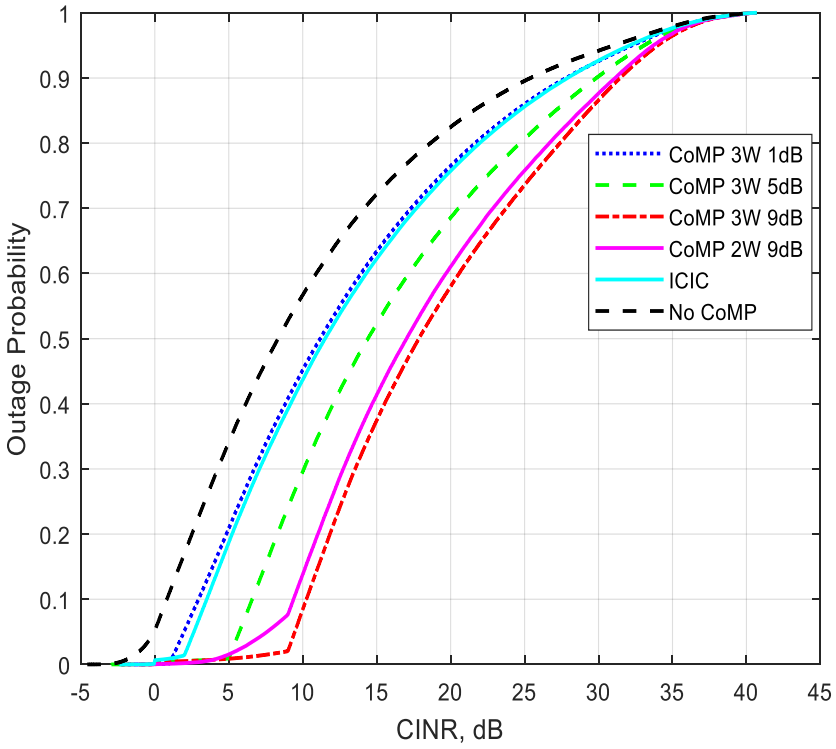

Figure 5-6 The outage probability of different γ with $\mathcal{C}_{3w}$, $\mathcal{C}_{2w}$ and ICIC.

From the previous graph, the higher the γ, the better the CINR performance improvement. However, there is a trade-off, because by including more users into the CoMP region in order to increase the CINR levels means that the amount of bandwidth that can be allocated per user is decreased. Despite the improvement shown in CINR levels, user capacity will reach its peak and the performance will start to decline. The mean CINR and mean capacity per user performance is presented in Figure 5-7 to directly compare the performance of CINR and capacity per user. It is shown that while the mean CINR keeps increasing with increasing of γ, the mean capacity for all schemes starts to drop after γ = 10 dB. The mean capacity starts to drop because at that point the system has started to include the users that have better performance without CoMP. These users receive less bandwidth when included in CoMP region, and the CINR level increase cannot compensate for the reduction in bandwidth. The cut in bandwidth is also caused by the unevenness of the number of users in cooperative cells.

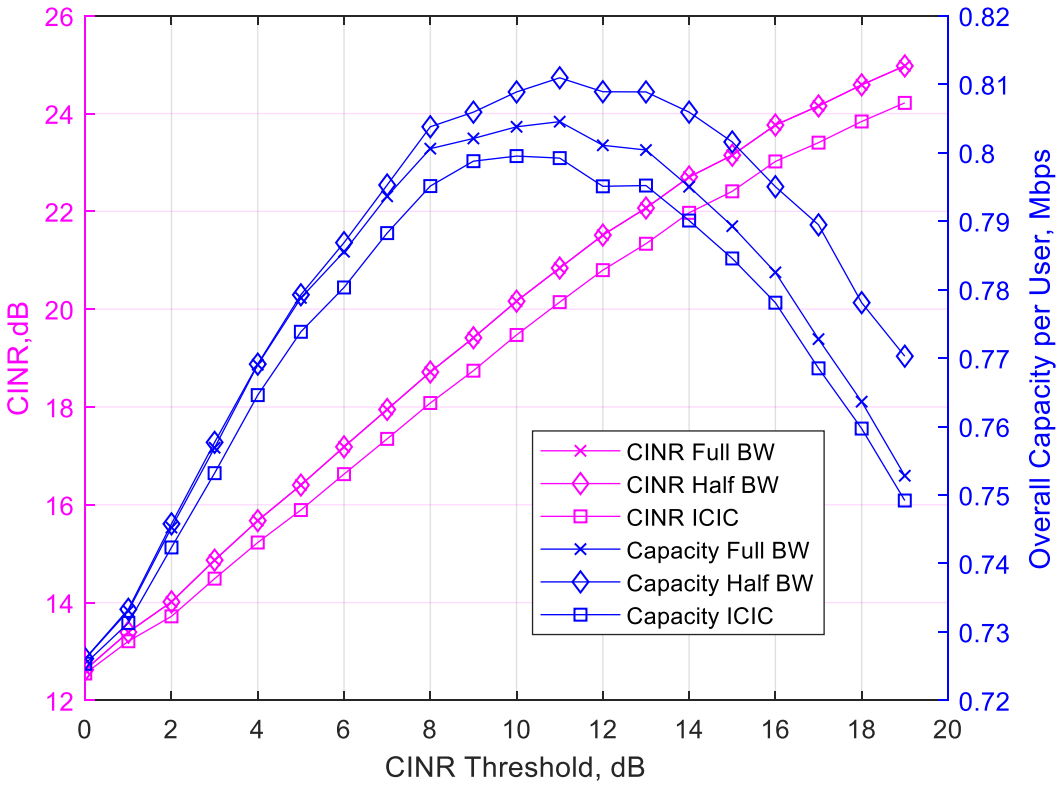

Figure 5-7 Mean CINR vs mean capacity per user for all schemes.

Figure 5-8, Figure 5-9, Figure 5-10, and Figure 5-11 present the capacity difference which indicates whether the system benefits (positive difference) or loses (negative difference). Capacity difference is the difference between the final capacity which refers to the users' capacity after CoMP is implemented, and the initial capacity which refers to the users' capacity before CoMP is implemented. Figure 5-8 shows the mean capacity difference of both FBW and HBW schemes for $\mathcal{U}e_i$, $\mathcal{U}e_c$ and $\mathcal{U}e_n$ users. The $\mathcal{U}e_n$ capacity difference keep increasing as the CINR threshold, γ increases, while the $\mathcal{U}e_c$ will reach a peak before having a degradation in capacity difference performance. The $\mathcal{U}e_n$ capacity difference keep increasing because when more users are being included into CoMP region, the $\mathcal{U}e_n$ will receive more bandwidth in results of less bandwidth sharing. On the other hand, $\mathcal{U}e_c$ performances degrade at a certain point of the simulation because the users that can perform better without CoMP start to be included. This kind of user receives less bandwidth with CoMP, and the CINR improvement is not sufficient to compensate for the bandwidth loss.

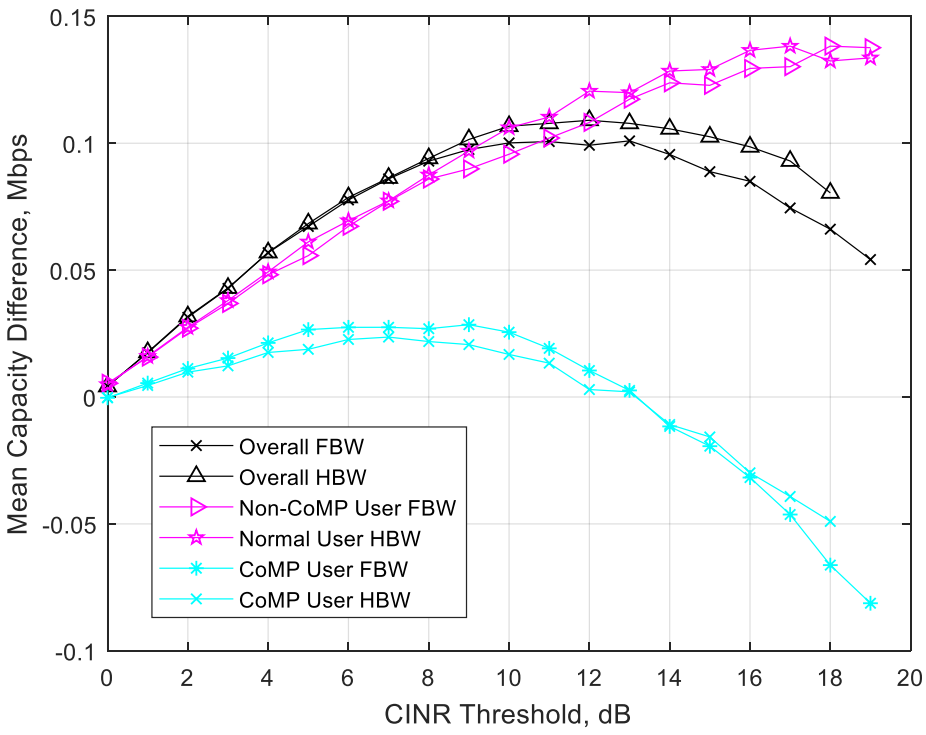

Figure 5-8 The average capacity difference of FBW and HBW for all types of users.

To go deeper into the behavior of the capacity difference, Complementary CDF (CCDF) graphs are presented in Figure 5-9, Figure 5-10, and Figure 5-11 for $\mathcal{U}e_i$, $\mathcal{U}e_c$ and $\mathcal{U}e_n$ respectively. The capacity differences of four different schemes are compared to establish the most suitable scheme to use in this scenario. The schemes are FBW with 9 dB γ, HBW with 9 dB γ, Flexible FBW, and Flexible HBW. The 9 dB performance threshold was chosen for both FBW and HBW because it was determined based on Figure 5-7, which illustrates that it is an optimal value of γ. For the $\mathcal{U}e_i$ capacity difference, it is shown in Figure 5-9 that 9 dB HBW has both the highest increase and decrease in performance. This is followed by 9 dB FBW, Flexible HBW, and Flex FBW respectively. The users in the system, $\mathcal{U}e_i$ consists of two different user groups when CoMP is applied to the system, which is the CoMP users ($\mathcal{U}e_c$) and non-CoMP users ($\mathcal{U}e_n$). Thus, this graph represents the overall performance.

In Figure 5-10, the $\mathcal{U}e_n$ capacity difference is presented. All the schemes show that 80% of users gain benefit from CoMP with 9 dB HBW being the best followed by 9 dB FBW, Flexible HBW, and Flexible FBW. Both HBW based schemes are better than the FBW based schemes because with HBW, $\mathcal{U}e_c$ are only allocated half of what they originally get without CoMP which leaves the $\mathcal{U}e_n$ extra bandwidth. While on the negative difference side, both HBW based schemes perform worse than the FBW based schemes because of the maximum value agreement as discussed in section 5.4.2 based on equation (5.25). Some $\mathcal{U}e_n$ of HBW will lose more bandwidth compare $\mathcal{U}e_n$ of FBW.

For the $\mathcal{U}e_c$ capacity difference, a CDF graph is presented in Figure 5-11. It can be seen that the Flex FBW out performs the other schemes by having 75% of $\mathcal{U}e_c$ benefitting from CoMP, while having less degradation (negative difference) compared with other schemes. The 9 dB FBW and 9 dB HBW have almost the same performance with both having a great loss of capacity, while 9 dB FBW has slightly better than 9 dB HBW in term of capacity gain. For the $\mathcal{U}e_c$, it is expected that FBW based scheme has better performance because of the nature of the scheme, which allocates more bandwidth to the CoMP region compared to the HBW.

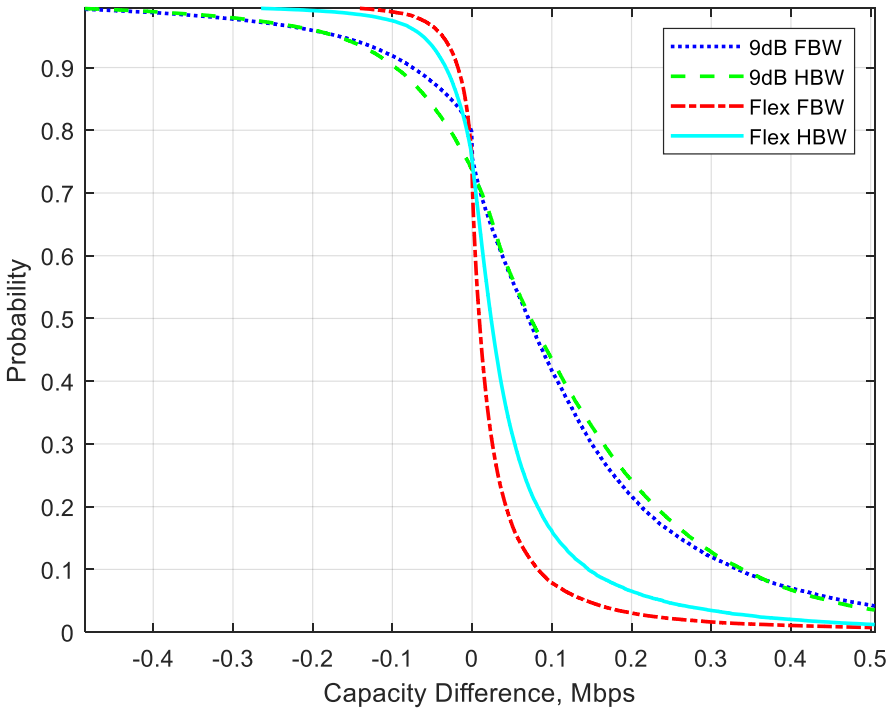

Figure 5-9 Overall users capacity difference CCDF for all schemes.

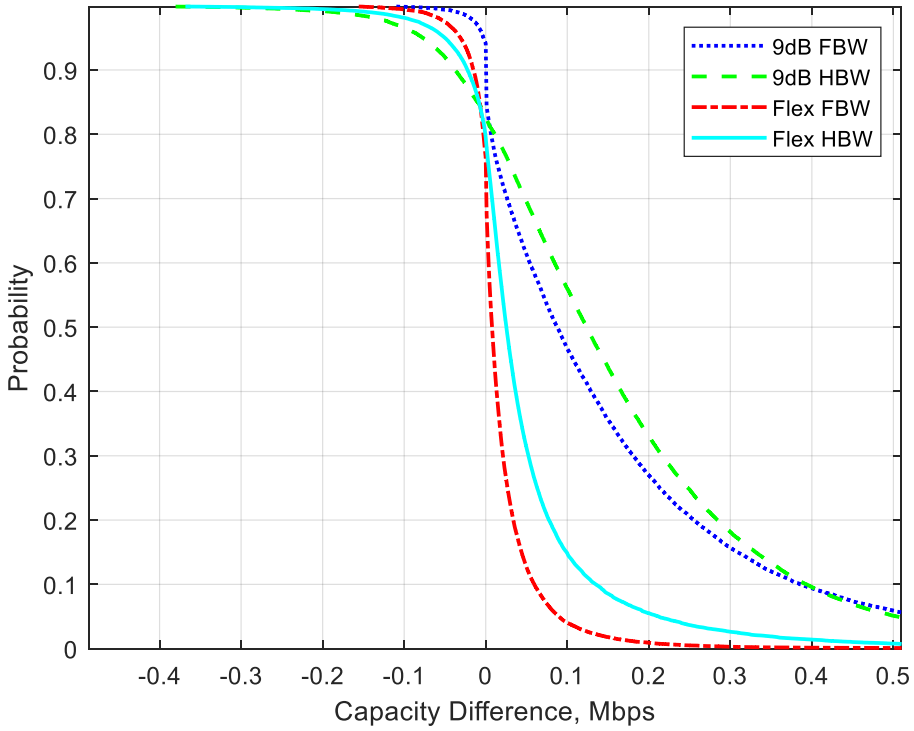

Figure 5-10 Non-CoMP users capacity difference CCDF for all schemes.

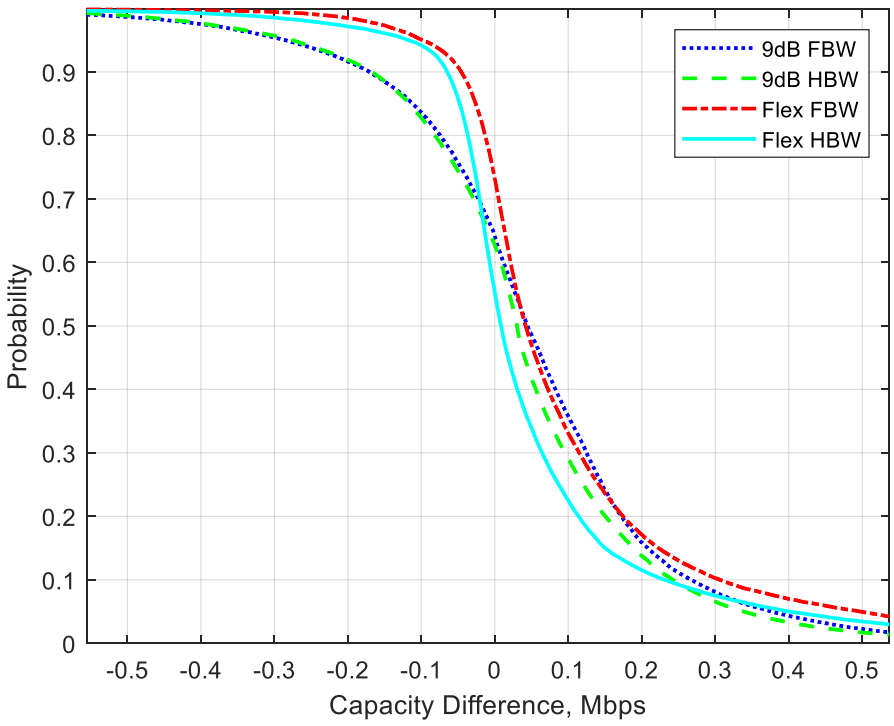

Figure 5-11 CoMP users capacity difference CCDF for all schemes.

In Figure 5-12 the percentage of benefitting users which represents the users that have at least a 20% capacity increase. While the percentage of losing user represents the users that have at least a 20% capacity loss. The 20% threshold is considered by the author to make sure that the increment really represents the users that are benefitting from CoMP, likewise for the decrement. This measure can be used to help determine which scheme works the best, because the trade-off between benefitting and losing users for each scheme can be compared directly. For the case of HBW and FBW the parameters of 1, 5, and 9 dB γ is used to show the effects of using different threshold level. The scheme with the lowest number of losing users is the FBW, however the benefitting user percentage is not that impressive. The highest percentage of benefitting users occurs with the HBW scheme, however it also has more drawbacks. Obviously, the best possible performance is to have maximum benefitting users and very low losing users but this depends on what is valued for the system. In terms of capacity increase, the Flex HBW is better than the Flex FBW while the capacity decrease is similar for both.

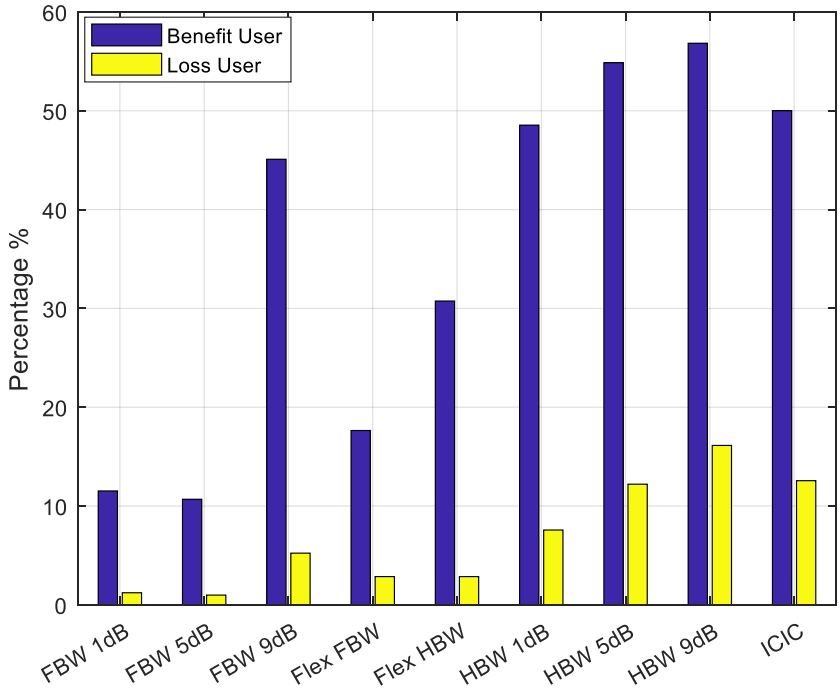

Figure 5-12. Benefit and loss trade-off for all schemes.

Figure 5-13 presents a coverage plot showing the HAP cells covering the service area for approximately 96% of the total users, prior to CoMP. The white area is the area that is not covered

by the HAP cells. The red colour in between the cells illustrates the region where the users have a CINR level lower than the operational threshold (1.8 dB). It also represents the overlapping region of the cells. The colour bar in Figure 5-13 and Figure 5-14 represents capacity per user in bits per second.

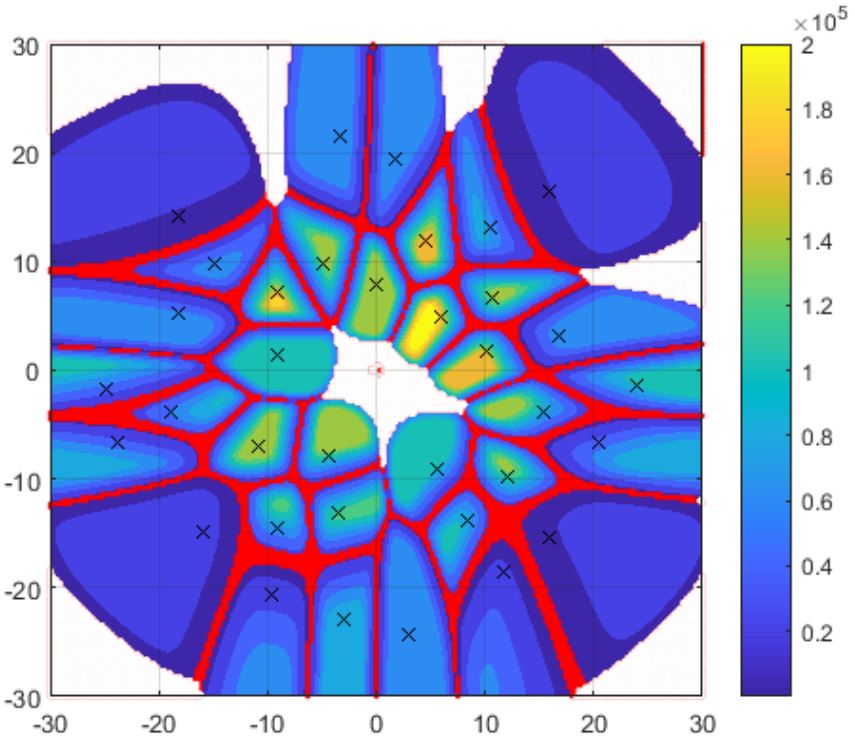

Figure 5-13 Contour plot of HAP cells. White regions indicate areas without HAP cells, the dark blue to yellow regions indicate the lowest to highest capacity per user respectively, 'X' marks are the centre of the HAP cells, and red regions are where the users have CINR levels of below 1.8 dB before implementation of CoMP in 30 km service area.

After implementing CoMP in the system, certain areas are improved as seen in Figure 5-14. An obvious improvement can be seen is that almost all red marks that represent a user having CINR below 1.8 dB are removed. This is an indication that the CINR of the cell edge users have been improved. In terms of capacity increase, a clear difference can be seen in Figure 5-15 and Figure 5-16 below.

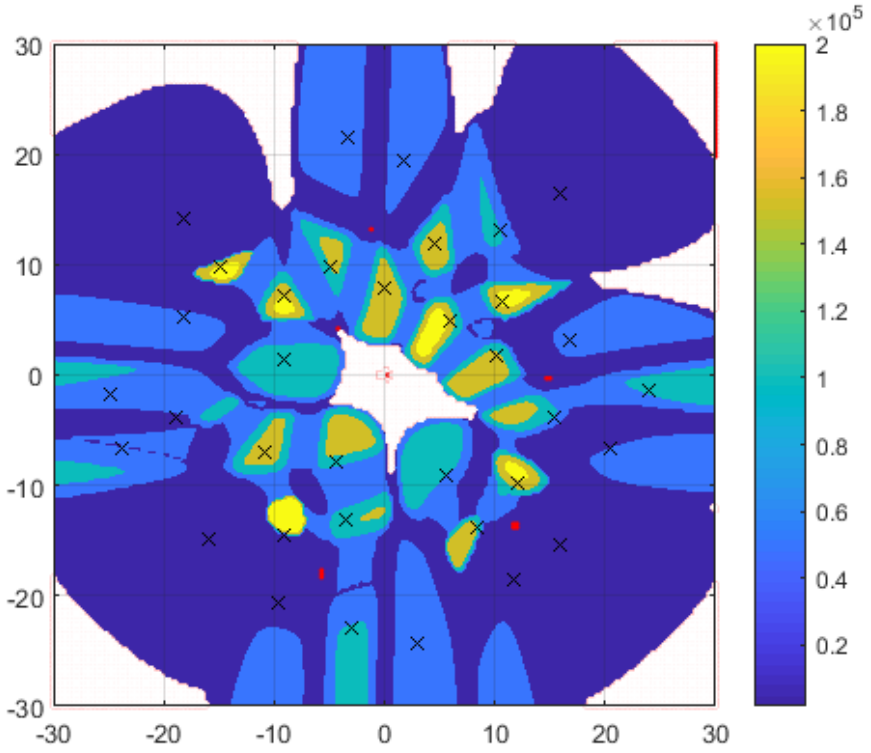

Figure 5-14 Contour plot of HAP cells. White regions indicate area without HAP cells, the dark blue to yellow regions indicate the lowest to highest capacity per user respectively, 'X' marks the center of the HAP cells, and red regions show where the users have CINR levels below 1.8 dB after implementation of CoMP with FBW (γ 9 dB) in 30 km service area.

The spatial effects of implementing CoMP with FBW, γ of 9 dB in a HAP system can be seen in Figure 5-15. It is clearly shown how the overlapping region is improved after being significantly affected by the interference as seen in Figure 5-13 earlier. As previously discussed, this is where users are located which have a degradation in performance when CoMP is applied. The darker region represents the area where the users are have a degradation. From the authors' perspective this sacrifice can be made when it is important to have consistent wide area coverage.

Lastly in Figure 5-16, a contour plot of flexible FBW is presented. It shows how this flexible scheme helps reduce the users included into the CoMP region, restricting membership to those who can really benefit from CoMP.

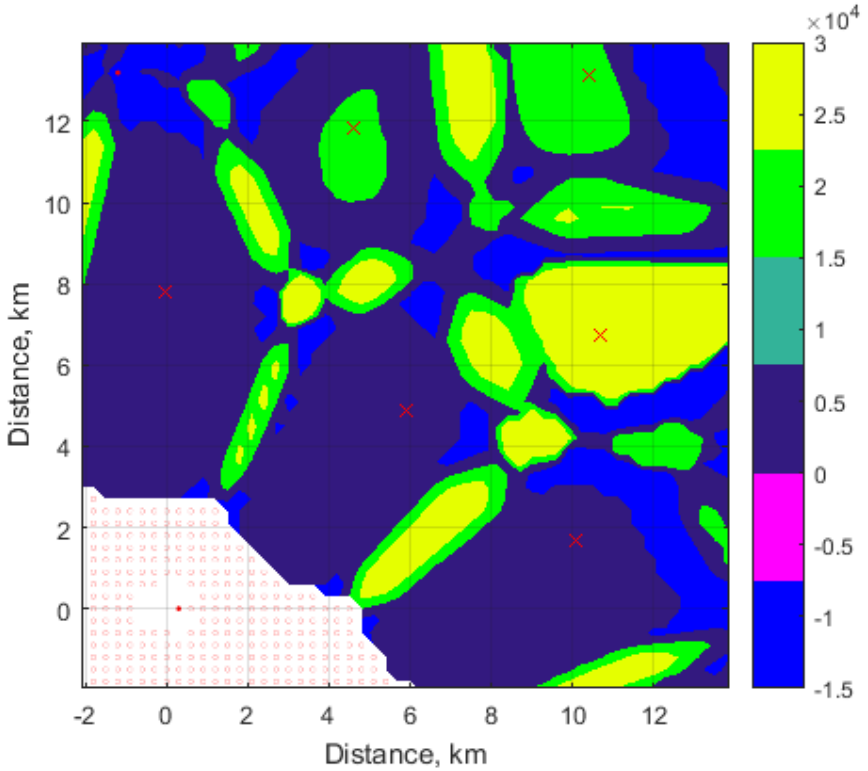

Figure 5-15 Contour plot focusing on overlapping areas (zoom in from the 30 km service area). The yellow areas indicate the areas with most improved users, dark blue areas indicate the areas with almost unaffected users, and light blue areas indicate the areas with highest loss users with 9 dB FBW CoMP (colourbar indicates capacity difference in bits per second).

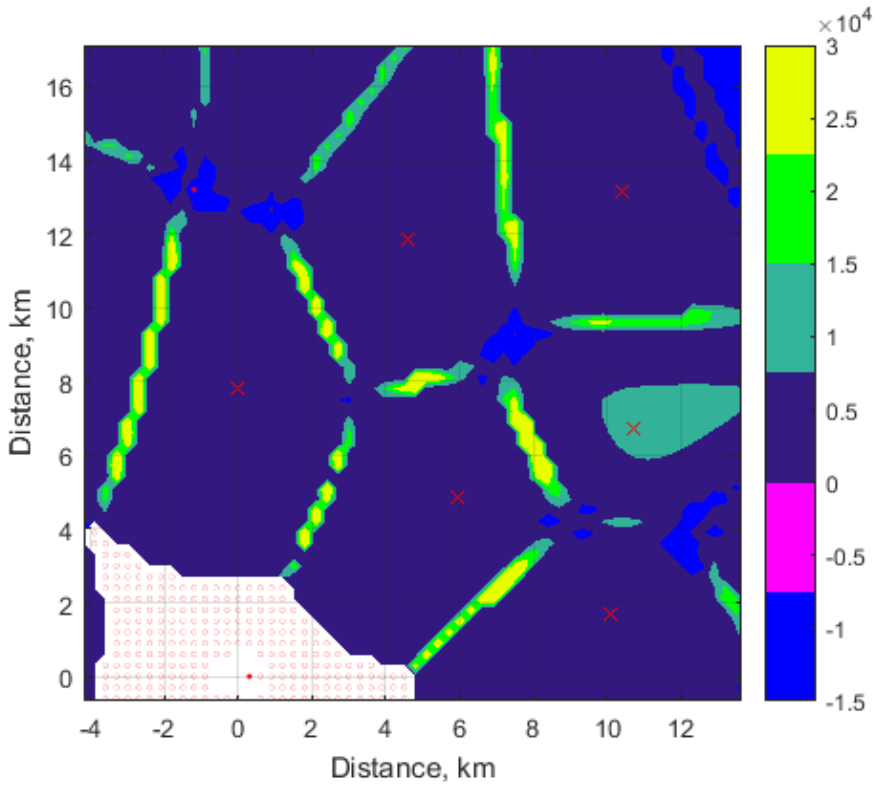

Figure 5-16 Contour plot focusing on overlapping areas (zoom in from the 30 km service area). The yellow areas indicate the areas with most improved users, dark blue areas indicate the areas with almost unaffected users, and light blue areas indicate the areas with highest loss users with Flex FBW CoMP (colourbar indicates capacity difference in bits per second).

5.6 Summary

JT-CoMP is shown to give significant benefits to the users at the cell edge in a HAP multi-beam system by improving both CINR levels and capacity per user and at the same time benefitting the overall performance of the system. By identifying the trade-off between CINR and capacity, two types of threshold are proposed which are the centralised CINR threshold, and the flexible CINR threshold. To deal with the unevenness of users in each cell, a flexible CINR threshold is implemented with each individual cell having a different threshold. Two different methods of allocating the bandwidth between the non-CoMP and CoMP regions have been proposed; the FBW and HBW schemes both bring benefits to 57% and 46% of users respectively. The FBW scheme works better for the CoMP region improving the user experience at the cell-edge. It is shown how γ can be used to control overall user capacity and reaches an optimum. A flexible threshold is proposed in order to carefully select the users to be included into the CoMP region. With this approach the users that lose capacity can be minimized. Implementing CoMP is possible because of the newly proposed HAP architecture that enables the system to treat individual HAP beams as a serving cell which can be managed by virtual eNodeBs. This provides equivalence to the traditional cell approach used with the terrestrial systems, thus providing the capability to perform such functions in a flexible way.

CHAPTER 6

6. Network Functional Split for a 5G C-RAN Based System Exploiting Joint High Altitude Platform and Terrestrial Segments

Contents

6.1 Overview

The purpose of this chapter is to demonstrate how HAP and terrestrial segments can be integrated together to allow dynamic coordination between the two segments to deliver a more network integrated system deployment. No coordination between HAP and terrestrial systems will result in more conservative interference mitigation techniques being adopted to ensure coexistence between these two systems which operate in a common spectrum allocation. One of the techniques to control the degradation in terrestrial user performance when deploying the HAP cells is to use an INR threshold as shown in Chapter 4. However, this will leave a gap between HAP cells and a terrestrial macro cell meaning that users in that region go unserved if the same spectral bands are used. Conventional wireless communication service provisioning from HAPs

considers that complete base stations are located on the HAP itself where all the signals from the RRU are processed, demodulated and decoded on the platform. This approach results in significantly more hardware being required on the HAP, which results in increased payload requirements in terms of weight, volume and power compared to situation where more processing is carried out on the ground. This limits network utility and feasibility when considering the state-of-the-art with HAP aircraft technologies. At the other extreme, a fully centralised system like Centralised Radio Access Network (C-RAN) will move as much of the hardware to the ground, reducing payload requirements, but will increase the burden of the fronthaul link between the RRU which is located on the HAP and the CU and DU on the ground. This chapter will specifically consider the best network functional splits to balance these two competing aspects, while considering the state-of-the-art and future HAP technologies. JT-COMP is used to facilitate the coexistence and interworking of the two systems.

The contributions of this chapter are:

1. A joint HAP and terrestrial network using a C-RAN based system and Network Function Virtualisation (NFV).
2. Application of a network functional split on the HAP C-RAN segment to reduce fronthaul load with the exploitation of Software Defined Networking (SDN).
3. Implementation of Joint Transmission Coordinated Multipoint (JT-CoMP) across the joint network (HAP and terrestrial) as an application of the newly proposed architecture to mitigate interference.
4. A HAP system fronthaul link deployment and GRS site diversity that can adapt to specific implementations of the network functional split.

There has been a considerable research effort addressing the coexistence of HAP and terrestrial systems. In [66], the downlink coexistence performance of WiMAX services in HAP and terrestrial systems was investigated. The performance of the WiMAX service from a HAP is optimised by comparing the performance of different antenna pointing offsets, and by narrowing

the transmit and receive antenna beamwidths. The HAP system performance is enhanced while also efficiently coexisting with the terrestrial WiMAX system. Authors in [67] which also investigated the coexistence of a HAP and terrestrial WiMAX system suggested that the user antenna which is at the receiver end (assuming downlink transmission) should not exceed 30^{o} for the coexistence to be effective. Based on findings in the literature, there are no studies that consider tight coordination between HAP and terrestrial systems, instead relying on conservative interference isolation techniques to ensure effective coexistence between the two systems.

6.2 Network Functional Split for a C-RAN Based System using Joint HAP and Terrestrial Segments

Adapting conventional C-RAN is an ideal way for a HAP system to minimise the hardware required on the platform, thus providing a lighter payload for the HAP and reduced data processing required on the platform side. Both should in principle reduce the energy required on the HAP to maintain the flight and deliver wireless communication services. However, the large amount of unprocessed data from the RRU presents a significant offload burden for the fronthaul link. An estimated 625 Gbps fronthaul link capacity is required to carry the unprocessed data of 25 × 25 antenna elements or up to 42 HAP cells from a single HAP according to [93]. Fibre optic cable technology is not usable with the HAP, as it is assumed to be free flying. The best option in terms of providing the necessary capacity is to use free space optic (FSO) technology to provide the fronthaul link from the platform to the ground. In [121] the author has carried out an experiment with an FSO link and successfully achieved 228 Gbps in a lab. Even though it is only for a short distance, it shows the technical feasibility and in time it should be possible to extend the transmission distance to several kilometres. Should at least 228 Gbps be achieved for an actual HAP scenario, a single FSO link will still only provide approximately 40 % of the required capacity, so other solutions are required so that the remaining 60 % can be transferred.

One of the solutions is to reduce the amount of data to be offloaded through the fronthaul link. This can be achieved by the application of a network functional split, dividing the functionality of the RRU and CU and DU into different options. Options 8 through to 1 shown in Figure 6-1 move progressively more CU and DU functionality towards the core network, in the case of the HAP functionality, it is moved from the air to the ground, where the CU and DU pool (centralised processing) are located leaving the RRU side (on the platform) requiring less data processing. The less data processing carried out on the RRU side means that a larger amount of data must be offloaded through the fronthaul link [93]. Thus, option 8 (conventional C-RAN) has the largest amount of data to be offloaded through the fronthaul link. There is a trade-off between

the degree of centralised functionality of CU and DU, and the amount of data to be offloaded through the fronthaul link. In the HAP case, the payload must be minimised in terms of payload mass and power available on the specific platform (e.g. Zephyr T with a 20 kg payload allowance). Thus, the lighter the payload and the less data processing done on HAP, the lower the amount of energy required for the HAP to operate. Given the high data rates required with an option 8 split, it is likely to put severe strain on the fronthaul link so lower splitting options must be considered.

The authors in [97] suggest that a split-PHY layer, which in this context is option 7, could achieve a capacity requirement cut of over 90 %. The configuration to divide the functionalities should be possible through SDN. Option 7 would be the best network functional split option for a HAP based system. It means that the platform will have:

- Less hardware, thus a lighter payload compared to a conventional HAP system.
- Less data processing done on the platform compared to a conventional HAP system.
- Less data offloading through the fronthaul link compared to a conventional C-RAN system (option 8).
- Easier integration with terrestrial segments
- More centralised functionality compared to a conventional HAP system which will additionally enable dynamic coordination of the system.

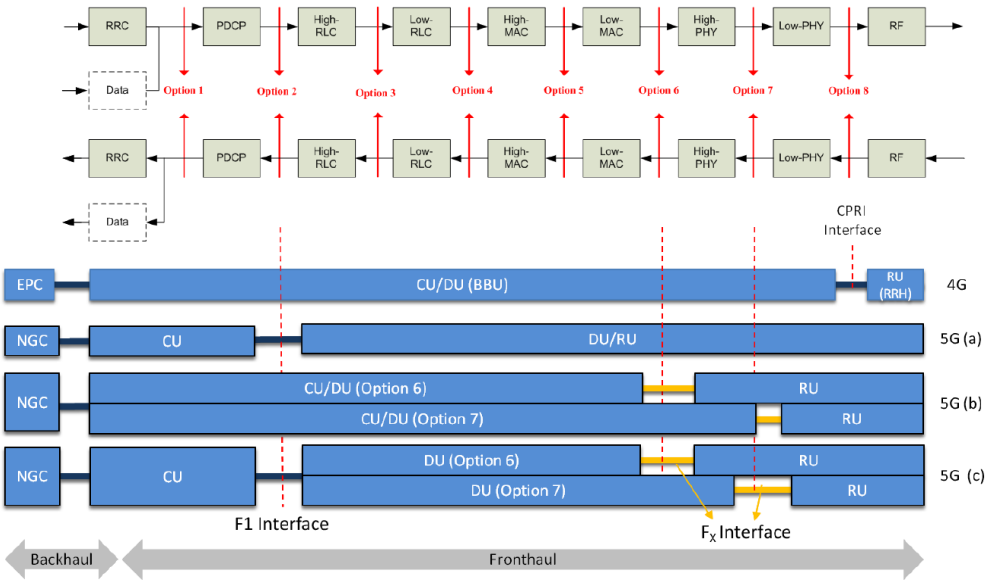

Figure 6-1 Joint HAP and terrestrial system adapting option 7 network functional split in a 5G C-RAN based system (directly taken from [93]).

6.2.1 Joint HAP and Terrestrial Architecture

Figure 6-2 shows the newly proposed joint HAP and terrestrial system architecture. To enable coordination between the HAP and terrestrial segments, a centralised based system must be adapted to join the two segments together. The C-RAN based system is chosen because it implements the centralised processing concept (CU and DU pool) allowing connection to multiple distributed RRUs. A single HAP can deliver multiple cells and each cell is considered in terms of functionality as an RRU, because each of them are managed by a virtual eNodeB exclusively. This is achievable through network function virtualisation (NFV). Similarly, a terrestrial macro base station is also considered as a RRU. All RRUs are virtually connected to the CU and DU pool. With SDN, the whole system configuration is relatively straightforward with each sub-system. In this case the HAP and terrestrial segments, configured with different split options depending on the sub-system requirement. Here both sub-systems adapt an option 7 network split as both need some parts of the physical layer to be centralised to simplify the implementation of the JT-CoMP coordination technique to provide a solution for the cell-edge users. The option 7 network functional split will still have the capability to support JT-CoMP [122].

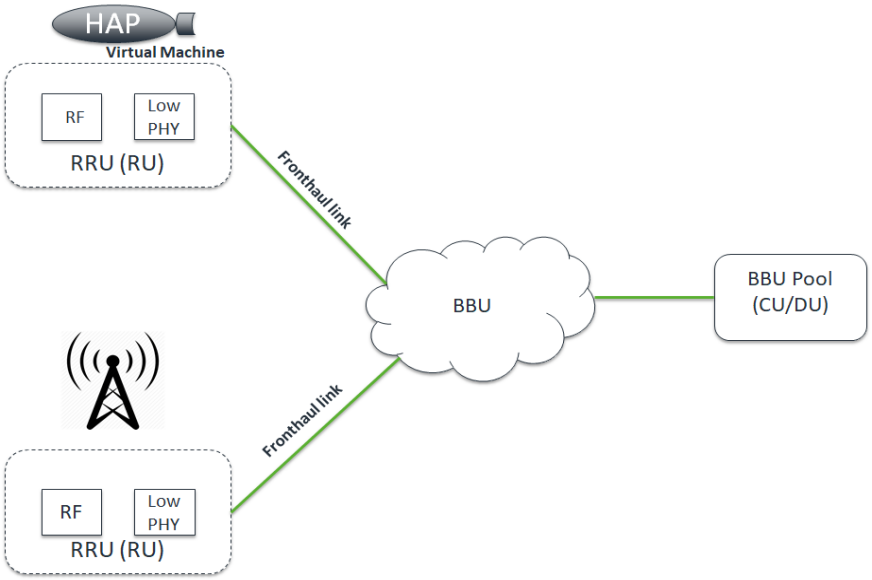

Figure 6-2 Joint HAP and terrestrial segments architecture adapting option 7 network functional split on a 5G C-RAN based system.

Since both segments enable coordination and are now part of the same system, JT-CoMP can be performed across the two segments, providing a combined solution to address the interference issue especially the cell-edge users. The synchronisation requirement by JT-CoMP can also be more straightforwardly achieved as all the RRUs have centralised processing in the CU and DU pool. This novel joint architecture based on C-RAN system features a new coexistence environment between HAP and terrestrial networks.

6.3 HAP Fronthaul Link Deployment for Network Functional Split Implementation

To implement this new system for HAPs, there are a few factors that need to be considered. These factors are the maximum payload the platform can carry, the amount of energy required (for both flight and wireless communication provision), and the fronthaul requirement to deliver wireless communication services, which is a challenge for HAPs especially. Each of these factors impact differently on the network functional split options. In this section, the main focus is to determine the best deployment for the fronthaul link of a system where free space optic (FSO) and millimeter-wave (mm-wave) are suitable options for the fronthaul link.

In the previous section, it is stated that option 7 of the network functional split is to be adapted to the HAP C-RAN based system. This will see part of physical layer function located on the RF side (on the platform) and the other part of the physical layer function together with the rest of the BBU function centrally located on the ground. According to a survey [122], there is a sub-splitting within the physical layer which can further divide the physical layer function. The split-PHY which is known as option 7 according to Figure 6-3, can be further split into option 7-1, 7-2, and 7-3.

To determine the fronthaul requirements of the different degrees of network splitting, this work considers option 7-1 and 7-3. Option 7-1 and option 7-3 would have the least and most processing done on the platform respectively which can be adopted with different fronthaul link technologies depending on the scenarios that are being considered. The whole low-physical layer hardware would be on the platform (near the RRU), and a dynamic configuration to select the degree of network splitting, implemented through software defined networking (SDN), depending on the HAP's condition (e.g. power, fronthaul link capability, or payload limitations). For comparison, the requirements of a conventional C-RAN system (using option 8) fronthaul will also be considered as a benchmark. The fronthaul requirements for the network functional split can be estimated as follows:

For option 8,

$$\mathbf{FH_{op8}\,(Gbps)} = \boldsymbol{N_{SR}BTWN_{AP}N_{CH}}\ [122] \tag{6.1}$$

For option 7-3,

$$\mathbf{FH_{op7-3}\,(Gbps)} = \sum_k \frac{\mathbf{1}}{\boldsymbol{T_{TTI}}} \boldsymbol{M_{O-UL}} . \boldsymbol{N_{SYM}N_{SC}N_{STRM}N_{q-LLR}}\ [97] \tag{6.2}$$

For option 7-1,

$$\mathbf{FH_{op7-1}\,(Gbps)} = \boldsymbol{N_{SC}N_{SYM}N_{AP}BTW}.\mathbf{2.1000} + \boldsymbol{MAC\ info}\ \ [122] \tag{6.3}$$

where N_{SR}, BTW, N_{AP}, N_{CH}, T_{TTI}, M_{O-UL}, N_{SYM}, N_{SC}, N_{STRM} and N_{q-LLR} are the sample rate, the bandwidth based on modulation scheme used, the number of antenna ports, the number of LTE channels, the transmission time interval, the modulation order in the uplink, the number of symbols per TTI, the number of sub-carriers of the system (in 20 MHz), the number of streams in the uplink, and the number of quantisation bits for LLR, respectively.

Parameter	Values
Sample Rate (N_{SR})	30.72 MHz
Bitwidth (*BTW)*	32
No. of Antenna Port (N_{AP})	25 × 25
No. of LTE Channel (N_{CH})	1
Transmission Time Interval (T_{TTI},)	1 ms
Modulation Order in Uplink (M_{O-UL})	2,4,6
No. of Symbol per TTI (N_{SYM})	14
No. of Sub-carriers (N_{SC})	1200
No. od Streams in Uplink (N_{STRM})	42
No. of Quantisation Bits for LLR(N_{q-LLR})	2

Table 6-1. Parameters for Fronthaul Requirements

In Figure 6-3, the fronthaul requirements are obtained from the equations in (6.1, 6.2, 6.3) based on the parameters in Table 6-1. The parameters are based on the LTE standard for a 20 MHz channel bandwidth. It shows that a traditional C-RAN option 8 system will require a fronthaul link with capacity of at least 614.4 Gbps which is not significantly different to the fronthaul link requirement as mentioned earlier in [93]. Option 7-1 provides up to 65% capacity reduction, where the fronthaul link requires at least 210 Gbps capacity. The reduction is due to

reduced physical layer processing as a result of removing the Cyclic Prefix (CP) and the fast fourier transform (FFT) that converts IQ symbols in the time domain to sub-carriers in frequency domain. For a lower level split, which is option 7-3, it can be seen that the fronthaul requirements drop another 32% compared to option 7-1, now requiring a fronthaul link with only 16.9 Gbps. More physical layer processing is done at the RRU side at this point compared to option 7-1, such as the port expansion and resource element mapper where the sub-carriers are converted into symbols by mapping the sub-carriers to resource elements. Overall, compared to a conventional C-RAN system, option 7-3 reduces the capacity requirement by 97%. As more processing is done at the RRU side, the complexity of the RRU increases.

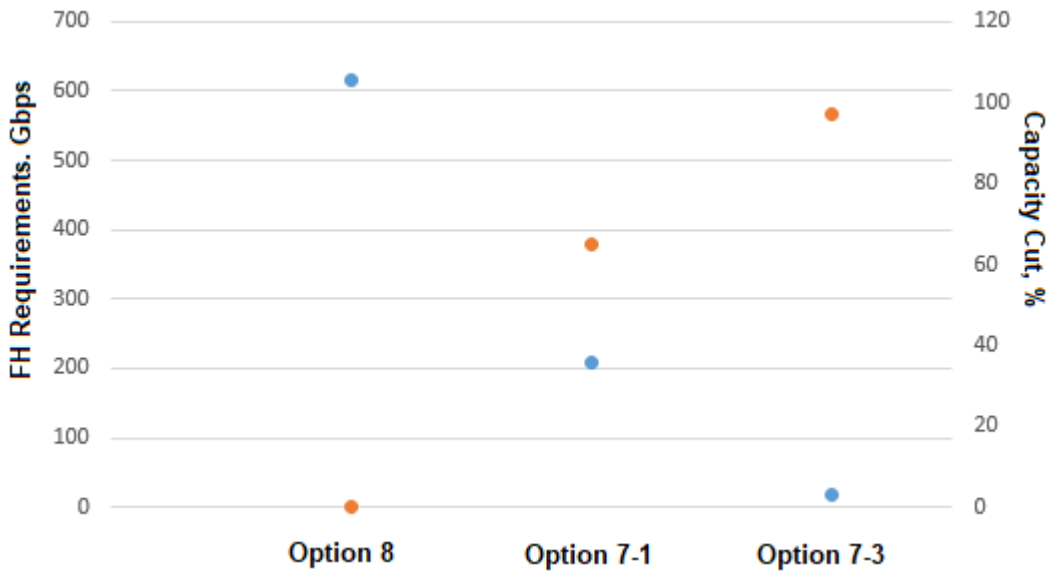

Figure 6-3 The fronthaul requirements and capacity cut down for network functional split with option 8, 7-1, and 7-3 as more data processing are done on the RF side.

With the fronthaul requirements of option 8, 7-1 and 7-3 presented earlier, we can now choose a suitable fronthaul deployments that enable a HAP to operate with a C-RAN based system. There are two possible technologies considered suitable for HAP fronthaul links which are mm-wave and FSO – it is assumed that these can achieve link capacities of 1.25 and 250 Gbps respectively considering current state of the art of both technologies. However, both mm-wave and FSO require LoS connectivity, which can be affected by rain events for mm-wave, and cloud

and fog for FSO [123]. The FSO uses the infrared portion of spectrum between visible light and microwaves, therefore atmospheric effects like fog will cause attenuation of the infrared signal [123]. To overcome these weather related link attenuations, ground relay station (GRS) diversity for both FSO and mm-wave is needed. To achieve full spatial decorrelation (where events at each GRS site can be considered as being independent) for rain events affecting mm-wave link availability, GRSs should be separated by at least 10 km, while to achieve full cloud decorrelation for FSO the GRS separation distance should exceed 200-300 km [124]. Thus, in the case of mm-wave, full decorrelation can be achieved by multiple GRSs being served by the same HAP, while to achieve full cloud decorrelation requires a system of multiple HAPs connected via inter-platform links. The inter-platform link network is well above maximum cloud height, so it is not affected by cloud cover.

The minimum required GRS to be able to carry the capacity assuming full GRS availability for each network functional split options can be defined as follows:

$$\boldsymbol{GRS_{\chi}} = \left\lceil \frac{\mathbf{FH}_{\chi}}{\boldsymbol{C_{FH}}} \right\rceil \tag{6.4}$$

where GRS_{χ} is the minimum ground relay station needed to correspond to FH_{χ} which is the fronthaul link requirement in Gbps for χ which is either option 8, 7-1, or 7-3 respectively depending on the technology considered for C_{FH} which is the maximum capacity link for fronthaul in Gbps.

To ensure that the links always have a certain availability so that the system can work with the minimum required GRS, site diversity is needed. The minimum GRS with site diversity can be estimated using the Binomial distribution as follows:

$$\binom{n}{k}\boldsymbol{p^{k}}(\mathbf{1}-\boldsymbol{p})^{\boldsymbol{n-k}} \leq \mathbf{1} - \boldsymbol{P_{availability}} \tag{6.5}$$

where n is number of GRS needed with site diversity, k is number of unavailable GRS, p is the probability of unavailability of a single link, and $P_{availability}$ is the overall available fronthaul

link probability. In the case of individual link availability is less than the required system availability then we can calculate the minimum GRSs are needed which is *n*.

To determine *n*,

$$\boldsymbol{n - k = GRS_{\chi}} \tag{6.6}$$

The difference between n and k is equal to GRS_{χ}. The value of GRS_{χ} is identified in (6.4), k is unknown, and n is to be determined, thus substituting k with $n - GRS_{\chi}$ in (6.5) means that the equation can be expressed as follows:

$$\binom{\boldsymbol{n}}{\boldsymbol{n-GRS_{\chi}}} \boldsymbol{p^{n-GRS_{\chi}}(1-p)^{GRS_{\chi}} \leq 1 - P_{availability}} \tag{6.7}$$

where,

$$\boldsymbol{n \geq GRS_{\chi}/(1-p)} \tag{6.8}$$

Due to the behaviour of the binomial distribution, there are two sets of solutions available, mirroring each other with $GRS_{\chi}/(1-p)$ as an axis. Due to physical constraint needed for site diversity, n has to be greater or equal to $GRS_{\chi}/(1-p)$ as stated in (6.8) as the additional constraint. The expression (6.5) can be used to obtain the number of GRS needed taking into account the diversity factor in which p can be used with real statistical data regarding rain and cloud events. To realise a conventional C-RAN system on HAPs, at least 3 FSO fronthaul links are required based on (6.4). For diversity purposes, as each GRS is assumed to be 300 km apart for clouds at each station to be uncorrelated. Thus, using (6.7), the minimum number of GRS required for option 8 to have 99.9% system availability is 5 GRSs, assuming a link availability of 90%, which can only be realised via inter-platform links as shown in Figure 6-4. On the other hand, adapting the option 7-1 network functional split on a C-RAN system according to the equation above would only require a single FSO fronthaul link to operate in a clear sky environment, but for diversity purposes in the situation where the system availability must be greater than the individual link availabilities, at least two more GRSs are needed.

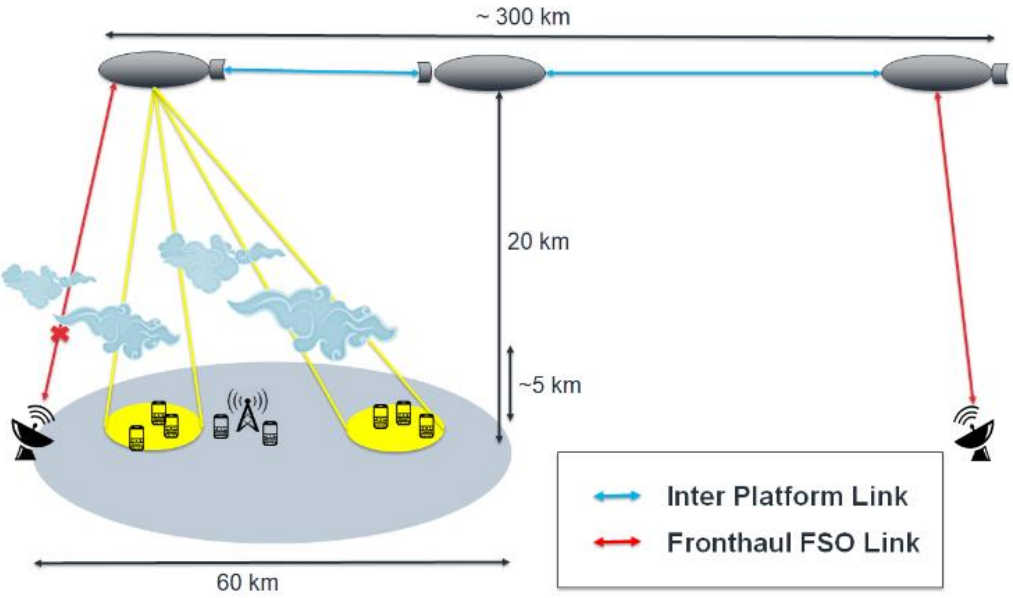

Figure 6-4 HAPs network connecting via the interplatform link to enable GRS site diversity.

For option 7-3, where the fronthaul requirements are reduced by 97% compared with option 8, because of the processing done on the platform, only a 16.9 Gbps capacity link is needed. With this fronthaul requirement, it is now possible to consider mm-wave technology for the fronthaul link. Based on (6.4), the minimum number of mm-wave fronthaul GRSs needed for HAPs system to operate on option 7-3 is 14. The mm-wave fronthaul GRS could be placed in a circular ring with a radius of 10 km and in a rain events, with a spatial correlation of 10 km approximately assuming that the rain events are uncorrelated when the ground stations are far enough away from each other. As a link margin (in dB) can be provided to compensate for the rain attenuation in the link budget, it is useful to consider several different availability probabilities for a mm-wave link by way of example. The number of GRS (n) needed depends on the overall system availability requirement and the availability of an individual link as shown in Table 4 which assumes GRS_{χ} is 14. In the case of unavailability of the GRS due to rain, a fronthaul link can switch to another GRS completely, or both stations could operate using a lower modulation scheme which has lower link quality requirement switching from for example 256 QAM to 64 QAM, 16 QAM or QPSK. In an event where the two nearest GRSs are affected by the rain, these two GRSs can operate with a lower order modulation scheme while the back-up GRSs operate using the 256 QAM modulation scheme.

	$P_{availability}$		
$1-p$	99.9 %	95.0 %	90.0 %
99.9 %	16	15	15
90.0 %	22	19	18
70.0 %	33	26	24

Table 6-2. The number of GRS, *n* needed for different requirements assuming mm-wave GRS with minimum number of GRS is 14 (when there is 100% availability)

The best option for a HAP system considering what has been discussed earlier is the option 7-1 which requires a single FSO fronthaul link connecting to a GRS on the ground which has a fiber connection to the CU and DU pool. In a cloudy environment, diversity could be achieved through an IPL link to the next HAP and then connecting to the next GRS which is 300 km away. Alternatively, the HAPs C-RAN system could be reconfigured using SDN and move to the lower option of option 7-3 so that a mm-wave link could be used for the fronthaul link which could maintain the link in cloudy weather. This would be at the expense of increased complexity on the HAP, resulting in a short-term increase in energy usage. If individual link availability is equal to or greater than the system availability required then no diversity is required, therefore GRS_{χ} is the number of GRS needed.

6.4 JT-CoMP Application across HAP-Terrestrial Access Network

Simulation is used to evaluate the performance of a JT-CoMP application for a network employing HAP and terrestrial segments on the access network, as a way of facilitating coexistence between the two segments. The system layout for the simulation consists of a HAP located at the centre of a 30 km radius service area in the stratosphere at a height of 20 km above ground. Also at the centre of the service area, a three sector macro base station is deployed. This models the situation where a small town or large village is served terrestrially to provide the necessary capacity density, with the surrounding area of lower capacity density served by the HAP. Two types of user are considered in this scenario; HAP users and terrestrial users. Users are uniformly distributed across the service area and the type of user (terrestrial or HAP) will be determined by which segment delivers the strongest CNR level. The HAP is considered to be equipped with 25×25 element planar phased array antenna which can perform beamforming creating multiple beams, each forming a cell, thereby providing coverage and capacity over the service area. The antenna profile is modelled based on [4]. The locations of the HAP cells are determined using the K-Means clustering algorithm. The algorithm determines the optimum location to point the beams based on the mean positions of the users prior to beam activation. With this algorithm, it is also possible to spot high density user groups inside the service area according to work in [2].

In the author's previous work, JT-CoMP has been evaluated in a HAP-only scenario where the Flex scheme together with full bandwidth (FBW) and half bandwidth (HBW) allocation schemes was shown to provide the best balance between benefit and loss users. To evaluate the proposed joint architecture, simulations using MATLAB based on the scenario described above have been performed and the methodology of JT-CoMP such as the flexible CINR threshold, and bandwidth allocation techniques are applied as in the previous work in [4]. The traffic is generated based on the full-buffer traffic model and the parameters are listed as follows:

Parameter	Values
Macro BS Transmit Power	40 dBm
HAP Transmit Power	40 dBm
Receiver Antenna Gain	0 dBi
HAP Antenna Gain (Boresight)	27.9 dBi
Three-sector Antenna Gain (Boresight)	14 dBi
Carrier Frequency	2.6 GHz
Noise Power	-100 dBm
CNR Threshold	9 dB
CINR Threshold	0 dB
INR Threshold	0 dB
Number of Users	2900

Table 6-3. Parameters for Simulation

Figure 6-5 presents the percentage of CoMP and non-CoMP of terrestrial users with the variation of γ. Approximately just below 0 dB CINR threshold, the non-CoMP users is 100% and should be considered as a scenario where CoMP is not applied into the system (no CoMP). As the threshold γ increases, the percentage of non-CoMP users decreases and on contrary, the percentage of CoMP users increases. This is due to more and more users being included into the CoMP regions as γ increases. Varying γ will show the impact of having different ratio of non-CoMP and CoMP users in the system and also show the relationship of resource allocation and the number of users. In the latter graphs, the performance will be shown and compared with different γ values to represent different scales of non-CoMP and CoMP users.

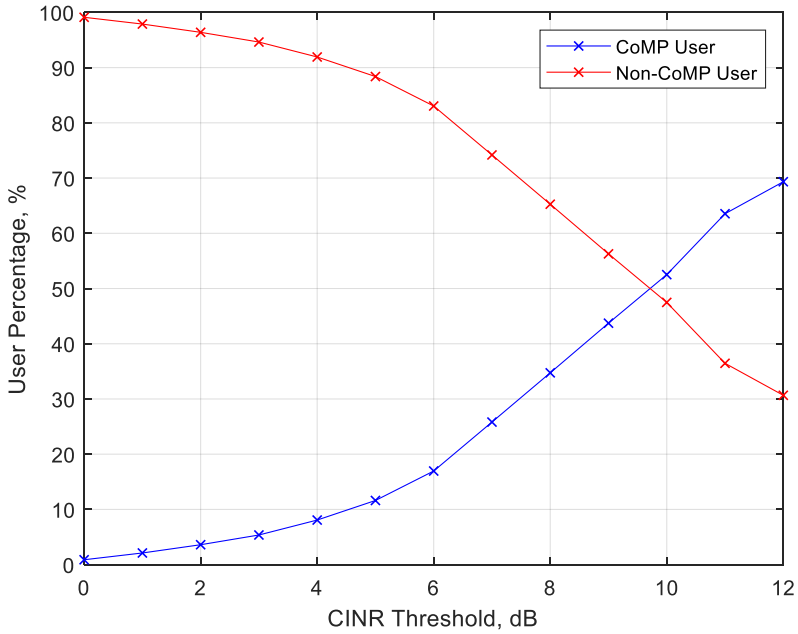

Figure 6-5 The percentage of terrestrial users with the variation of CINR threshold, γ.

When implementing JT-CoMP, it is expected that the CoMP user CINR levels will improve, which thereby improves the overall CINR levels. In Figure 6-6 and Figure 6-7, the CDF plots of the CINR levels of all users (HAP + terrestrial) and terrestrial users are shown respectively. The overall improvement of CINR levels depends on the ratio of non-CoMP and CoMP users, so to compare the performance, CINR levels of no CoMP, γ 5 dB, γ 8 dB, and the Flex scheme are presented in both Figure 6-6 and 6-7. It can be seen that in Figure 6-6 the CINR levels of the users keep increasing with the increases in the threshold, γ. The trend is consistent for the terrestrial users in Figure 6-7. With the Flex scheme, 50% of the users have a lower CINR compared to CoMP with a γ of 5 dB. The reason for that is because of the smaller group of CoMP users in the system. With the Flex scheme, fewer users are included in the CoMP region because with the equation $\log_2(1 + CINR) \leq k\log_2(1 + CINR_c)$, specific thresholds for each individual cell can be obtained instead of using one global threshold for all the cells. This will result in users that are potentially not going to benefit from CoMP being filtered out, hence fewer CoMP users in the group. For users outage, looking at 10 dB CINR threshold, without CoMP, 29% of users are excluded from the system, but it is improving with the implementation of CoMP. The outage improved, with 25%, 20%, and 15% users are excluded for Flex CINR, CoMP 5 dB, and CoMP 8 dB respectively. While in Figure 6-7 , the terrestrial users' outage also shown a similar trend. It shows that JT-CoMP has improved the CINR levels for both HAP and terrestrial users making it possible to deploy HAP cells close to the terrestrial macro cell. However, as discussed in Chapter 5, the best scheme need to be considered for CoMP to make sure it is beneficial for the users in the system.

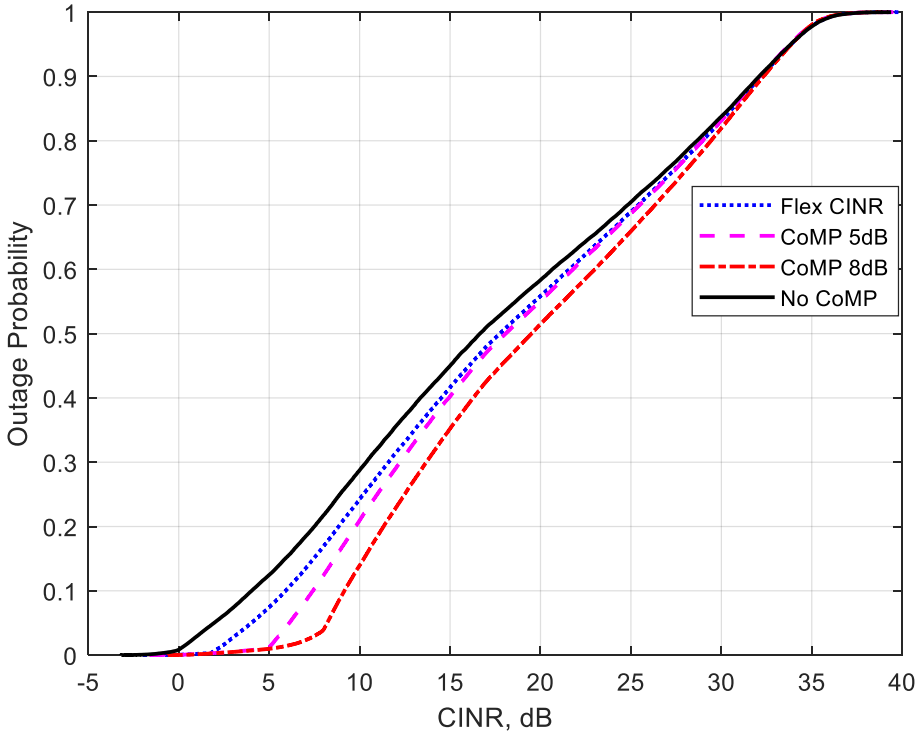

Figure 6-6 CINR levels of overall users for no CoMP, γ = 5dB, γ = 8dB and flexible CINR.

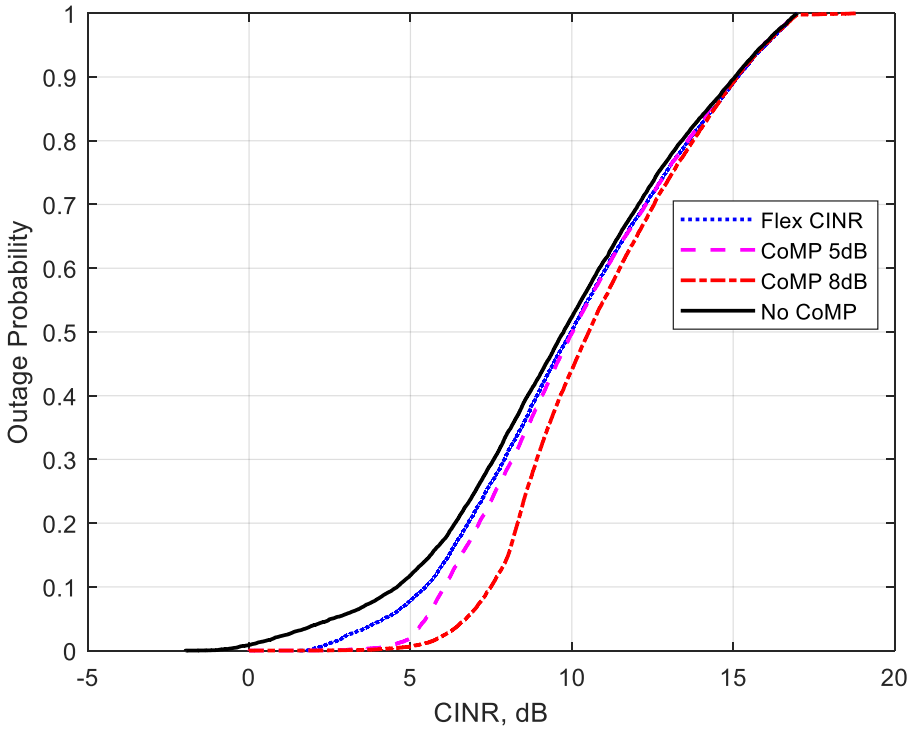

Figure 6-7 CINR levels of terrestrial users for no CoMP, γ = 5dB, γ = 8dB and flexible CINR.

In Figure 6-8, the percentage of users which have a positive increase in capacity performance (benefiting users), and the percentage of users which suffer a decrease of capacity performance is presented. The group that is shown is the 5th percentile user group that has the worst performance before CoMP is implemented which makes these users are the most affected by the interference. The performance of these groups are measured after CoMP is implemented with different schemes and parameters in order to determine which schemes and parameters will provide the most benefit to these users. Based on Figure 6-8, it can be seen that for all (HAP + terrestrial) users, almost all the schemes are acceptable for CoMP implementation. It is the same performance from what we seen in Chapter 5 for HAP users. However, for terrestrial, it will be more complicated for CoMP to be implemented. The reason why CoMP perform poorly for terrestrial users is because of the unevenness between terrestrial macro cell and HAP cell. From the bar graph, it can be concluded that CoMP is beneficial for the terrestrial users, given that 71% of the users are benefitting, while the rest (29%) are losing. Such a loss may be acceptable given that 71% users benefit. Some of the losing users may have insufficient CINR to operate at all prior to CoMP being implemented.

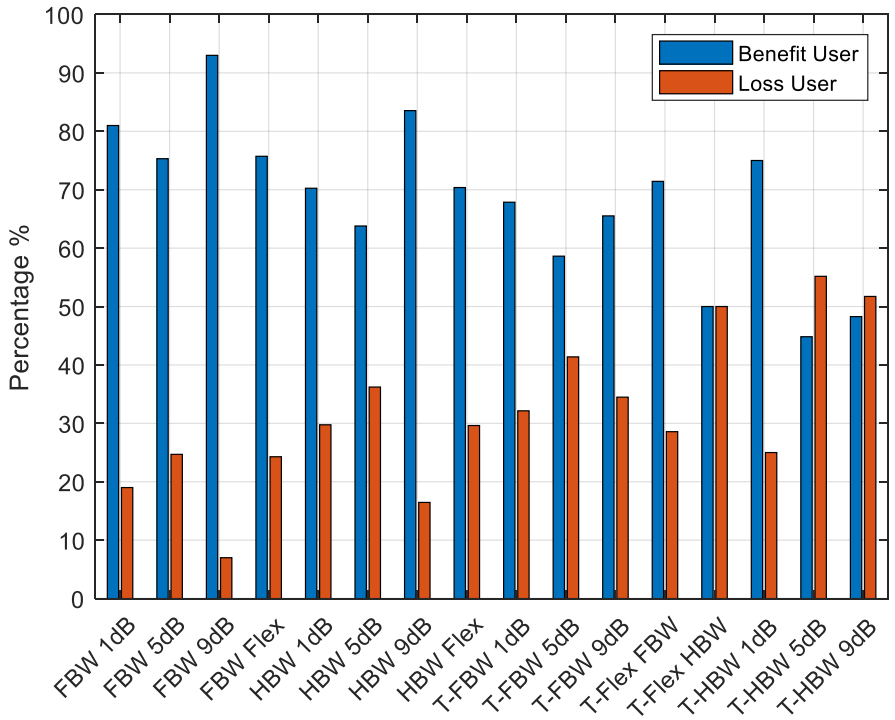

Figure 6-8 5th percentile user group performance in terms of benefit and loss users for all schemes.

6.5 Summary

The C-RAN based system is shown to be efficient to enable a joint HAP and terrestrial system through the implementation of a network functional split. With the split options considered, option 8 (conventional C-RAN), option 7-1 and option 7-3, provide several solutions regarding the HAP fronthaul link. A dynamic configuration through a software defined networking results in a flexible system, allowing the functional split option to be varied according to need in terms of HAP payload constraints. Considering the case of fronthaul link unavailability due to cloud or rain, ground relay station diversity is needed. The minimum number of GRS needed for a specific overall system availability such as 99.9%, 90%, or 70% is estimated using binomial distribution. Assuming a network functional split option 7-1 is adopted for both HAP and terrestrial system, enables the two systems to use JT-CoMP to control inter- and intra-segment interference because of the centralisation achieved by both systems. The performance of JT-CoMP with schemes like FBW, HBW, Flex FBW, and Flex HBW are shown. It is shown that for JT-CoMP to work across HAP and terrestrial system, only Flex FBW is likely to provide net benefits to the users in the system - 71% of users benefit and only 29% users lose capacity when compared to a no JT-CoMP scenario. This will provide a new degree of coexistence between HAP and terrestrial users where the two systems enable coordination, which enable more applications to be implemented, not only limited to CoMP.

CHAPTER 7

7. Conclusion and Future Work

Contents

7.1 Conclusion

In this thesis we have identified the challenges to enable the coexistence between HAP and terrestrial segments which are mainly caused by the interference between the cells sharing the same spectrum. Also, there may be a lack of coordination between the two segments which make some interference mitigation techniques such as CoMP difficult to implement across the two segments. In such situations to enable coexistence, the interference level caused by one cell to another should be maintained under a certain threshold to ensure a good QoS for all the users in the system, especially for the users in the existing terrestrial network. Several solutions were suggested and tested in this work ranging from an intelligent beam-pointing technique, JT-CoMP for a HAP system, and JT-CoMP in an integrated C-RAN system which showed that coexistence between the two segments is achievable and at the same time can improve the overall system performance.

A novel beam-pointing technique that relies only on the RF signalling has been proposed, to determine the number of users in a particular area to be clustered together. This RF clustering technique is shown to be accurate in spotting dense user groups inside the service area even with a lower number of beams. The efficiency of the RF clustering approach can be improved with algorithms like K-means clustering. Simulation results have shown that the RF based schemes (RF clustering and RF + K-means clustering) provide the best performance compared to Random and Regular pointing, and the K-means clustering scheme is shown to provide up to 96% coverage of the population in the service area. Although there is a technique in the literature which also offers high accuracy in spotting dense user groups, it is based on direction of arrival and comes at the cost of high complexity. RF clustering, on the contrary, will only use the regular signalling exchange as employed in the normal cell association process as in terrestrial systems, whereas DOA will consume additional power as an extra service.

In adapting JT-CoMP for a HAP system, we identified a trade-off between CINR gain and the reduction of a user's allocated bandwidth because of the bandwidth reserved to reduce interference. To counter this compromise, we provided several bandwidth allocation techniques (FBW and HBW) to balance the distribution of bandwidth between the CoMP region and Non-CoMP region. Aware of the effect of the number of users on the bandwidth allocation, which contributes to the overall performance, we provided two ways to define the boundary of the overlapping regions between the cells which are the centralised and flexible CINR threshold schemes. They provide differing sets of CoMP and Non-CoMP users which reflect the disparate impact of JT-CoMP to the system. On top of that, the newly proposed HAP system architecture in Chapter 3 was used to best provide the tight synchronisation needed to perform JT-CoMP. Most of the existing research regarding JT-CoMP, as explained in Chapter 2, has focused on improving the CINR levels of the cell-edge users. 57% of the users are shown to benefit from the JT-CoMP which means we are able to balance the trade-off and efficiently implement CoMP on HAPs.

In order to enable coordination between the HAP and terrestrial segments which were outlined in objective III, a joint architecture based on a Cloud – Radio Access Network (C-RAN) system was introduced. Apart from adapting C-RAN based system to connect the two segments together centrally, the network functional split which varies the degree of the centralised processing is also considered to deal with the limitations of HAP fronthaul link requirements. Based on the fronthaul link requirements acquired from the different splitting options, the ground relay station diversity to connect the HAP to centralised and distributed units (CUs and DUs) has also been considered. As an application of enabled coordination through the proposed joint architecture, JT-CoMP is implemented across the two segments which improved the user experience at the edge of both HAP and macro cells. It is shown to be effective in increasing the throughput for 71% of users in the bottom 5^{th} percentile. To the best of the author's knowledge, there is no work done in the past that dealt with the coexistence problem by enabling coordination between the HAP and terrestrial segments using a C-RAN based system. Adapting the C-RAN based system not only allows coordination with its centralisation feature but also solves the power limitation issues on HAPs, while suggesting the ground relay station diversity implementation. This novel system architecture contributes in preparing the HAPs for 5G deployment that will be commercialised shortly.

The contributions and novelties beyond the state of the art that was achieved in this thesis are as follows:

- Demonstration of the use of new HAP system architecture which integrates applications like JT-CoMP [4].
- The development of novel intelligence based beamforming approaches based on an RF clustering algorithm to achieve effective and dynamic coexistence with the terrestrial system [1, 2].
- A method to better balance the CINR gain and capacity loss trade-off via a new bandwidth allocation technique [3, 4].

- A new flexible CINR threshold that better selects users who will benefit from CoMP [4].

- A joint HAP and terrestrial network using a C-RAN based system and Network Function Virtualisation (NFV).
- Application of a network functional split on the HAP C-RAN segment to reduce fronthaul load with the exploitation of Software Defined Networking (SDN).
- Implementation of Joint Transmission Coordinated Multipoint (JT-CoMP) across the joint network (HAP and terrestrial) as an application of the newly proposed architecture to mitigate interference.
- A HAP system fronthaul link deployment and GRS site diversity that can adapt to specific implementations of the network functional split.

7.2 Future Work

This section suggests a number of items of future work based on the areas that have been explored in this thesis.

7.2.1 Determination of Appropriate Number of HAP Cells for HAP Network Deployment

There are many scenarios where HAP deployment is needed. Some of them are; providing coverage in rural areas, providing extra capacity for events like a concert, providing coverage during disaster relief, and etc. HAP beam deployment later forming cells would be different depending on the scenario. For example, in rural areas many beams are needed to achieve a total coverage (at the same time not to deploy excessive cell to avoid waste of energy), while for temporary event, like concert would only require a few beams to increase capacity in a dedicated area. Extending from the intelligent beam-pointing strategies in Chapter 4, deciding the appropriate number of HAP cells should also be done intelligently. It would be useful to develop an algorithm to determine an appropriate number of beams that are needed regardless the scenario.

7.2.2 Varying the Number of Antenna Elements of the Phased Array Antenna

Extending or reducing the size of the antenna array will directly affect the size of the beams produced by the array, hence it will affect the size of the cell mapped on the ground. Reducing the number of antenna elements means that the beams would be more prominent in size that may result in more overlapping between the cells, which means the algorithms used in the previous work might produce poorer performance for the RF clustering when compared to the K-Means clustering algorithm. Likewise, if the size of the antenna array is extended. It would be useful to deeply study how the algorithms proposed in the previous work would perform under a different number of antenna elements which resulting different size of HAP cells.

7.2.3 Exploiting the Use of HAP on Television White Space (TVWS)

The use of TVWS for delivering broadband services has been successfully tested, for example in Jamaica and Taiwan (ecosystem tourism broadband) in recent years [15]. Terrestrial systems are very constraining in terms of antenna directivity and TVWS research has concentrated on the terrestrial scenario to date, therefore it would be good to investigate whether HAP can work satisfactorily in these circumstances considering the nature of the HAP antenna systems that are able to control the roll-off of the antenna beam and have the flexibility to pointing the beam throughout the service area, enabling better control of the interference. Figure 7-1 shows that a HAP antenna (with 40x40 elements phased array) has a steep power roll-off rate compared to a terrestrial system, which enables a HAP cell to be deployed closer to high population areas (where the primary system has high demand). A HAP cell can be deployed as close as 2.5-3 km while meeting the regulation of Digital Terrestrial Television (DTT) by OFCOM (not to exceed -114 dBm per 8 MHz) [125]. Both HAP and terrestrial base stations have the same transmit power of 40 dBm for a fair comparison. The Ultra High Frequency (UHF) band used for television broadcast is highly underutilised in rural areas due to geographical factors (inaccessible to deploy fixed networks) [126]. So, utilising the TVWS band to deliver broadband services from HAP for secondary users without harming the primary users in the television broadcast and wireless microphone system is crucial for this work. Spectrum databases could be used to keep track of the spectrum activity, thus controlling the interference level to preserve the primary service, and delivering the broadband service as secondary service using TVWS spectrum. If the results of this work show that the coexistence of HAP (secondary system) and terrestrial (primary system) is possible, it would be a significant contribution in increasing the utilisation of the TVWS spectrum.

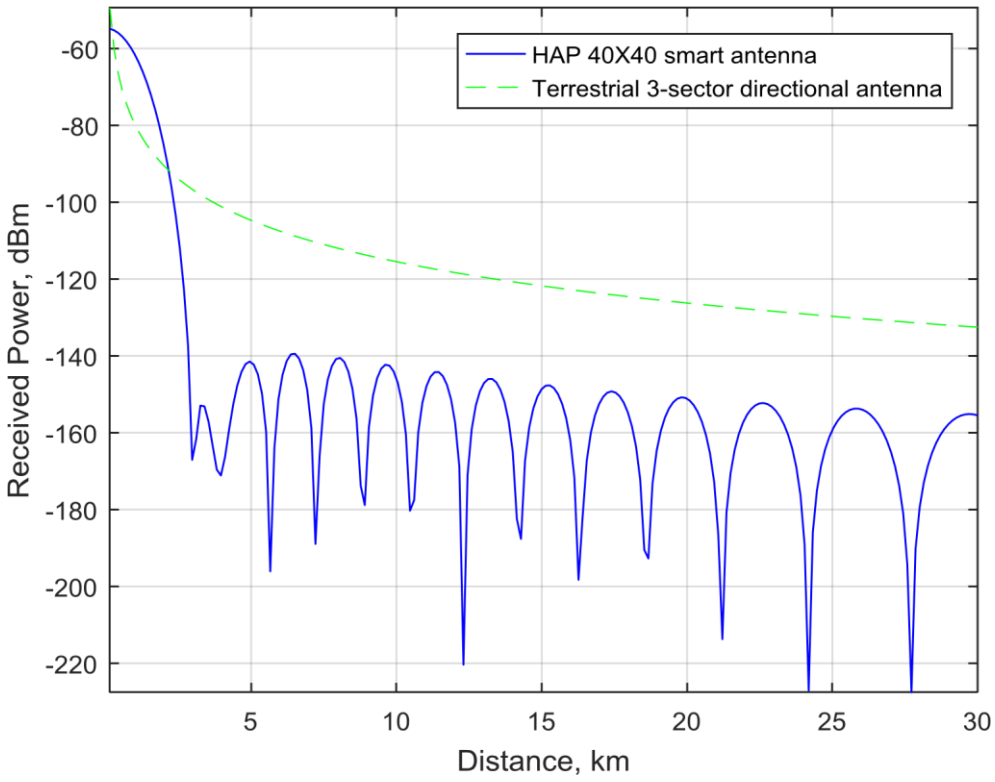

Figure 7-1 HAP and terrestrial systems power roll-off.

7.2.4 RF Clustering Further Optimisation Using Particle Swarm Optimisation (PSO)

RF clustering performance can be further enhanced by optimising each of individual centroids to point to a better position, which can avoid a high degree of cell overlap causing high co-channel interference. This can be achieved by using an algorithm which was shown in Chapter 4 with K-Means clustering algorithm, however it is good to study how PSO algorithm optimises the centroid of the listening cells compared to the K-Means clustering algorithm. PSO works by finding an optimum value resulting from each individual centroid point (particle) from a set of possible centroid points (swarm). Several iterations are needed to find an optimum centroid and at each iteration there will be one particle that is selected with the best CINR value, and then, based on PSO equations all other unselected particles are updated to be closer to the best particle. This is to find out an optimum centroid point of a certain location.

7.2.5 Zero Forcing Beam-pointing Technique for High Altitude Platform

The zero forcing beamforming (ZF) technique in downlink transmission is an algorithm to allow the transmitter (in this case the phased array antenna) to transmit data in the desired direction, while at the same time nulling out interference in other directions which can possibly cause interference to other users reusing the same spectrum. With the HAP architecture proposed in Chapter 3, it is possible to provide accurate channel state information (CSI) because of the centralisation of the virtual eNodeBs on HAP. However, the amount of centralised processing will be very high which will be one of the challenges that needs to be considered because of limitations with many types of HAP. In normal cases, when two cells are placed very close to each other it will cause high interference because of the unwanted signal that arises from an unwanted direction like the sidelobes. Therefore, it is expected to have better overall performance in terms of CINR of all users in the system and also improves the coexistence between HAP and terrestrial segments when the ZF technique is applied. The ability to control the nulls means that there will be less interference between the beams and also with the terrestrial segment which can improve the coexistence performance.

References

[1] M. D. Zakaria, D. Grace, and P. D. Mitchell, "Service Cell Selection," United Kingdom Patent 1901060.2 2019.

[2] M. D. Zakaria, D. Grace, and P. D. Mitchell, "Antenna array beamforming strategies for high altitude platform and terrestrial coexistence using K-means clustering," in *2017 IEEE 13th Malaysia International Conference on Communications (MICC)*, 2017, pp. 259-264.

[3] M. D. Zakaria, D. Grace, P. D. Mitchell, and T. M. Shami, "User-centric JT-CoMP for High Altitude Platforms," in *2018 26th International Conference on Software, Telecommunications and Computer Networks (SoftCOM)*, 2018, pp. 1-6.

[4] M. D. Zakaria, D. Grace, P. D. Mitchell, T. M. Shami, and N. Morozs, "Exploiting User-Centric Joint Transmission – Coordinated Multipoint with a High Altitude Platform System Architecture," *IEEE Access*, pp. 1-1, 2019.

[5] S. Chen and J. Zhao, "The requirements, challenges, and technologies for 5G of terrestrial mobile telecommunication," *IEEE Communications Magazine*, vol. 52, no. 5, pp. 36-43, 2014.

[6] J. G. Andrews, S. Buzzi, W. Choi, S. V. Hanly, A. Lozano, A. C. K. Soong, and J. C. Zhang, "What Will 5G Be?," *IEEE Journal on Selected Areas in Communications*, vol. 32, no. 6, pp. 1065-1082, 2014.

[7] F. Tariq, M. Khandaker, K.-K. Wong, M. Imran, M. Bennis, and M. Debbah, "A Speculative Study on 6G," *IEEE COMMUNICATIONS MAGAZINE*, 2019.

[8] D. Grace, M. Mohorcic, M. Oodo, M. Capstick, M. B. Pallavicini, and M. Lalovic, "CAPANINA—communications from aerial platform networks delivering broadband information for all," *Proceedings of the 14th IST Mobile and Wireless and Communications Summit*, 2005.

[9] T. C. Tozer and D. Grace, "High-altitude platforms for wireless communications," *Electronics & communication engineering journal*, vol. 13, no. 3, pp. 127-137, 2001.

[10] J. Thornton, D. Grace, C. Spillard, T. Konefal, and T. Tozer, "Broadband communications from a high-altitude platform: the European HeliNet programme," *Electronics & Communication Engineering Journal*, vol. 13, no. 3, pp. 138-144, 2001.

[11] S. Karapantazis and F. N. Pavlidou, "The role of high altitude platforms in beyond 3G networks," *IEEE Wireless Communications*, vol. 12, no. 6, pp. 33-41, 2005.

[12] K. Gomez, S. Kandeepan, M. M. Vidal, V. Boussemart, R. Ramos, R. Hermenier, T. Rasheed, L. Goratti, L. Reynaud, D. Grace, Q. Zhao, Y. Han, S. Rehan, N. Morozs, T. Jiang, I. Bucaille, T. Wirth, R. Campo, and T. Javornik, "Aerial base stations with opportunistic links for next generation emergency communications," *IEEE Communications Magazine*, vol. 54, no. 4, pp. 31-39, 2016.

[13] F. Dong, Y. He, X. Zhou, Q. Yao, and L. Liu, "Optimization and design of HAPs broadband communication networks," in *2015 5th International Conference on Information Science and Technology (ICIST)*, 2015, pp. 154-159.

[14] D. Yuniarti, "Regulatory challenges of broadband communication services from high altitude platforms (HAPs)," in *2018 International Conference on Information and Communications Technology (ICOIACT)*, 2018, pp. 919-922: IEEE.

[15] K. H. Anabi, R. Nordin, and N. F. Abdullah, "Database-Assisted Television White Space Technology: Challenges, Trends and Future Research Directions," *IEEE Access*, vol. 4, pp. 8162-8183, 2016.

[16] D. Kimura and H. Seki, "Inter-cell interference coordination (ICIC) technology," *FUJITSU Sci. Tech. J*, vol. 48, no. 1, pp. 89-94, 2012.

[17] T. M. Shami, D. Grace, A. Burr, and M. D. Zakaria, "User-centric JT-CoMP clustering in a 5G cell-less architecture," presented at the IEEE International Symposium on Personal, Indoor and Mobile Radio Communications (PIMRC), Bologna, Italy, 2018.

[18] D. Grace, M. Mohorcic, M. Oodo, J. Horwath, M. Capstick, M. B. Pallavicini, and M. Lalovic, "An overview of the European CAPANINA project-broadband for all from high altitude platforms," in *Proc. 5th Stratospheric Platforms Syst. Workshop*, 2005, pp. 1-8.

[19] F. A. d'Oliveira, F. C. L. d. Melo, and T. C. Devezas, "High-Altitude Platforms—Present Situation and Technology Trends," *Journal of Aerospace Technology and Management*, vol. 8, no. 3, pp. 249-262, 2016.

[20] H. Zhai and A. Euler, "Material challenges for lighter-than-air systems in high altitude applications," in *AIAA 5th ATIO and16th Lighter-Than-Air Sys Tech. and Balloon Systems Conferences*, 2005, p. 7488.

[21] T. E. Noll, S. D. Ishmael, B. Henwood, M. E. Perez-Davis, G. C. Tiffany, J. Madura, M. Gaier, J. M. Brown, and T. Wierzbanowski, "Technical findings, lessons learned, and recommendations resulting from the helios prototype vehicle mishap," NATIONAL AERONAUTICS AND SPACE ADMIN LANGLEY RESEARCH CENTER HAMPTON VA2007.

[22] A. J. D. Rapinett, Department of Physics, University of Surrey, "Zephyr: a high altitude long endurance unmanned air vehicle," 2009.

[23] A. Skippins and S. Taccheo, "High Altitude Platforms to Provide Internet in Developing Countries A Review of Technology," 2017.

[24] L. Reynaud, S. Zaïmi, and Y. Gourhant, "Competitive assessments for HAP delivery of mobile services in emerging countries," in *2011 15th International Conference on Intelligence in Next Generation Networks*, 2011, pp. 307-312: IEEE.

[25] S. Chandrasekharan, K. Gomez, A. Al-Hourani, S. Kandeepan, T. Rasheed, L. Goratti, L. Reynaud, D. Grace, I. Bucaille, T. Wirth, and S. Allsopp, "Designing and implementing future aerial communication networks," *IEEE Communications Magazine*, vol. 54, no. 5, pp. 26-34, 2016.

[26] Z. Yang, A. Mohammed, and T. Hult, "Performance Evaluation of WiMAX Broadband from High Altitude Platform Cellular System and Terrestrial Coexistence Capability," *EURASIP Journal on Wireless Communications and Networking*, journal article vol. 2008, no. 1, p. 348626, 2008.

[27] D. Grace, J. Thornton, G. White, C. Spillard, D. Pearce, M. Mohorcic, T. Javornik, E. Falletti, J. Delgado-Penin, and E. Bertran, "The european helinet broadband communications application-an update on progress," in *Japanese Stratospheric Platforms Systems Workshop (Invited Paper)*, 2003.

[28] S. Dutta, F. Hsieh, and F. W. Vook, "HAPS Based Communication using mmWave Bands," in *ICC 2019 - 2019 IEEE International Conference on Communications (ICC)*, 2019, pp. 1-6.

[29] K. Harb, A. T. Abdalla, M. Mohamed, and S. Abdul-Jauwad, "HAPs communication in Saudi Arabia under dusty weather conditions," in *2013 IEEE 11th Malaysia International Conference on Communications (MICC)*, 2013, pp. 379-380.

[30] M. Wood and A. Martines. *Why Did Wireless Networks Fail After Hurricane Sandy?* (Accessed). Available: https://www.freepress.net

[31] A. S. Yazid, T. F. F. Tengku, A. A. Abdullah, W. N. W. Daud, F. Salleh, and M. R. Husin, "Flood Risk Mitigation: Pressing Issues and Challenges," *International Review of Management and Marketing*, vol. 7, no. 1, 2017.

[32] Y. Wang, Y. Xu, Y. Zhang, and P. Zhang, "Hybrid satellite-aerial-terrestrial networks in emergency scenarios: a survey," *China Communications*, vol. 14, no. 7, pp. 1-13, 2017.

[33] P. Lähdekorpi, T. Isotalo, K. Kylä-Liuhala, and J. Lempiäinen, "Replacing terrestrial UMTS coverage by HAP in disaster scenarios," in *2010 European Wireless Conference (EW)*, 2010, pp. 14-19: IEEE.

[34] I. R Palma-Lázgare and J. A. Delgado-Penín, "High altitude platform stations in design solutions for emergency services," *Buran*, vol. 17, no. 25, pp. 26-30, 2010.

[35] S. Sibiya and O. O. Olugbara, "Reliable Internet of Things Network Architecture Based on High Altitude Platforms," in *2019 Conference on Information Communications Technology and Society (ICTAS)*, 2019, pp. 1-4.

[36] K. Xiao, C. Li, and J. Zhao, "LSTM Based Multiple Beamforming for 5G HAPS IoT Networks," in *2019 15th International Wireless Communications & Mobile Computing Conference (IWCMC)*, 2019, pp. 1895-1900.
[37] X. Wang, L. Li, and W. Zhou, "The Effect of HAPS Unstable Movement on Handover Performance," in *2019 28th Wireless and Optical Communications Conference (WOCC)*, 2019, pp. 1-5.
[38] M. Smith and L. Rainwater, "Applications of scientific ballooning technology to high altitude airships," in *AIAA's 3rd Annual Aviation Technology, Integration, and Operations (ATIO) Forum*, 2013, p. 6711.
[39] M. Lee, I. Smith, and S. Androulakakis, "High-Altitude LTA Airship Efforts at the US Army SMDC/ARSTRAT," in *18th AIAA lighter-than-air systems technology conference*, 2009, p. 2852.
[40] I. Smith, M. Lee, M. Fortneberry, and R. Judy, "HiSentinel80: flight of a high altitude airship," in *11th AIAA Aviation Technology, Integration, and Operations (ATIO) Conference, including the AIAA Balloon Systems Conference and 19th AIAA Lighter-Than*, 2011, p. 6973.
[41] K. Eguchi, Y. Yokomaku, M. Mori, N. Yamauchi, M. Maruhashi, N. Tabo, K. Oogaki, J. Kimura, and H. Nakamura, "Feasibility study program on stratospheric platform airship technology in Japan," in *13th lighter-than-air systems technology conference*, 1999, p. 3912.
[42] M. Onda and M. Sano, "Test vehicle proposal to next Japanese stratospheric LTA developments," in *6th AIAA Aviation Technology, Integration and Operations Conference (ATIO)*, 2006, p. 7715.
[43] M. Nakadate, "Development and flight test of SPF-2 low altitude stationary flight test vehicle," in *AIAA 5th ATIO and16th Lighter-Than-Air Sys Tech. and Balloon Systems Conferences*, 2005, p. 7408.
[44] S. Okaya, "R&D status of RFC technology for SPF airship in Japan," in *9th Annual International Energy Conversion Engineering Conference*, 2011, p. 5896.
[45] Y.-G. Lee, D.-M. Kim, and C.-H. Yeom, "Development of Korean High Altitude Platform Systems," *International Journal of Wireless Information Networks*, vol. 13, no. 1, pp. 31-42, January 01 2006.
[46] S. Lee, J. Jang, H. Ryu, and K. H. Lee, "Matching trajectory optimization and nonlinear tracking control for HALE," *Advances in Space Research*, vol. 54, no. 9, pp. 1870-1887, 2014.
[47] H. Bang, S. Lee, and H. Lee, "Nonlinear trajectory tracking using vectorial backstepping approach," in *2008 International Conference on Control, Automation and Systems*, 2008, pp. 169-174: IEEE.
[48] *Solar-Powered UAV Succeeds in Flying 14 Km above Sea Level*. (Accessed, 18/2/2019). Available: http://www.businesskorea.co.kr/news/articleView.html?idxno=11694
[49] *STRATOBUS: HALFWAY BETWEEN A DRONE AND A SATELLITE*. (Accessed, 18/2/2019). Available: https://www.thalesgroup.com/en/worldwide/espace/case-study/mi-drone-mi-satellite-stratobus
[50] T. Dargent, "Airship equipped with a compact solar generator using local concentration and bifacial solar cells," ed: Google Patents, 2018.
[51] *Stratospheric Broadband*. (Accessed, 18/2/2019). Available: http://capanina.org/
[52] *The Promise of ERAST*. (Accessed, 18/2/2019). Available: https://www.nasa.gov/centers/dryden/news/X-Press/stories/102904_people_erast.html
[53] *Helios Prototype*. (Accessed, 18/2/2019). Available: https://www.nasa.gov/centers/dryden/news/ResearchUpdate/Helios/index.html
[54] *Pioneering the Stratosphere*. (Accessed, 16/2/2019). Available: https://www.airbus.com/defence/uav/zephyr.html
[55] *Airbus Zephyr Solar High Altitude Pseudo-Satellite flies for longer than any other aircraft during its successful maiden flight*. (Accessed, 17/10/2018). Available: https://www.airbus.com/newsroom/press-releases/en/2018/08/Airbus-Zephyr-Solar-High-Altitude-Pseudo-Satellite-flies-for-longer-than-any-other-aircraft.html

[56] *Facebook cancels its internet drone program, will partner with Airbus instead*. (Accessed, 17/10/2018). Available: https://www.geekwire.com/2018/facebook-cancels-internet-drone-program-will-partner-airbus-instead/

[57] *Self-described serial entrepreneur takes on his next challenge: ultra-long-endurance unmanned aircraft*. (Accessed, 19/2/2019). Available: http://aviationweek.com/awin/vlj-pioneer-bets-atmosat-uav-market

[58] *Solara 50 Atmospheric Satellite*. (Accessed, 19/2/2019). Available: https://www.aerospace-technology.com/projects/solara-50-atmospheric-satellite/

[59] *AeroVironment Announces Joint Venture and Solar High-Altitude Long-Endurance Unmanned Aircraft System Development Program*. (Accessed, 17/10/2018). Available: https://www.businesswire.com/news/home/20180103005647/en/AeroVironment-Announces-Joint-Venture-Solar-High-Altitude-Long-Endurance

[60] *A 'super cell tower' in the stratosphere: AeroVironment and SoftBank's 5G vision*. (Accessed, 13/03/2019). Available: https://www.cnbc.com/2018/09/13/aerovironment-and-softbanks-5g-vision-cell-tower-in-the-stratosphere.html

[61] *SoftBank Corp. Develops Aircraft That Delivers Telecommunications Connectivity from the Stratosphere*. (Accessed, 13/10/2019). Available: https://www.hapsmobile.com/en/news/press/2019/20190425_01/

[62] *New HAPS Products Ready to Be Enjoyed in Indonesia in 2 Years*. (Accessed, 13/10/2019). Available: https://teknologi.bisnis.com/read/20191002/101/1154530/produk-haps-baru-siap-dinikmati-di-indonesia-2-tahun-lagi

[63] *STRATOBUS OR THE LEGAL STATUS OF HIGH ALTITUDE PLATFORM STATIONS*. (Accessed, 13/10/2019). Available: https://www.spacelegalissues.com/space-law-stratobus-or-the-legal-status-of-high-altitude-platform-stations/

[64] Z. Yang, A. Mohammed, T. Hult, and D. Grace, "Assessment of Coexistence Performance for WiMAX Broadband in HAP Cellular System and Multiple-Operator Terrestrial Deployments," in *2007 4th International Symposium on Wireless Communication Systems*, 2007, pp. 195-199.

[65] Z. Yang, D. Grace, and P. Mitchell, "Downlink performance of WiMAX broadband from high altitude platform and terrestrial deployments sharing a common 3.5 GHz band," in *Proceedings of the IST Mobile and Wireless Communications Summit*, 2005.

[66] Z. Yang, A. Mohammed, T. Hult, and D. Grace, "Optimizing downlink coexistence performance of WiMAX services in HAP and terrestrial deployments in shared frequency bands," in *2007 International Waveform Diversity and Design Conference*, 2007, pp. 79-82.

[67] Z. Yang, A. Mohammed, T. Hult, and D. Grace, "Downlink Coexistence Performance Assessment and Techniques for WiMAX Services from High Altitude Platform and Terrestrial Deployments," *EURASIP Journal on Wireless Communications and Networking*, vol. 2008, no. 1, p. 291450, 2008// 2008.

[68] P. Likitthanasate, D. Grace, and P. D. Mitchell, "Coexistence performance of high altitude platform and terrestrial systems sharing a common downlink WiMAX frequency band," *Electronics Letters*, vol. 41, no. 15, pp. 858-860, 2005.

[69] Z. Peng and D. Grace, "Coexistence Performance of High-Altitude Platform and Terrestrial Systems Using Gigabit Communication Links to Serve Specialist Users," *EURASIP Journal on Wireless Communications and Networking*, no. 1, p. 892512, 2008.

[70] J.Holis and P.Pechac, "Coexistence of terrestrial and HAP 3G networks during disaster scenarios," *Radioengineering*, 2008.

[71] J. Thornton, D. Grace, M. H. Capstick, and T. C. Tozer, "Optimizing an array of antennas for cellular coverage from a high altitude platform," *IEEE Transactions on Wireless Communications*, vol. 2, no. 3, pp. 484-492, 2003.

[72] J. Holis, D. Grace, and P. Pechac, "Effect of Antenna Power Roll-Off on the Performance of 3G Cellular Systems from High Altitude Platforms," *IEEE Transactions on Aerospace and Electronic Systems*, vol. 46, no. 3, pp. 1468-1477, 2010.

[73] Iskandar and A. Abubaker, "Co-channel interference mitigation technique for mobile WiMAX downlink system deployed via Stratospheric Platform," in *2014 8th International Conference on Telecommunication Systems Services and Applications (TSSA)*, 2014, pp. 1-5.
[74] B. V. D. Bergh, A. Chiumento, and S. Pollin, "LTE in the sky: trading off propagation benefits with interference costs for aerial nodes," *IEEE Communications Magazine*, vol. 54, no. 5, pp. 44-50, 2016.
[75] P. Likitthanasate, D. Grace, and P. D. Mitchell, "Spectrum etiquettes for terrestrial and high-altitude platform-based cognitive radio systems," *IET Communications*, vol. 2, no. 6, pp. 846-855, 2008.
[76] D. Grace, C. Spillard, J. Thornton, and T. C. Tozer, "Channel assignment strategies for a high altitude platform spot-beam architecture," in *PIMRC*, 2002, pp. 1586-1590.
[77] K. Katzis, D. Pearce, and D. Grace, "Fixed channel allocation techniques exploiting cell overlap for high altitude platforms," *Cell*, vol. 1, no. A2, p. B1, 2004.
[78] K. Katzis, D. Pearce, and D. Grace, "Fairness in Channel Allocation in a High Altitude Platform Communication System exploiting Cellular Overlap," in *Wireless Personal Multimedia Communication Conference (WPMC), Abano Terme, Italy*, 2004: Citeseer.
[79] Z. Gao, Z. Wei, Z. Wang, J. Zhu, G. Deng, and Z. Feng, "Spectrum Sharing for High Altitude Platform Networks," in *2019 IEEE/CIC International Conference on Communications in China (ICCC)*, 2019, pp. 411-415.
[80] R. Zong, X. Gao, X. Wang, and L. Zongting, "Deployment of High Altitude Platforms network: A game theoretic approach," in *2012 International Conference on Computing, Networking and Communications (ICNC)*, 2012, pp. 304-308.
[81] O. Anicho, P. B. Charlesworth, G. S. Baicher, A. Nagar, and N. Buckley, "Comparative Study for Coordinating Multiple Unmanned HAPS for Communications Area Coverage," in *2019 International Conference on Unmanned Aircraft Systems (ICUAS)*, 2019, pp. 467-474.
[82] J. Thornton, D. A. J. Pearce, D. Grace, M. Oodo, K. Katzis, and T. C. Tozer, "Effect of Antenna Beam Pattern and Layout on Cellular Performance in High Altitude Platform Communications," *Wireless Personal Communications*, journal article vol. 35, no. 1, pp. 35-51, 2005.
[83] Z. Wang, X. Liu, and Z. Li, "Steerable antennas movement compensation for high altitude platform," *Journal of Electronics*, vol. 28, no. 2, p. 154, 2011.
[84] Y. Albagory and A. E. Abbas, "Smart cell design for high altitude platforms communication," *AEU-International Journal of Electronics*, vol. 67, no. 9, pp. 780-786, 2013.
[85] Y. Albagory, "An Efficient 2D-DOA Estimation Technique for High-Altitude Platforms Mobile Communications," *Wireless Personal Communications*, vol. 88, no. 3, pp. 429-448, 2016.
[86] Q. Zhang, Q. Xi, C. He, and L. Jiang, "User Clustered Opportunistic Beamforming for Stratospheric Communications," *IEEE Communications Letters*, vol. 20, no. 9, pp. 1832-1835, 2016.
[87] P. Viswanath, D. N. C. Tse, and R. Laroia, "Opportunistic beamforming using dumb antennas," in *Proceedings IEEE International Symposium on Information Theory*, 2002, p. 449: IEEE.
[88] M. Sharif and B. J. I. T. o. i. T. Hassibi, "On the capacity of MIMO broadcast channels with partial side information," vol. 51, no. 2, pp. 506-522, 2005.
[89] O. Neji, N. Chendeb, O. Chabbouh, N. Agoulmine, and S. B. Rejeb, "Experience deploying a 5G C-RAN virtualized experimental setup using OpenAirInterface," in *2017 IEEE 17th International Conference on Ubiquitous Wireless Broadband (ICUWB)*, 2017, pp. 1-5.
[90] E. A. R. d. Paixão, R. F. Vieira, W. V. Araújo, and D. L. Cardoso, "Optimized load balancing by dynamic BBU-RRH mapping in C-RAN architecture," in *2018 Third International Conference on Fog and Mobile Edge Computing (FMEC)*, 2018, pp. 100-104.

[91] R. T and B. O, "A New SDN-Based Next Generation Fronthaul Interface for a Partially Centralized C-RAN," in *2018 IEEE 32nd International Conference on Advanced Information Networking and Applications (AINA)*, 2018, pp. 393-398.
[92] T. Salman, "Cloud RAN: Basics, Advances and Challenges," *Wireless Mobile Networking*, 2016.
[93] ITU-T, "Transport network support of IMT-2020/5G," ed: ITU-T, 2018.
[94] D. Harutyunyan and R. Riggio, "Flex5G: Flexible Functional Split in 5G Networks," *IEEE Transactions on Network and Service Management*, vol. 15, no. 3, pp. 961-975, 2018.
[95] K. Ramantas, A. Antonopoulos, E. Kartsakli, P. Mekikis, J. Vardakas, and C. Verikoukis, "A C-RAN Based 5G Platform with a Fully Virtualized, SDN Controlled Optical/Wireless Fronthaul," in *2018 20th International Conference on Transparent Optical Networks (ICTON)*, 2018, pp. 1-4.
[96] S. Costanzo, I. Fajjari, N. Aitsaadi, and R. Langar, "DEMO: SDN-based network slicing in C-RAN," in *2018 15th IEEE Annual Consumer Communications & Networking Conference (CCNC)*, 2018, pp. 1-2.
[97] K. Miyamoto, S. Kuwano, T. Shimizu, J. Terada, and A. Otaka, "Performance evaluation of ethernet- based mobile fronthaul and wireless comp in split-PHY processing," *IEEE/OSA Journal of Optical Communications and Networking*, vol. 9, no. 1, pp. A46-A54, 2017.
[98] K. Miyamoto, S. Kuwano, J. Terada, and A. Otaka, "Performance evaluation of mobile fronthaul optical bandwidth reduction and wireless transmission in Split-PHY processing architecture," in *2016 Optical Fiber Communications Conference and Exhibition (OFC)*, 2016, pp. 1-3.
[99] C. Chang, R. Schiavi, N. Nikaein, T. Spyropoulos, and C. Bonnet, "Impact of packetization and functional split on C-RAN fronthaul performance," in *2016 IEEE International Conference on Communications (ICC)*, 2016, pp. 1-7.
[100] A. Azeez, H. Amer, A. Alaameria, G. Su, and L. Tan, *Hybrid Inter Cell Interference Coordination in 5G Networks*. 2018.
[101] M. Yassin, "Inter-cell interference coordination in wireless networks," Université Rennes 1, 2015.
[102] "Coordinated multi-point operation for LTE physical layer aspects," in *3rd Generat. Partnership Project (3GPP), Tech. Rep. 36.819 R11 v11.2.0*, ed, 2013.
[103] G. Nigam, P. Minero, and M. Haenggi, "Coordinated multipoint joint transmission in heterogeneous networks," *IEEE Transactions on Communications*, vol. 62, no. 11, pp. 4134-4146, 2014.
[104] V. Garcia, Y. Zhou, and J. Shi, "Coordinated multipoint transmission in dense cellular networks with user-centric adaptive clustering," *IEEE Transactions on Wireless Communications*, vol. 13, no. 8, pp. 4297-4308, 2014.
[105] T. M. Shami, D. Grace, A. Burr, and M. D. Zakaria, "Radio resource management for user-centric JT-CoMP," presented at the International Symposium on Wireless Communication System (ISWCS), Lisbon, Portugal, 2018.
[106] H. S. Kang and D. K. Kim, "User-centric overlapped clustering based on anchor-based precoding in cellular networks," *IEEE Communications Letters*, vol. 20, no. 3, pp. 542-545, 2016.
[107] A. H. Sakr and E. Hossain, "Location-aware cross-tier coordinated multipoint transmission in two-tier cellular networks," *IEEE Transactions on Wireless Communications*, vol. 13, no. 11, pp. 6311-6325, 2014.
[108] W. Nie, F.-C. Zheng, X. Wang, W. Zhang, and S. Jin, "User-centric cross-tier base station clustering and cooperation in heterogeneous networks: Rate improvement and energy saving," *IEEE Journal on Selected Areas in Communications*, vol. 34, no. 5, pp. 1192-1206, 2016.
[109] S. Bassoy, M. Jaber, M. A. Imran, and P. Xiao, "Load aware self-organising user-centric dynamic CoMP clustering for 5G networks," *IEEE Access*, vol. 4, pp. 2895-2906, 2016.

[110] L. Liu, Y. Zhou, V. Garcia, L. Tian, and J. Shi, "Load aware joint CoMP clustering and inter-cell resource scheduling in heterogeneous ultra dense cellular networks," *IEEE Trans. Veh. Technol*, vol. 67, no. 3, pp. 2741-2755, 2017.
[111] J. C. Rudell, J. A. Weldon, J.-J. Ou, L. Lin, and P. Gray, "An integrated GSM/DECT receiver: Design specifications," *UCB Electronics Research Laboratory Memorandum*, 1998.
[112] A. Burr, A. Papadogiannis, and J. Tao, "MIMO Truncated Shannon Bound for system level capacity evaluation of wireless networks," in *2012 IEEE Wireless Communications and Networking Conference Workshops (WCNCW)*, 2012, pp. 268-272.
[113] C. A. Balanis, *Antenna theory: analysis and design*. John wiley & sons, 2016.
[114] 3GPP, "Universal Mobile Telecommunications System (UMTS);Spacial channel model for Multiple Input Multiple Output (MIMO) simulations," in *3GPP TR 25.996 version 6.1.0 Release 6*, ed.
[115] 3GPP, "3rd Generation Partnership Project (3GPP);Technical Specification Group (TSG) RAN;Working Group 4 (WG4);RF System Scenarios," in *TR25.942 V 2.0.0 (1999-09)*, ed.
[116] A. Ramli and D. Grace, "Rf signal strength based clustering protocols for a self-organizing cognitive radio network," in *2010 7th International Symposium on Wireless Communication Systems*, 2010, pp. 228-232: IEEE.
[117] A. Ramli and D. J. T. o. E. T. T. Grace, "Reinforcement learning-based clustering protocols for a self-organising cognitive radio network," vol. 27, no. 4, pp. 544-556, 2016.
[118] "System-wide Simulations Analysis and Results," in "FP7-ICT-2011-8-318632-ABSOLUTE/D2.6.2," 2015.
[119] ITU-R, "System parameters and considerations in the development of criteria for sharing or compatibility between digital fixed wireless systems in the fixed service and systems in other services and other sources of interference," in *Rec. F. 758*, ed, 2015.
[120] X. Fan, S. Chen, and X. Zhang, "An Inter-Cell Interference Coordination Technique Based on Users' Ratio and Multi-Level Frequency Allocations," in *2007 International Conference on Wireless Communications, Networking and Mobile Computing*, 2007, pp. 799-802.
[121] J. Zhang, F. Li, J. Li, and Z. Li, "228 Gb/s vector-mode-division-multiplexing signal transmission in free-space based on optical frequency comb," in *2017 16th International Conference on Optical Communications and Networks (ICOCN)*, 2017, pp. 1-3.
[122] L. M. P. Larsen, A. Checko, and H. L. Christiansen, "A Survey of the Functional Splits Proposed for 5G Mobile Crosshaul Networks," *IEEE Communications Surveys & Tutorials*, pp. 1-1, 2018.
[123] R. M. Pierce, J. Ramaprasad, and E. C. Eisenberg, *Optical attenuation in fog and clouds* (ITCom 2001: International Symposium on the Convergence of IT and Communications). SPIE, 2001.
[124] Jialu Lun, David Grace, Nils Morozs, Paul D. Mitchell, Yi Chu, Abimbola Fisusi, Olusegun Awe, and R. E. Sheriff, "TV White Space Broadband for Rural Communities Using Solar Powered High Altitude Platform and Terrestrial Infrastructures," University of York, 2017.
[125] D. Noguet, R. Datta, P. H. Lehne, M. Gautier, and G. Fettweis, "TVWS regulation and QoSMOS requirements," in *2011 2nd International Conference on Wireless Communication, Vehicular Technology, Information Theory and Aerospace & Electronic Systems Technology (Wireless VITAE)*, 2011, pp. 1-5.
[126] C. Gomez and R. Bureau, "TV White Spaces: Managing spaces or better managing inefficiencies?," in *13th Global Symposium for Regulators "4th Generation regulation: driving digital communications ahead*, 2013.